Integrating Hydrodynamic Models and High Resolution DEM (LIDAR) For Flood Modelling

Alemseged Tamiru Haile
March, 2005

Integrating Hydrodynamic Models and High Resolution DEM (LIDAR) For Flood Modelling

by

Alemseged Tamiru Haile

Thesis submitted to the International Institute for Geo-information Science and Earth Observation in partial fulfilment of the requirements for the degree of Master of Science in Geo-information Science and Earth Observation, Specialisation: Watershed Management, Conservation and River Basin Planning

Thesis Assessment Board

Chairman	Prof. Dr. Ir. Z. Su
External Examiner	Dr. P. Reggiani (WL-Delft Hydraulics)
Primary Supervisor	Dr. T.H.M. Rientjes
Second Supervisor	G.N. Parodi, M.Sc

INTERNATIONAL INSTITUTE FOR GEO-INFORMATION SCIENCE AND EARTH OBSERVATION
ENSCHEDE, THE NETHERLANDS

Disclaimer

This document describes work undertaken as part of a programme of study at the International Institute for Geo-information Science and Earth Observation. All views and opinions expressed therein remain the sole responsibility of the author, and do not necessarily represent those of the institute.

Abstract

In late October 1998, Hurricane Mitch event resulted in destructive landslides, flooding, and other associated disasters that overwhelmed the Honduras's resources and ability to quickly rebuild itself. As it is also the case in other parts of the world, the government started giving a great attention to flood problems. This study integrates State of Art techniques in data processing and Earth observation and hydrodynamic flood models to study flood hazard in Tegucigalpa, Honduras. Integrating Earth observation systems, **GIS**, and complex **flood models** which display impressive three dimensional outputs undeniably will have the potential to increase our capability to manage flood events. However, models may have their hidden vices, and **model uncertainty** is often not addressed. The models, **SOBEK** (coupled one and two dimensional) and **HECRAS** (one dimensional), solve the mass balance and the full momentum equations governing flow in rivers and floodplains and as such offer the simulation a strong physical basis. This makes novice users to overrate the models reliability. Differences in the two approaches relate to the designed model structure, selected model algorithms and applied model resolutions of various inputs. The overall objective of this study is to investigate model reliability and uncertainty where model performance is tested for various model inputs as obtained through geo-processing and earth observation. Variables of interest in this regard are flood inundation extent, flood depths and flow velocities. A very important aspect of flood modelling also addressed in this thesis, deals with representing topography of the river and floodplain. Commonly, hydrodynamic models are successful in topographically simple areas, which have lesser heterogeneity, where DEM's of low resolution are used in the model setup. Low resolution **DEM**, however, has the limitation of dropping out or generalizing some of the important features affecting flow dynamics. At present, a need is identified to use high resolution data for flood simulation studies since society demands more accurate and detailed information on hazardous flood events.

In this study, a **DEM** generated from LIDAR data with a grid cell size of 1.5 m was selected and served as a base line case for comparing various flooding simulations. The **DEM** was resampled, by nearest neighbour, bilinear, and bi-cubic algorithms, to lower resolutions that range from 1.5 to 15 m, and comparisons were performed. One-and two dimensional hydrodynamic models were used to simulate the flood inundation, for part of the Tegucigalpa city, for peak discharges having 50 and 100 year return periods as obtained from regional flood frequency analysis. The original **DEM** was also used to extract buildings using geomorphologic filters, and channel attributes, using **GIS** operations. Buildings were represented as solid, partially solid, and hollow objects. For the upstream boundary conditions of the main and tributary rivers, triangular discharge hydrographs were specified and a free flow was allowed at the downstream end. The effect of channel roughness and hydrograph shape were also investigated.

The **DEM** resampling procedure resulted in significant loss of information, and downstream boundary condition sensitivity analysis confirmed that the effect does not propagate to the study area. Another sensitivity analysis to **DEM** resolution revealed that topographic representation is critical for the reliability of model output: using **SOBEK**, 15m resolution resulted in an inundation area of about 3.4 times that obtained using 5m, and for twelve hour hydrographs, 2.5m **DEM** required a simulation time of about 15 days compared to the 26 minutes time for the 15m. The one dimensional model sensitivity to surface roughness indicated the model's weakness to solve supercritical flow, and the difficulty to obtain an 'optimum' parameter set.

Hydrodynamic models, High resolution DEM and GIS were integrated, and the need to investigate **model uncertainty** before employing sophisticated hydrodynamic models for flood study was pointed out. Recent advances in **high resolution** topographic data acquisition encourage modellers to use and develop more complex models. However, this has to be weighted with the disadvantage of using excessive computational time, and the difficulty of defining an optimum parameter set. Advances in computational resources and development of effective numerical solvers could limit the computational time. The difficulty of obtaining optimum parameter set may also be coped with the potential ability of incorporating methods for investigating uncertainty in the model approaches.

Key words: GIS, LIDAR, SOBEK, DEM, HECRAS, Flood modelling, Model uncertainty

Acknowledgements

Thanks to all members of the Water resource department at ITC for making my stay in the Netherlands very pleasant. I would also like to thank Dr. Cees Van Westen for providing me with all the necessary data for my thesis and Drs. Dinand Alkema for his support at the proposal level of my work. The contribution of my second superivisor Ir. Gabriel Parodi for the success of my work was also significant and I would like to thank him for his contribution.

A special thanks to my first supervisor Dr. Tom Rientjes for his dedication and critical comments on my work. I have learnt three main things from him: to know what I am doing, how to present my work and models are uncertain. Though the time was too short to master all these lessons during the period of the thesis work, I hope there will be sufficient time in the future to exercise and get benefit out of them. I will also try to ‘speak up’, Tom.

Table of contents

List of figures

List of tables

1. Introduction

The repeated occurrence of major flooding, as in China, or the Indian sub-continent, or in North America where catastrophic flooding has occurred in every year since 1993, and the use of phrases like 'the worst in half a century' and the 'worst in living memory', give the impression that floods are getting worse (Smith 1998). It also illustrates that man's attempts to control rivers have often had only little or no success. The greatest natural disasters come as a result of ignorance or, even worse, half-knowledge (Ward 1978). There are several definitions for a 'flood'. Two of these are:

> 'A flood is any relatively high flow that overtops the natural or artificial banks in any reach of a stream'
>
> Chow (1956)

> 'A flood is a body of water which rises to overflow land which is not normally submerged'
>
> Ward (1978)

Floods are one of the major society's concerns in the floodplain area. The ever growing population and economic activities in these areas have boosted the interest of the public, planners and decision makers to understand the cause and effect of floods. Floods are due to natural causes such as overflow of rivers by precipitation, extreme events like hurricanes, earthquake and/or man induced causes such as dam failures, and floodplain encroachments. The information on these devastating events has a vital role in improving our decision making, planning, design, and construction activities in the floodplain. Such information can be inferred from mathematical flood modelling which simulates the spatial and temporal characteristics of flood events.

Mathematical models for flood simulation solve a set of governing flow equations, and provide specific information on flood characteristics. The equations governing the water flow are the conservation of mass (continuity), momentum and energy equations. These equations have a form of non-linear partial differential equations and seeking their solution requires replacing them with a set of algebraic equations (discretization), which in turn must be solved with the aid of computers. In the past, simulating a flood event required simplification of the full governing flow equations owing to the lack of computational power and inadequacy of input data. However, advances in computational power combined with larger and more extensive meteorological data monitoring (when available) and topographic data acquisition techniques have allowed for the use of simulation models which solve the full governing flow equations to describe hydraulic transport processes. A major advantage of flood simulation models is that alternative schemes for development or flood control can be quickly tested and compared. Moreover, these physically based distributed simulation models allow for parameter variation in space and time. However, there is a difficulty to acquire all the necessary data, for analysis, calibration and evaluation, for each element of their problem domain in time and space. Where data is available, larger computational time could be another problem when high resolution

simulation is desired. Currently, there is a significant advance in this aspect. Despite their limitations, flood simulation models still play a vital role for the success of our decisions in the floodplains.

Reliable simulation of flooding events helps in estimating human, economic and financial impacts expected from a certain flood recurrence interval. Model approaches can also be used to forecast the future by studying the response of the catchment for different meteorological stresses. This can be used to define flood hazard zones; estimate expected maximum flood damage and the vulnerability of people and structures to floods, normally called "risk" analysis. Use of model results for decision making presupposes that the information is reasonably reliable. The accuracy of reproduction or prediction of 'real' situations depends upon the definition of an accurate "conceptual model" and the amount of data available when setting up a model. The model itself cannot substitute for lack of data. On the contrary, additional field data are often required before reliable results can be obtained. As stated by (Rientjes 2004) since their early development, frequently heard criticisms are that models are 'unreliable, uncertain, not trustworthy and that the performance of a model often is not sufficient'. Thus, the quality of the input data should be checked and the model approaches need to be validated in order to get a relatively accurate prediction of flood inundation depth, duration, velocity and area.

Flood modelling suffers from in adequacy of data such as hydrometric and topographic data. With regard to topographic data, recent advances in high resolution topographic data acquisition for instance LIDAR may have the potential to improve problem. Therefore their potential for flood modelling needs to be tested that also is the objective of this thesis.

1.1. Floods and society

In all countries of the world, rivers and their floodplains create assets as well as liabilities: resources as well as hazards (Rowsell and Tunstall 1996). The main stimuli for research in the floodplain can be generalized as 'our desire to build and live in the floodplain'. Society considers them as a means for survival and development. This can easily be explained by the fact that ancient civilized society lived along river courses; for instance, the Egyptians civilization along Nile River, the role of the twin rivers Euphrates and Tigris in ancient Middle East. There are many evidences that man has fought against flood hazards since ancient times. A good example is the Noah flood mentioned in the bible. 'Where did the water at that time come from?' A similar history is also there in Babylonian tradition (Ward 1978). In the Babylonian flood saga, king Atra-hasis was given seven days by the god Enki to pull down his reed house and build a boat with the materials. The boat was loaded with his possessions, animals and birds. The entire human race except the king and his passengers and family was destroyed. The flood lasted seven days and seven nights.

Whether society is living in the floodplains of large rivers such as the Mississippi and Nile or small river tributaries there is always a threat to flood inundation. Historically, China's problems have been dominant. The Huang Ho (Yellow River) has often been termed 'China's Sorrow'. As recently as 1931, over 3,500,000 people were killed in the flooding on the Chang Chiang (Yangtze) when some $3.5*10^6$ hectares were inundated (Smith and Ward 1998). To mention some of recent large floods: floods of December 1993, January 1995 and December 1998 in the Netherlands (Rientjes 2004), the 2004 flood due to multiple storms in the Philippines, and the devastating earthquake triggered flood event (Tsunami) of the Indian subcontinent in the late December 2004. The 1995 flood resulted in the

largest evacuation of people in the Netherlands (about 250,000) since the great North Sea flood of 1953. Along river banks, there is an adverse increase of agricultural activities, industrialization and urbanization. The ever growing economic activities in these areas mean that the more we become vulnerable to flood damage. Losses due to floods are classified as tangible, expressed in terms of monetary units, or intangible. The losses can be related to disruption of economic and social activities, especially in urban areas, immediately after a flood, or caused by the long term effects of floods. Figure 1-1 shows types of losses due to a flood. The flooding damage is also exacerbated by inadequate attention, maps, regulations and management approaches. Water resource managers and politicians are interested in stopping the unwise developments in the floodplain: there is a need to cope with floods. "Coping with floods" is defined as all those measures, with necessary policies and strategies of implementation, which a society may apply to alleviate the consequences of flood events (Yevjevich 1994). Some of the management activities in the floodplain include: floodplain zoning, evacuation plans, flood insurance studies, and other developmental activities. These activities boost the need for more accurate information on timing, magnitude and extent of floods by the public, water resource managers and politicians. This information can be obtained by use of hydrodynamic models.

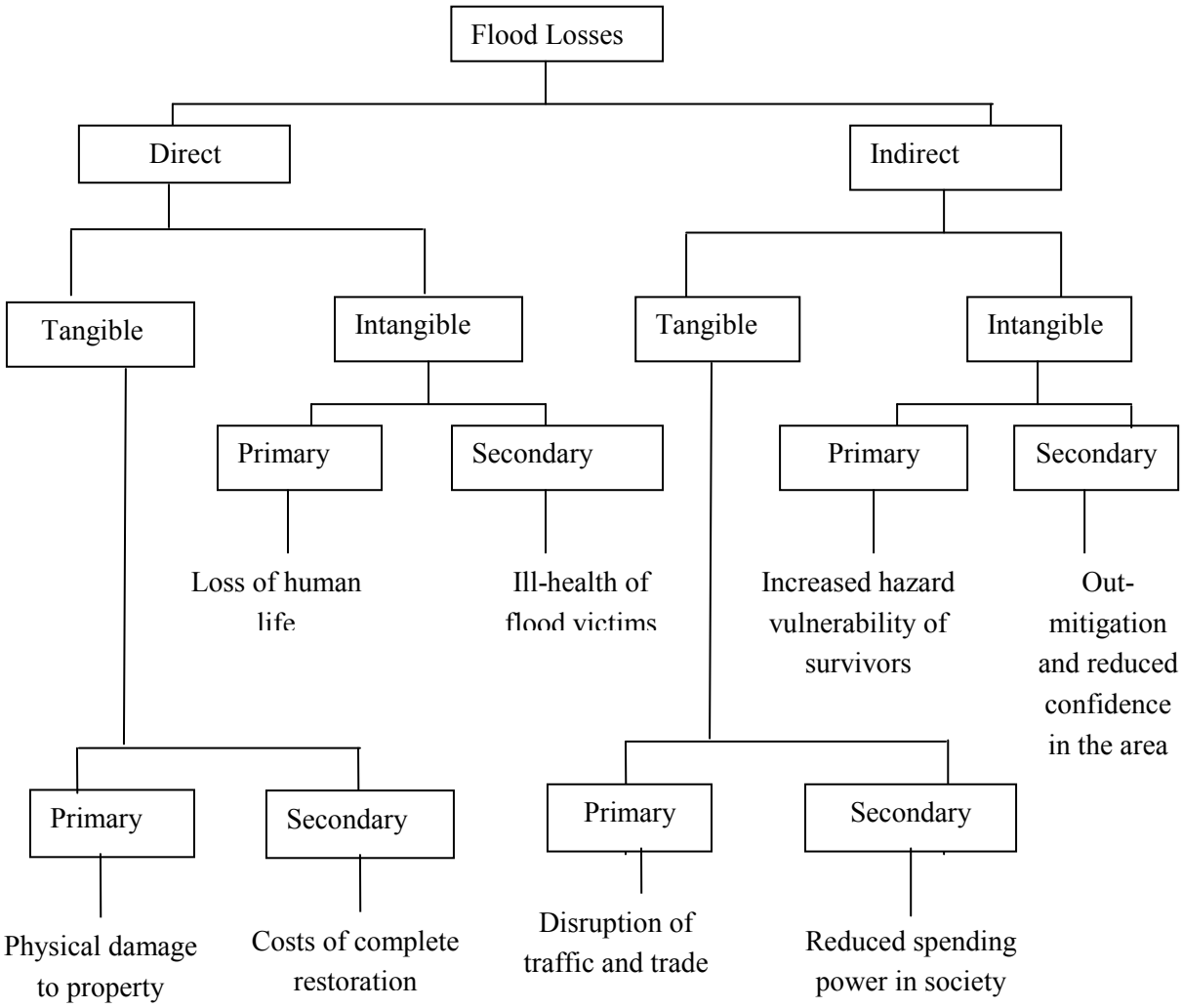

Figure 1-1: The categories of flood loss potential. Source: Smith et al.(1998)

1.2. Structure of the thesis

There are several questions which need an answer in relation to floods for a certain area. These include: what are the causes of floods? Can we really predict flood events? If yes, to what accuracy? What types of data are required for such a purpose? How reliable are the data sources? How often could flood of a certain magnitude be expected to occur? What will be the magnitude? How long would flood of a certain magnitude be expected to stay? To what extent will it spread in the floodplain? What will be the spatio-temporal variation and magnitude of the depth and velocities of flow over a floodplain and its channel? Can we estimate the expected damage? and others. This study attempts to deal with some of these questions. However, as it is expected, the study is limited by our current understanding of the subject, data availability and accuracy, and to a small extent by limited computational resources.

Chapter two explains the context of research in floodplains and the role of State-of-Art technique remote sensing and GIS for hydrodynamic flood modelling. Three possibilities to integrate models in GIS, and LIDAR topographic data acquisition technique are discussed in this chapter. Moreover, this chapter gives a general description on the solution procedure for flood modelling, model inputs and sources of errors in hydrodynamic modelling. The calibration and sensitivity analysis procedures are also covered in this chapter.

A description of the study area and the problem statements are presented in Chapter three. Chapter three also reviews related previous studies for the study area. The objectives and research questions are stated here.

The material and methods followed in the thesis are discussed in chapter four. The assumptions and the solution procedures specifically for the two models used for flood simulation are explained. Preparation of model inputs using geo-processing and other procedures are also described briefly.

Chapter five mainly focuses on presentation and discussion of simulation results, and chapter six summarises the limitations, investigations of the study and the recommendations.

2. Literature review

2.1. The context of research in the floodplains

Research activities for floodplain processes include hydrodynamic modelling of flow, topographic evolution of floodplains, water quality, and sediment erosion and deposition. Understanding hydrodynamic overbank processes is essential to know the risks associated to living in these areas, and also predict suspended sediments and associated contaminants. The developments in flood modelling can be linked to advances in data capturing techniques, computational facilities and theoretical developments (mainly the governing flow equations and their solutions). For this field of study, the governing flow equations for hydrodynamic modelling are well known. However, there is still a research concern to obtain improved numerical solvers for these equations. Some of the topics which need research attention in hydrodynamic flood modelling include the interaction between the floodplain and channel processes, which processes to include, how to represent turbulence, what solution procedures (numerical solvers, wetting and drying) to follow, which dimensions to consider and how to estimate parameters. In addition to these, (Bates et. al. 1996) identified two aspects as particularly significant in terms of research direction. The first is the inclusion of uncertainty methods in the modelling to provide further insights into model parameterization needs, predictive outcomes and process dominance. The second is the nature of the linkages between the floodplain environments (hitherto treated as hydraulically isolated) and the hillslope and floodplain subsurface (hitherto modelled hydrologically without comprehensive regard for channel hydraulics). Some of the terms mentioned above are explained in the sections to follow.

2.2. The role of geoinformatics

A geographic information system (GIS) assists in all stages of flood disaster management: preparation, prevention, mitigation, and post disaster activities. It provides a powerful, interactive, and graphics oriented data platform and user environment. However, prior to utilizing available data and model approaches, analysis of the problem's information requirements, the data base contents and the given boundary conditions is necessary to configure models and data in a most effective and economical way (Arnold et. al. 1989). Hydrologic and hydraulic modelling can also benefit much from the data base management system of GIS. Use of GIS facilitates automated extraction of topographic and drainage information and the other data layers (soil, land cover, etc) as an input to models. Once the data have been entered into a GIS data base in the form of overlays, the overlays can be analysed, combined, revised, changed in scale, and manipulated in some other way. In addition to data preparation and processing, GIS helps to display and disseminate model outputs in a manner that can be understood by the public, water resource managers and politicians. Some of the functions of GIS for hydrology are listed by (Band and Moore 1995) as:

i. Determining the spatial patterns of surface attributes at scales or resolution appropriate to route water through the terrain or represent spatial dependence of certain processes (such as net erosion, run-off infiltration or advection).

ii. Extracting and representing the watershed structure by the nested system of the stream network and associated hillslope and subcatchment drainage areas.
iii. Sampling and constructing statistical descriptions of key surface variables including variance and covariance structures or joint distribution functions.
iv. Determining the effects of scale on the distribution functions of key land surface variables and the correlation structures between these variables, and investigating the scaling behaviour of these distributions as they are sampled across different resolutions.
v. Optimal partitioning of the surface into sufficiently homogeneous land units minimizing within unit variance, or into functional watershed units at a scale corresponding to the REA (representative elementary area), if it can be shown to exist.
vi. Facilitating the storage and retrieval of observed biophysical data for comparison with a set of state and flux variables predicted by the model, such that modelled spatial and temporal patterns of variables not used for calibration can be assessed.

Hydrologic and hydrodynamic models benefit from GIS through GIS-model integration. There are three levels of GIS-model integration: loosely coupled, tightly coupled through shared database, and tightly coupled through embedded model. This is illustrated in Figure 2-1.

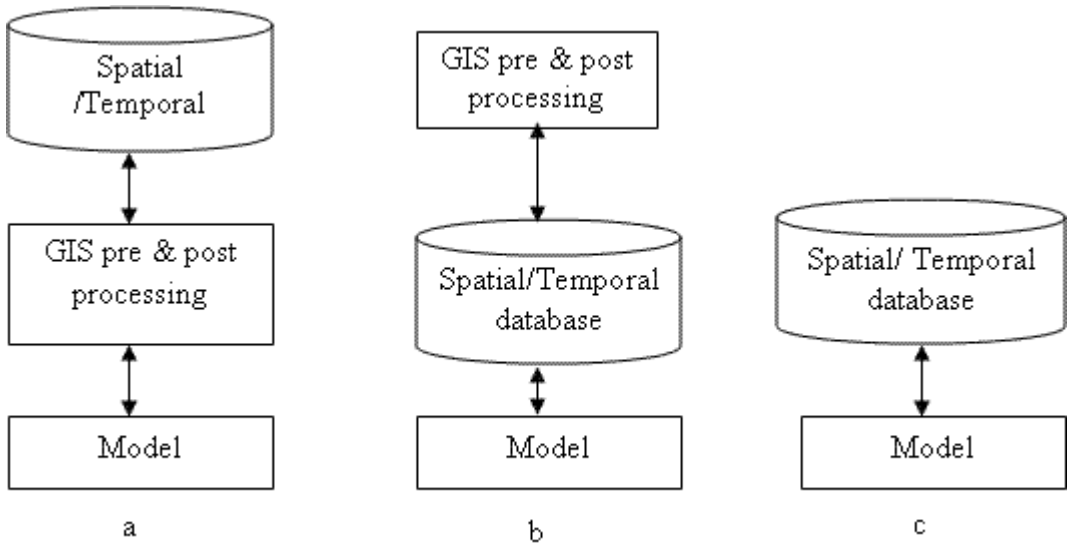

Figure 2-1: Levels of GIS-model integration (a) loosely coupled; (b) tightly coupled through shared database; (c) tightly coupled through embedded model. Source :(Werner 2004)

Aspects of data capture and management integration are at risk of being isolated by the respective demands for analytical "solutions" and political "solutions". And yet both of these solutions are comparatively starved of the very data most often needed. This situation places at risk the methods, directions and outcomes of the science in the field of floodplain processes (Anderson et. al. 1996). However, there are new emerging sources for data acquisition such as remote sensing imagery. Remote sensing has the capability to provide us with spatial data which is in favour of hydrodynamic models as their governing equations are solved over a distributed model domain. The spatial data are, in some cases, of high resolution and can be used to get information on land cover and topographic information. The pre-processed data can be used directly as an input to the models or for

parameterization. This allows us to have more physically based approaches. GPS assists flood outline mapping. Radar is improving the robustness of weather prediction models and rainfall-runoff models. Flash flood forecasting is also improved by using satellite imagery in conjunction with radars. Measurement of wave height by radar altimeters improves our understanding and forecasting of coastal flooding. One of the challenges in flood modelling is the calibration aspect. However, inundation extent before, during, and after a flood event can be obtained from remote sensing images which can be used for calibration purpose provided the appropriate hydrometric data is available at the site. In general, remote sensing could be utilized in different ways for a hydrodynamic modelling: (a) to estimate parametric inputs such as surface roughness values and precipitation mainly based on data from active and passive remote sensing instruments; (b) to estimate initial conditions such as river stage (mainly for large rivers); and (c) to obtain data for calibration for example in the form of flood extent map. One type of data from remote sensing which can be used to obtain topographic data is the LIDAR technology. This is explained in the next section.

2.2.1. LIDAR topographic data acquisition

The ability to map flood outlines, model catchment hydrology, and develop flood estimation procedures on the basis of relationships between the nature of a catchment and its flood hydrograph, are some of the aspects of flood studies which have been constrained in the past by the scarcity of point information on catchment characteristics (Smith 1998). In this regard, the recent developments in Digital Terrain Models (DTM), such as LIDAR topographic data acquisition, play a significant role. LIDAR is an acronym for Laser Imaging Detection And Ranging. FEMA (FEMA) defines it as an airborne laser system, flow abroad rotary or fixed-wing aircraft, that is used to acquire x, y, and z coordinates of terrain and terrain features that are both manmade and naturally occurring. Its main components are an airborne Global Positioning System (GPS) with attendant GPS base station(s), Inertial Measuring Unit (IMU), and light-emitting scanning scanner. Advances in airborne LIDAR topographic survey are due to the developments in three technologies: Laser range finding (the use of laser to measure distance), GPS and IMU. The system components for LIDAR topographic data acquisition are shown in Figure 2-2. LIDAR systems are usually carried by an aircraft flying at low altitudes and emit pulses of laser light to precisely measure distances. A scanning mirror directs the laser pulses back and forth across a wide swath. Timing of the round trip from the source to the target is measured and is converted to distance using the velocity of light ($3*10^8$ m/s). The precise location of the aircraft is estimated by the combination of GPS and IMU. The onboard GPS antenna is mounted directly above the laser head, and the GPS ground stations identify and correct errors in the aircraft's position. The x, y, and z coordinates of the aircrafts position are obtained from the GPS measurements. The pitch, roll and yaw of the aircraft's are measured by the IMU. This information is used to compute the angle and orientation of the beam with respect to the coordinate system used during the post processing. The density of elevation points generated can be adjusted by changing flying height, speed and scan angle/frequency. Denser and relatively more accurate dataset can be obtained using slow flight speed and narrower scan angle.

In forested and urban areas, the pulse may hit more than one object and reflected back several times. These several returns can be used to estimate the height and the shape of objects. The last return along with ground control points, sophisticated computer algorithms, and digital orthophotos is used to develop digital elevation models.

The improvements in LIDAR data acquisition have the potential to improve the problems associated with inadequate representation of topographic data. The primary advantage of the LIDAR data is the accurate digital nature, which is less subject to the horizontal errors inherent in using data sets derived from contour lines. LIDAR can produce maps of surface height over large areas with a height precision of about 15 cm (depending on the nature of the ground cover) and a spatial resolution of about 1m. Other advantages include its rapid collection and the future possibility of repeat flights over floodplains that may be subject to topographic change in the event of a flood. A high-resolution model will also be advantageous when small scale processes have a significant effect on model predictions, for example, where inundation extent is controlled by small topographic features such as dykes, levees and ditches.

Figure 2-2: System components for LIDAR

2.3. Flood hazard assessment

Floods are natural phenomenon, which will become a hazard when they have a potential to cause damage - mainly societal, environmental and economic. “Flood hazards result from a combination of physical exposure and human vulnerability to geophysical processes. Physical exposure reflects the type of flood events that can occur, and their statistical pattern, at a particular site, whilst human vulnerability reflects key socio-economic factors such as the number of people at risk on the floodplain or low-laying coastal zone, the extent of any flood defence works and the ability of the population to anticipate and cope with hazard. It is the balance between these two elements, rather than the physical event itself, which defines natural hazard and determines the outcome of a natural disaster.” (Smith 1998) Flood damage can be estimated either after a flood event through interview and observation or on the basis of depth-damage curves. Depth-damage curves are difficult to construct owing to their non-linearity and the variety of land uses in the floodplain. In addition, other factors such as velocity and duration of floods affect the magnitude of damage: for roads and agricultural land, the duration and velocity of floods may be more important. Flood water levels are

often used in land use planning. There could also be a problem of double counting. Transferring damage curves from one region to another is also a difficult task; for instance, due to differences in building materials. Moreover, the damage resulting from a flood event depends on the management actions taken: preparation, prevention, and mitigation.

As such flood simulation requires estimation of upstream area runoff associated to a certain return period which is obtained either through flood frequency analysis and a rainfall-runoff modelling. In order to estimate time of flooding and change in characteristics of flow with time, flood models require accurately representing the shape of the hydrograph for the upstream part of the floodplain, and such information is provided by rainfall-runoff simulation modelling by which the peak runoff as well as the shape of the hydrograph is estimated. The problem with this approach is how to obtain 'accurate' and 'sufficient' input data, and how to calibrate the model for the desired events. The output hydrograph can then be used as a boundary condition for the hydrodynamic flood model, which is used to simulate the flood inundation over the floodplain under study.

2.4. Flood modelling

Several processes are observable in a hydrologic system. A complete accounting and simulation of these processes is too complex to incorporate in the study of the system. Hydrologic and hydraulic models are a simplified representation of the 'real world', which try to simulate those processes, which are (at least we think) most dominant in simulating the natural phenomenon we want to study.

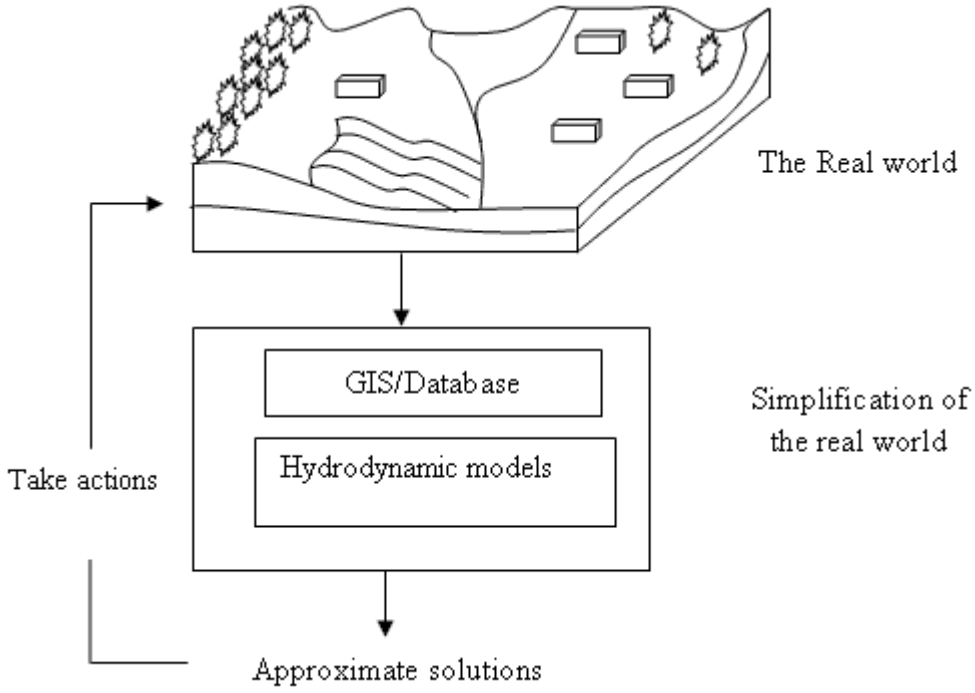

Figure 2-3: Representation of the 'real world' in hydrodynamic flood models

Flow in rivers is generally transient. For some practical applications, however, the variation may be considered so slow that a steady (or quasi-steady) flow situation can be assumed (Jansen et. al. 1979). Steady state approach considers flow characteristics variation with space only neglecting the variation

with time and is aimed at identifying the maximum water surface profiles associated to maximum flows. However, in the case of transient approach flow is considered to vary in both space and time. Rapid changes in flow and stage, and full stream networks require consideration of the transient nature of flows in a river. In urban areas, there is also a need to estimate the variation of flow characteristics with time since damages on property and life depend on the rate of change of these characteristics. In addition, flood evacuation plans require the time at which the flood reaches at each location of the floodplain.

Physically based flood inundation model approaches solve the Saint-Venant equation using one-dimensional (1D) or two-dimensional (2D) numerical schemes. 1D model assumes change of stage, velocity and discharge along the longitudinal direction disregarding the transverse and depth components of the flow field vectors. These models are competent with hydrometric observations. In these models, cross sections are taken at certain locations along the stream wise direction and the geometry is assumed to be constant or vary linearly between the cross sections. Hydraulic energy and pressure forces, flow depth and velocity are assumed constant in the transverse direction and locations of sections may predetermine flow directions and flow conditions. Some limitations of such an approach are that the direction of flow is determined beforehand, cross sections may not have been chosen to best represent the direction and distribution of flow and off-channel storage areas may have been neglected when surveying the cross-sections. On the other hand, 2D model approaches account for both the x and y components of the flow (not for z). These models have advantages in undefined and heterogeneous floodplains where the direction of flow is affected by factors in addition to the slope of the floodplain and the channel. However, these models are more difficult to calibrate, and detailed representation of channel cross sections in these models requires finer grid cells which could increase the simulation time. By using a 1D representation for the channel flow and a 2D representation for the floodplain, it is possible to incorporate the influence of the existing infrastructures such as buildings and roads (2D model) and narrow rivers and structures such as culverts and bridges (1D model) on the flooding processes. (M.S. Horritt et al. 2002) indicated that calibration and validation of a 1D flood model against 2D flood model has yet to be carried out and there is no indication of the relative performance of 1D and 2D approaches in predicting floodplain inundation.

2.4.1. Historic perspective

In 1871, Barrė de Saint-Venant formulated the basic theory for one-dimensional analysis of transient flow; however, in the past, owing to the mathematical complexity of the Saint-Venant equations, simplifications were necessary to obtain feasible solutions for the important characteristics of a flood wave and its movement. Examples of such simplified equations are the kinematic and diffusion (zero-inertia) equations. If the complete Saint-Venant equations are used, the routing model is known as a dynamic routing model. With the advent of high speed computers, Stocker first attempted in 1953 to use the complete Saint-Venant equations for routing Ohio River floods. Since then, much effort has been expended on the development of dynamic routing models (Maidment 1993). The development in GIS is also contributing to the development of hydrodynamic models by facilitating data preparation, processing and output visualization.

2.4.2. Solution procedure

In a flood routing problem a decision needs to be made whether to solve the full flow governing equations or not. After that, space and time discretization follows and the continuous partial differential form of the governing equations is converted to a discrete system of algebraic equations. Solving the linear system of algebraic equations requires specification of boundary and initial conditions. Different types of equation (matrix) solvers are available each having their own pros and cons. It is essential to remember that the solution from these solvers is an approximation of the solution for the continuous partial differential equations. Additional procedures include computer coding and interfacing with other systems such as GIS. The procedure is illustrated in Figure 2-4.

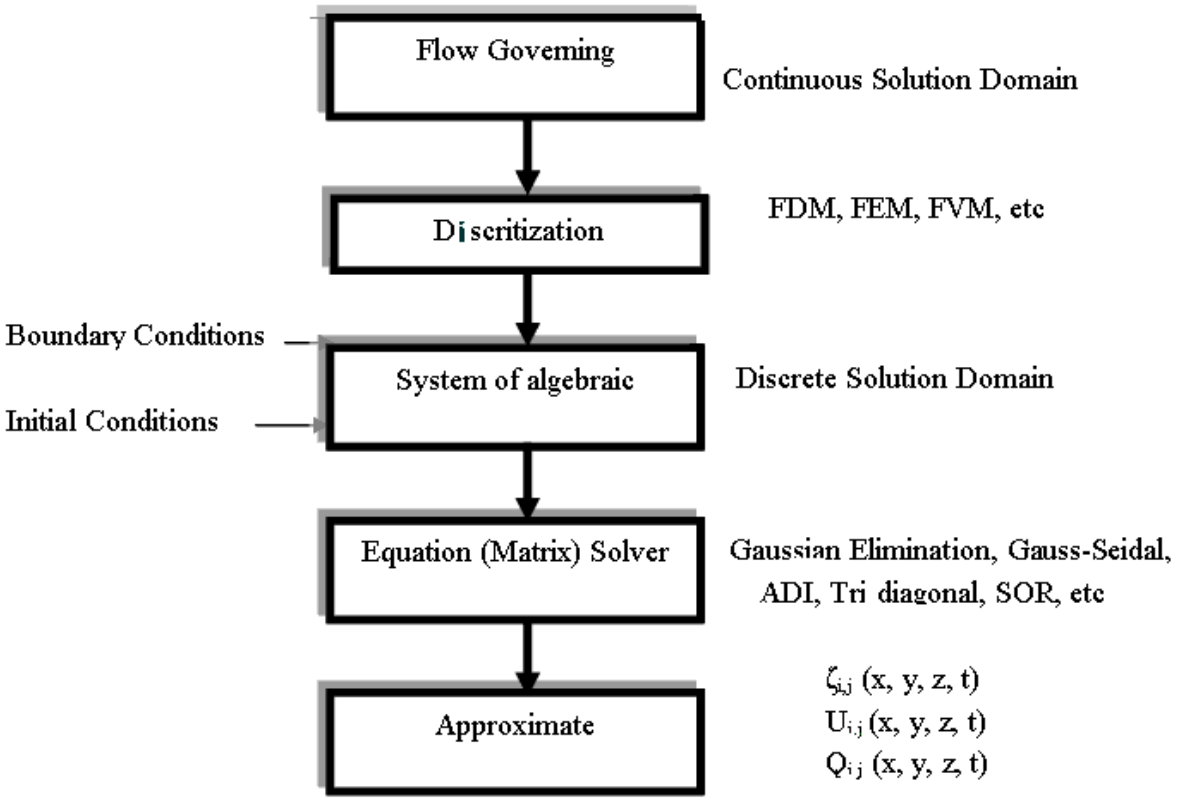

Figure 2-4: Typical computational procedures for a flood routing problem

Where ADI = Alternating Direction Implicit
SOR = Successive Over Relaxation
FDM = Finite Difference Method
FEM = Finite Element Method
FVM = Finite Volume method
$\zeta_{i,j}$ = Water level
$U_{i,j}$ = Velocity
$Q_{i,j}$ = Discharge

2.4.3. Solution domain discretization

The domain of the governing partial differential flow equations is continuous in space and time. Computational and data acquisition difficulties require us to replace this continuous domain by a

discrete domain. The scale of natural variation, the scale of the model approach, the chosen model domain and the sampling scale determine the degree of discretization. The commonly used spatial discretization methods include Finite Volume Method (FVM), Finite Difference method (FDM), and Finite Element Method (FEM). FVM has the advantage of capturing discontinuities. FEM discretizes the solution domain into a number of small subregions (i.e. finite elements) and requires approximating functions known as interpolation polynomials to represent the variation of the dependent variables over the elements. FDM is the most commonly used method and covers the domain including the boundary of the physical problem with a rectangular grid or mesh. The finite difference equations are applied at the calculation nodes. This replacement introduces an error in the solution of the problem which is proportional to the size of the grid cells. Figure 2-5 shows the solution domain and its discretization for a one dimensional flow problem. Figure 2-6 illustrates the loss of information in capturing the continuous space domain during data acquisition and transformation it to a model domain. It is a good illustration of how errors may accumulate from successive stages of DEM construction: data capture, data compilation, gridding and change of grid to model grid. In transferring the point data to generalized grid cells, some features with dimensions less than the internal grid cell spacing may be dropped out. Some of the commonly used flood models are listed in Table 2-1.

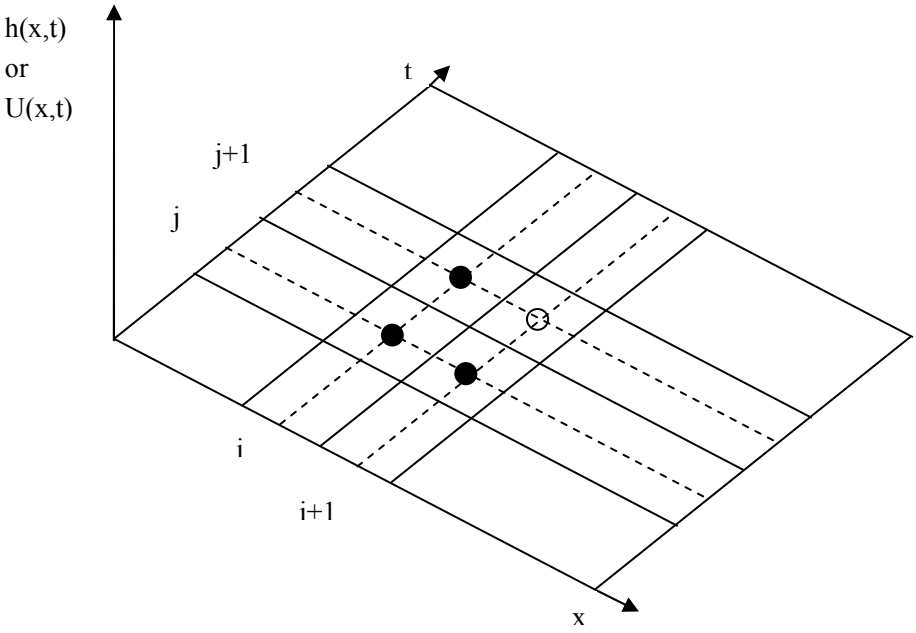

Figure 2-5: Descritization of the solution domain for a one dimensional flow problem

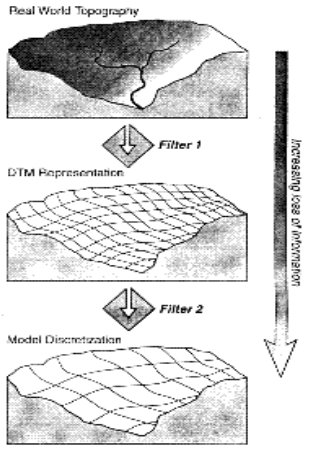

Figure 2-6: Loss of topographic information resulting from the filtering effect of DTM and model discretization (P.D. Bates 1996)

Table 2-1: ***Some of the widely used model approaches for flood inundation estimation***

Models	Dimensionality	Spatial Discretization	Comments
HEC-RAS	1D	Finite Difference	Has the capability to model sediment transport
FLDWAV	1D	Finite Difference	Has the capability to model sediment transport

Models	Dimensionality	Spatial Discretization	Comments
MIKE11	1D	Finite Difference	Has the capability to model sediment transport
MIKE21	2D	Finite Difference	Has the capability to model sediment transport
MIKE FLOOD	Coupled 1-& 2D	Finite Difference	Coupling of MIKE11 and MIKE21 Has the capability to model sediment transport
RMA2	2D	Finite element	
SOBEK	Coupled 1-&2D, 1D	Finite difference	Has Rainfall-Runoff, Water quality, and Sewer modules
TELEMAC-2D	2D	Finite element	
LISFLOOD-FP	Coupled 1-&2D		It is raster based Uses: Diffusive or kinematic wave for the channel Manning's equation for the floodplain

2.4.4. Model parameterization

The major inputs to a flood model include: surface roughness values, floodplain and channel topography, and initial and boundary conditions. The inputs are illustrated in figure 2-7. Roughness values mainly depend on the land cover conditions for the floodplain and on the type of bed materials, channel alignment and others for the channel system. Usually roughness values are defined based on tabulated values in hydraulics books. However, these values have often been obtained from laboratory estimates which had been performed under control conditions; hence, they may have some degree of empiricism. The second input, topographic data is mainly obtained from conventional surveying techniques, contour maps, and/or currently from other remote sensing sources such as LIDAR, ASTER, SPOT etc. Selection of the appropriate data source is mainly dictated by the characteristics of the system, required accuracy, and availability of data. The third input, initial conditions represent the hydraulic state of the system before the actual model simulation starts. It can be estimated by interpolation of the observations from available gauges, or simulated using models. Nevertheless, it is very difficult to specify representative estimate of the initial conditions before the main flood event. The other input to the model, the boundary condition, is commonly specified at the upstream and downstream ends of the system depending on the flow type.

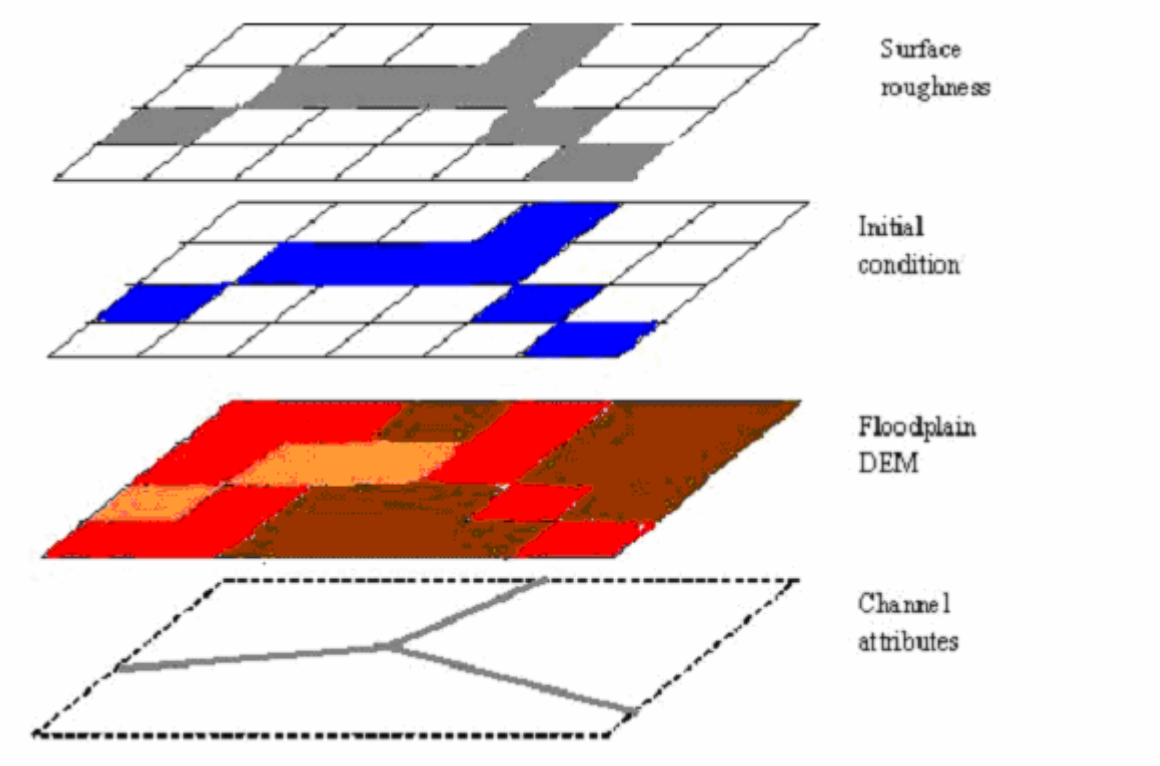

Figure 2-7: Main inputs for a hydrodynamic flood modeling

2.4.5. Boundary conditions

Flood modelling requires specification of the upstream and downstream boundary conditions. Downstream conditions might be specified as stage or discharge hydrograph, stage-discharge relationship, or hydraulic fall. Upstream boundary conditions are specified commonly as discharge hydrograph. When dealing with future events whose time or magnitude cannot be forecast, the peak of maximum discharge at the upstream location may be defined based on statements of probability or frequency with which a specified rate or volume of flow will be equalled or exceeded. From a practical point of view, the frequency analysis is only a procedure to fit the hydrologic data to a mathematical model of distribution (Chow 1964). These distributions are based on a number of assumptions which might not be satisfied in the real world. The analysis makes inferences from small observations, which are assumed to be random sample, the true population for the theoretical distribution considered. However, the observations represent a small subset of the many sets of physical conditions that could represent the population described by the theoretical probability distributions. Moreover, the variables might have interdependence due to their small size. Despite these limitations, it is a common practice to associate peak discharges with certain return period (the time period at which the peak discharges are expected to be equalled or exceeded at least once) as it is easier to present to the public and planners.

Chow (1959) expresses the magnitude X_T of a hydrologic event as

$$X_T = \overline{X} + \Delta X \qquad [2\text{-}1]$$

Where: X_T = the magnitude of a hydrologic event with a return period T

$\overline{X}$ = the mean of the variate

ΔX = the departure of the variate from the mean

The departure, ΔX, depends on the dispersion characteristics of X and on the recurrence interval T and other statistical parameters defining the distribution. The most popular methods of flood frequency analysis are the log-normal, Gumbel (extreme value type I), and log-Pearson type III distributions.

2.4.6. Sources of errors in flood modelling

As the use of hydrodynamic models matures, other modelling challenges are emerging. There is now a great concern by modellers and users to the reliability of these models. Differences between recorded data and simulated model output arise basically from four sources of errors:

i. Random or systematic errors in the input data (ε_i) ; for example, precipitation
ii. Random or systematic errors in the recorded data (ε_r); for example, river water levels
iii. Errors due to non-optimal parameter values (ε_{no})
iv. Errors due to an incomplete or biased model structures (ε_s)
v. Errors due to discretization of the model domain (ε_d)
vi. Errors due to rounding off (ε_{ro})

Thus the total error (ε_t) is

$$\varepsilon_t = \varepsilon_i + \varepsilon_r + \varepsilon_{no} + \varepsilon_s + \varepsilon_d + \varepsilon_{ro} \qquad [2\text{-}2]$$

Where: $\varepsilon_t = V_{obs} - V_{sim}$

V_{obs} = observed value

V_{sim} = simulated value

Note: the errors could be either positive or negative

In using a discrete model, the characteristics of the system are often assumed to be homogeneous within each element of the model domain. In reality, system characteristics vary even within smaller areas than the sizes of these discrete elements. Limitations in the available measurement techniques to provide measurements at any point of the simulation domain make defining an 'optimum' set of parameters, which results in an acceptable difference between model output and expected results, difficult and almost impossible. For instance, it is not easy to measure surface roughness values, topographic attributes, and other inputs in a spatially 'continuous' manner with the current measurement technique. This fact and the limitation of computational techniques and facilities to make computations in temporally continuous approach compel us to replace the model domain by a number of discrete units as illustrated in section 2.4.3. Difficulties in defining optimum parameter sets also lead to the concept of equifinality of parameter sets (and models). This concept states different parameter sets or model approaches could result in an equally acceptable model out put.

The difference between the exact solution of the governing partial differential equation and the exact solution of the difference equation used to approximate the partial differential equation is the discretization error. Its magnitude depends on the size of space and time steps used, and on the number of finite differences in the truncated serious employed to approximate the derivatives. The

discretization error can be reduced by decreasing the space and time steps; however, this is limited by computational time and memory. If the selected values are too small, the computations are inefficient, sometimes to the extent of making the application too expensive or time consuming and therefore infeasible; however if the values are too large, the resulting truncation (discretization) error can cause significant errors in the computed discharges and corresponding water surface elevations; and the errors may be so large as to make the computations unrealistic. Unrealistic solutions can cause the computer program to abort when computed elevations result in negative depths; also, unrealistic solutions can result in significant irregularities (spurious spikes) in the computed hydrographs (Fread). In addition to errors in the discretization, there are also errors in rounding off.

It is not sufficient to understand only the sources of model errors. There is also a need to

- Understand how these errors propagate
- Develop models of quantifying some of these errors
- Present expected magnitude of errors to model users
- Define the confidence interval for model results when decision has to be made based on these results

2.4.7. Flood model calibration, and sensitivity analysis

It is shown in section 2.4.5 that there are several sources of errors which introduce deviations between simulated and observed (expected) values. Therefore it is difficult to obtain the closest agreement between model simulations and field observations without going through a calibration stage. The traditional model calibration procedure deals about finding the most 'optimal' set of parameters which results in an acceptable difference between model output and expected results. Thus, it only treats the error listed in (iii) in section 2.4.5. For flood models, surface roughness values are usually selected as the calibrating parameter. The values of the calibrating parameter(es) are changed manually or automatically until a fixed calibration target has been met. The success of the model calibration can be evaluated visually comparing model results and observed values and/or using one or more accuracy criteria (or objective functions). Examples of these types of objective functions are the Nash-Sutcliffe model efficiency parameter, and root mean squared error.

$$RMSE = \frac{1}{n}\sum_{i=1}^{n}(V_{Obs(i)} - V_{Sim(i)})^2 \qquad [2\text{-}3]$$

Where: n = total number of observations

$V_{obs(i)}$ and $V_{sim(i)}$ are the observed and simulated variables. For flood modelling the flow depth could be used for such a purpose.

Complexities of river hydraulics make the setting of objective criteria for hydrodynamic models difficult. Hence, the models performance acceptability depends also on the study objectives, the reliability of field data and the sensitivity of model outputs. Sensitivity analysis is often performed by changing the values of one or more parameter or input data at a time. The purpose of this is to determine which parameter (or other inputs) has a dominant effect on the outputs for the selected model approach, and understand the reliability of the model. Hydrodynamics models are sensitive to DEM resolution, surface roughness, initial and boundary conditions, and/or numerical parameters.

After the calibration stage, the model must also be tested for its reliability using the calibrated parameters for a recorded event independent of that used for calibration. If it gives acceptable outputs for independent data set then it can be said that it is verified for other conditions in the study area. However, (Aronica et al 1998) describe the reason for loses of credibility of the traditional approach of obtaining an 'optimal' parameter sets as: same or very similar values of the objective function for different parameter sets (non-uniqueness of the solution of the inverse problem), or different inflow series (for different flood events) can give a different goodness of fit (agreement between observed and simulated values) for the same parameter set, or an equivalence of parameter sets, where different parameter sets and therefore model structures might provide equally acceptable simulators of the system.

"The presentation of models as software is becoming increasingly sophisticated, with links to geographical information systems and the display of impressive-three dimensional graphical outputs. It is easy to be seduced by these displays into thinking that the output of the model is a good simulation of the real catchment response, especially if few data are available to check on the predictions. However, even for the most sophisticated models currently available, this is not necessary so, and evaluation of the model predictions will be necessary."

Beven (2000)

The generalized likelihood uncertainty estimator (GLUE) approach, introduced by (Beven et al. 1992), transforms the problem of searching for optimum parameter set into a search for the sets of parameter values, which would give reliable simulations for a wide range of inflow series. The approach was not applied for this study due to the time limitations and the initial objectives of the study. Nevertheless, it has been found necessary to mention the steps, for the sake of completeness, as stated in (Beven et al. 1992):

i. Formulate the objective function that measures the performance in terms of modelling the behaviour of the system. This function should reflect the purpose of application.
ii. Select for each parameter considered a prior distribution. When other information is lacking a uniform distribution between appropriate bounds can be used.
iii. Use Monte Carlo simulation to draw random parameter sets and evaluate performance of the model for each. The likelihood that a set is a good simulator of the system is determined as a function of model performance.
iv. Select a likelihood value below which the model can be considered non-behavioural and remove all simulations with a likelihood below this threshold. Likelihood values of the remaining parameter sets are normalized between zero and one.
v. Construct an experimental distribution function of the model outcome by weighing with the likelihood. From the distribution function thus derived, prediction limits for the desired uncertainty bounds are easily derived by interpolation.

3. Study area, objective and research questions

3.1. Study area description

Tegucigalpa is the capital city of Honduras. It is located at about 15°06'N latitude and 87°11'W longitude. The city has an average altitude of about 1000m above mean sea level. January and February are the coolest months with mean maximum of 24°C, while March and April are the hottest featuring mean maximum around 29°C. The average minimum temperature values vary from 14°C in "winter time" to 18°C in spring. The dry season lasts from November till April. The rainy season normally begins in May/ June. It continues to November/December, often interrupted in August/September by a three- to six-week dry period.

Figure 3-1: Study area

In an area of Tegucigalpa, known as La Bolsa, Río Guacerique flows from the west and meets with Río Grande, flowing from the south, to become Río Choluteca. About 1 kilometer (km) north of this confluence, Río Chiquito flows into Río Choluteca. Figure 3-2 shows the river channel and floodplains of Río Choluteca, beginning about 2.7 km downstream of the Puente El Chile bridge and extending upstream to the confluence of Río Grande and Río Guacerique; from the mouth of Río Chiquito upstream 1.36 km; from the mouth of Río Guacerique upstream 1.27 km; and from the mouth of Río Grande upstream 4.80 km. The over bank areas of the channels are city streets and buildings in most areas. The flood simulation was performed starting near the location of the stadium below the junction of Rio Guacerique and Rio Grande.

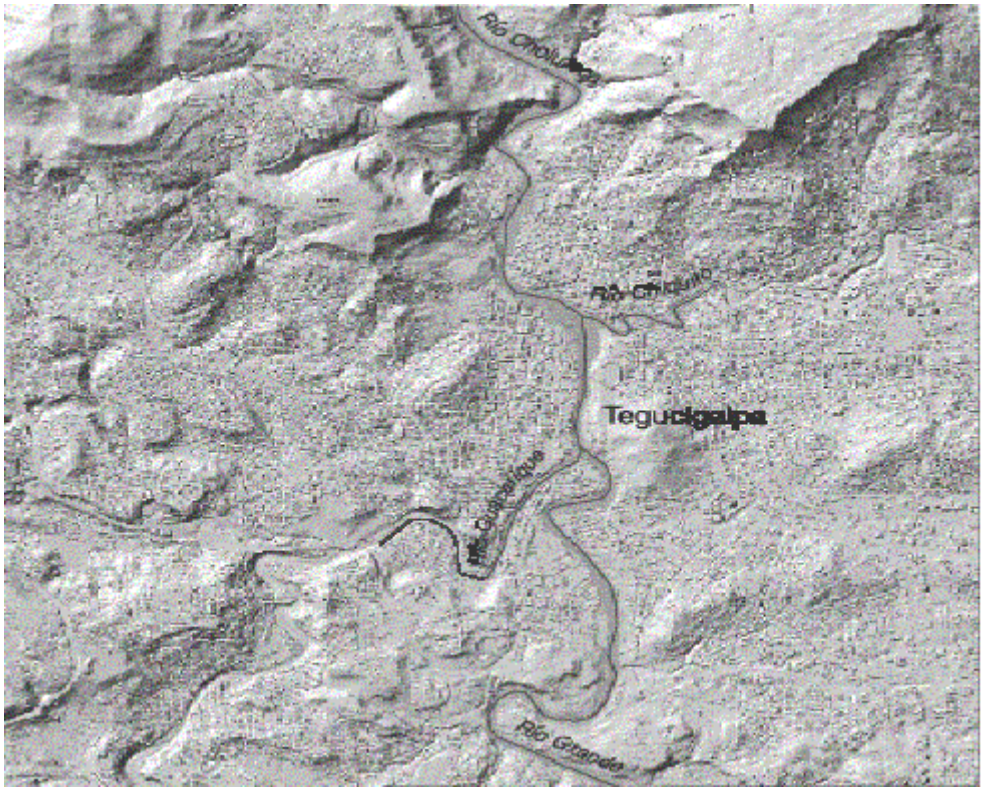

Figure 3-2: Schematic of the river passing through the city Tegucigalpa.

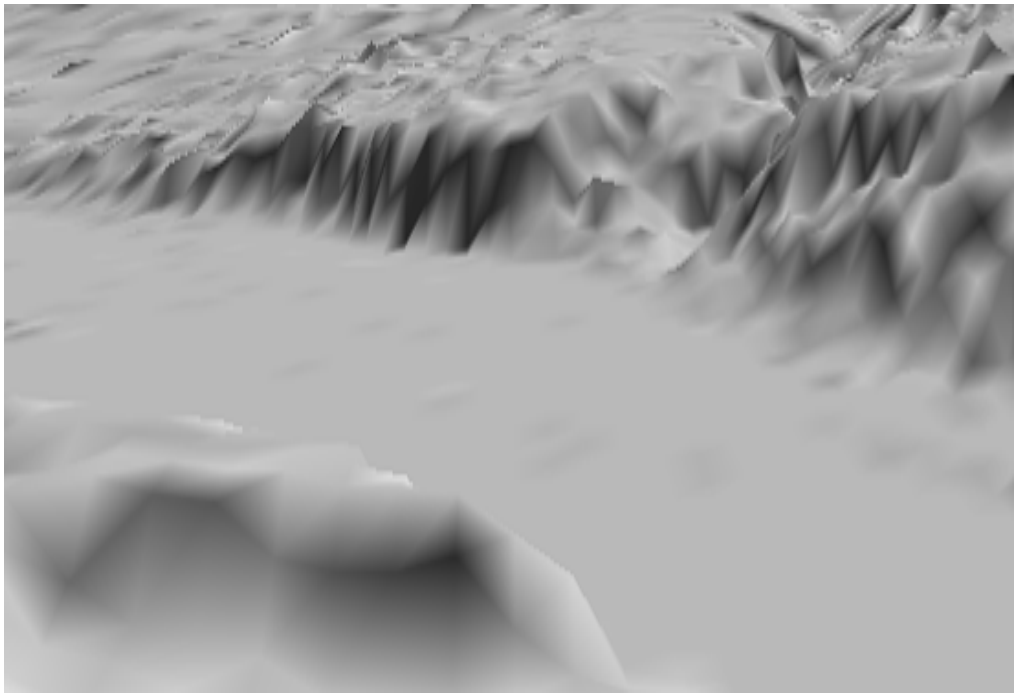

Figure 3-3: Channel condition at the junction of Rio Choluteca and Rio Chiquito as obtained from the LIDAR DEM

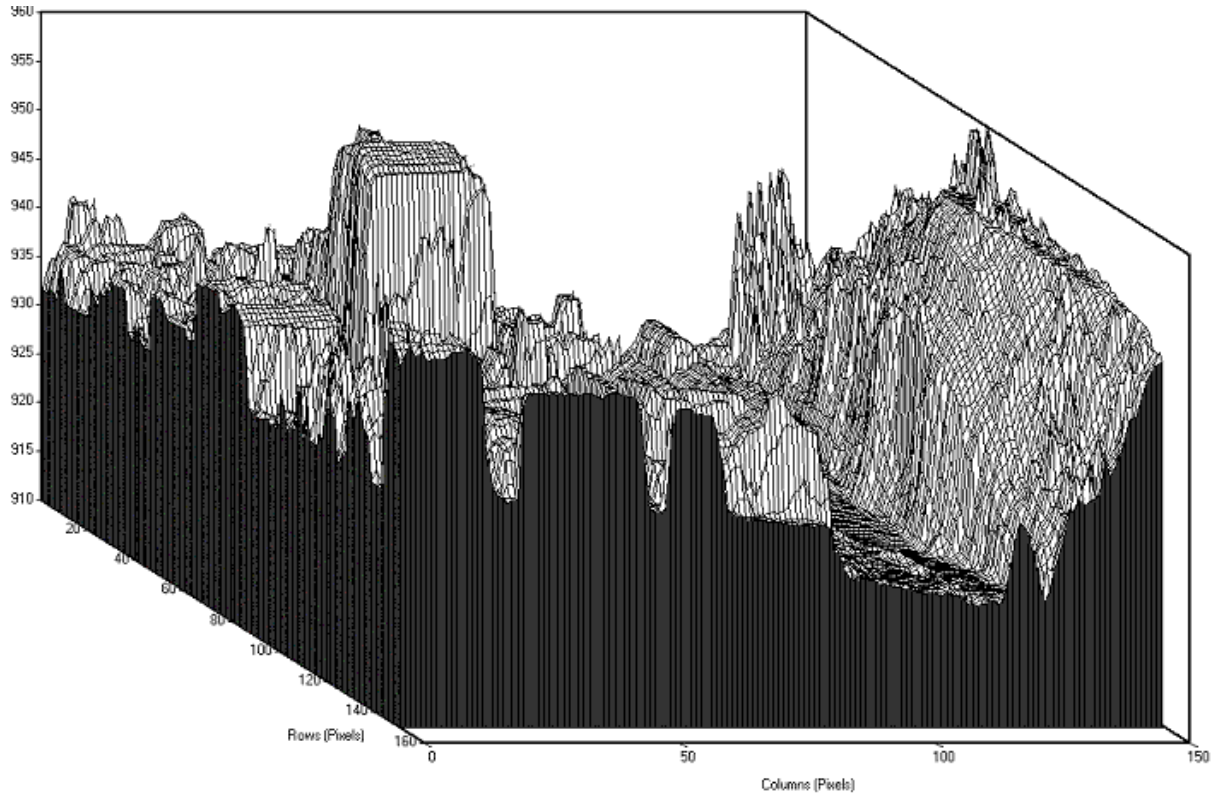

Figure 3-4: 3-D view of the floodplain of Rio Choluteca near the stadium (Note: the unit is meter)

Figure 3-2, Figure 3-3 and Figure 3-4 help in understanding how complex the hydraulic characteristics of a flood in the study area is due to several heterogeneities.

3.2. Problem description

In late October 1998 hurricane Mitch hit Central America. It is considered the strongest hurricane in the entire Atlantic basin for the past fifteen years and the worst natural disaster in Honduras in the last 200 years. More than 9,000 people died and 1.5 million people have lost their properties. Confirmed by official authorities the economic loss is about 3.7 billions US$, which equals approximately 70% of the annual gross national product. At least 70% of the national crop has been destroyed, including 80% of bananas, the main export product. The capital city Tegucigalpa also was severely affected by flooding and landslides.

Phrases, which nowadays are always the headlines of everyday news, such as the ‘worst flood in a half a century’ and ‘the worst flood in living memory’ indicate the devastating problem of floods is exacerbated. Their associated human and economical loss means that we have to take pre and post disaster measures in floodplain areas. Sound decision in these areas is in need of data and information. The major tool in this regard is use of hydrodynamic models. Its main problem in the past was low speed of computational facilities to solve the full governing flow equations and lack of input data especially topographic information. Currently, this problem is getting better with the advent of high-speed computers and improvements in topographic data acquisition techniques. However, other problems mainly associated to the modelling approach remain unsolved. To mention some of them, flood studies imply extrapolation of model parameters and boundary data to situations that have never been recorded. This raises the question of the reliability of current procedures of model calibration.

Other uncertainties of flood simulation modelling could arise from the difficulty to select the appropriate digital elevation model (DEM) resolution and representative boundary conditions. (Kate Marks et al 2000) broadly divided the problems in floodplain modelling into two: those concerning the methodological approach inherent in the modelling procedure (such as representation of wetting and drying processes, turbulence representation and the numerical solvers used) and those that result from inadequate data provision, particularly of topographic data.

Previously, flood inundation modelling has been constrained by the low spatial resolution of available topographic data sources. The current advances in airborne topographic data acquisition such as LIDAR have a positive bearing for the development of our predictive capability in the floodplains. However, to reduce simulation time and for other reasons, the input digital terrain model (DTM) for flood models need to be at a smaller resolution than that obtained from LIDAR and this might result in loss of important details such as roads. In relation to urban feature representation in the DTM, it was observed that continuous overland flow along roads cannot be represented in the model (in this case SOBEK) if the road width is less than $\sqrt{2}$ (Pixel resolution) (Tennakoon 2004). Thus, it is necessary to check whether important details are not lost while transferring high resolution DTM to model DTM.

3.3. Previous studies

After the 1998 Hurricane Mitch event, the USGS prepared a flood inundation map with a recurrence interval of 50 years at fifteen municipalities of Honduras including Tegucigalpa. The 50 year flood is estimated based on a national flood frequency analysis based approach for mean precipitation and catchment area. The flood simulation was done with steady state module of HEC-RAS 1-D flood model, a distributed event based model approach.

In Tegucigalpa, the Japan International Cooperation Agency (JICA) has conducted a concurrent project on flood control and has made estimates of the 50-year flood discharge on the Río Choluteca river system. They used a storage function approach to estimate runoff that was calibrated to the Hurricane Mitch peak flow (827 m^3/s) at Concepción Dam on the Río Grande with a drainage area of 139.5 km^2 and precipitation recorded at Toncontín Airport in Tegucigalpa. A transient flow-routing model was used to route flows estimated with the storage function approach for the sub basins through the stream network. Estimated 2-day maximum precipitation with a 50-year recurrence interval for the Toncontín precipitation record, distributed hourly using the pattern of observed precipitation during Hurricane Mitch, is input to their model that estimates the 50-year flood discharge of 2,600 m^3/s at Río Choluteca at the downstream end of Tegucigalpa, where 922 m^3/s was estimated by the regression method.(USGS 2002), (Note: the 922 m^3/s was estimated by the USGS based on the national flood frequency analysis for 50 year recurrence interval).

In the USGS study, most of the selected municipalities are not located near a long-term stream station. For these ungauged stations, they performed a regression analysis to obtain a relation between peak flows (50 year recurrence interval flood discharges) and drainage area and annual precipitation. This approach assumes the heterogeneity of the catchment to be accounted for by the regression coefficients. The relations may not be valid for streams in urban areas unless the effects of urbanization are insignificant as the hillslope hydrology is quite different from the floodplain

hydrology. On the other hand, the approach followed by JICA uses an estimated 2-day maximum precipitation with a 50-year return period. The estimates from the two approaches for the 50-year flood resulted in a difference of about 1678 m^3/s for the downstream end of Tegucigalpa indicating the larger uncertainty associated with using different methods. This implies the need for a further study to identify the reason for such discrepancies and getting a 'reliable' estimate of the 50-year discharge.

3.4. Objectives and research question

Research objectives:

- Obtain the area and depth of flood inundation in the municipality of Tegucigalpa using high-resolution topographic data and coupled 1- and 2-D hydrodynamic flood model.
- To investigate model reliability and uncertainty where model performance is tested for various model inputs as obtained through geo-processing and earth observation

In such approach, important research questions are:

- How to transform a high resolution DTM to a model DTM without losing information relevant for flood modelling?

- How to parameterize land surface roughness values?

- How does the grid resolution of a DEM affect the flood characteristics as simulated by a 2-D flood model approach?

- How can buildings be represented in hydrodynamic flood models: as solid objects, hollow objects or partially solid objects with large bed friction values? Does the type of representation employed affect the result significantly?

- Does the use of 1D model result in a significant change in flood characteristics as compared to a 2D simulation?

4. Materials and methods

One- and two dimensional hydrodynamic model approaches were used to simulate the flow characteristics of flood events with different return periods (50 and 100 years), for part of the Tegucigalpa city. With respect to data availability and purpose of the study, triangular discharge hydrographs were specified as upstream boundary conditions, and hydraulic free fall was allowed at the downstream end. LIDAR data and an ortho-photo were used to derive floodplain DEM, channel cross-sections, surface friction roughness values and buildings as inputs for the modelling purpose. The sensitivity of the model approaches for changes in inputs was also evaluated.

One of the main factors to be considered cautiously in hydrologic and hydrodynamic modelling is the assumptions and simplifications formulated. These assumptions are most of the time not respected in the complex and heterogeneous 'real world' and determine the degree to which we can mimic the 'real conditions'. The assumptions and simplifications inherent to SOBEK and HECRAS include:

- Constant water density
- A horizontal water surface is assumed for channel and floodplain transversally
- Exchange of momentum between channel and floodplain is neglected
- Discharge is distributed between floodplain and channel according to their conveyance (HECRAS only)
- The effect of friction is computed using a uniform flow equation
- The friction slope terms are replaced by an equivalent force (HECRAS only)
- Pressure is assumed to have a hydrostatic distribution
- The vertical acceleration is negligible
- The channel is not very steep
- No consideration for turbulent stress
- Rigid channel bed
- Long flood wave

The major software packages used for the study include GIS packages: ARCVIEW/GIS, ILWIS, ERDAS, HECGEORAS (an ARCVIEW extension), and Hydrodynamic flood models: HECRAS (1D) and SOBEK (coupled 1-and 2D) flood models.

4.1. SOBEK coupled one-and two-dimensional model approach

The coupled 1-and-2D raster based SOBEK flow modelling system, developed by WL/Delft hydraulics, integrates the SOBEK 1D (channel flow) module with the two dimensional (2D) raster based hydrodynamic prediction package known as Delft-FLS (Delft flooding system). In SOBEK 1- and 2-D, it is assumed that 1D and 2D networks are two independent map layers, with the 2D network map layer overlaying a 1D network. The computational code determines the connection between the 1D and 2D layers based on the map coordinates for the centre of the 2D grid cell and the 1D

connection node/calculation node. The water flow characteristics are computed by solving the complete Saint Venant equation. (Refer SOBEK online help www.sobek.nl).

For the 1D channel flow, the continuity equation is

$$\frac{\partial A_w}{\partial t} + \frac{\partial Q}{\partial x} = q_{lat} \qquad [4.1]$$

Where A_w = Wetted area [m^2]
q_{lat} = Lateral discharge per unit length [m^2/s]
Q = Discharge [m^3/s]
t = Time [s]
x = Distance [m]

The momentum equation for the 1D approach is

$$\frac{\partial Q}{\partial t} + \frac{\partial (Q^2 / A_w)}{\partial x} + gA_w \frac{\partial h}{\partial x} + \frac{gQ|Q|}{C^2 R A_w} - \frac{W_f \tau_{wi}}{\rho_w} = 0 \qquad [4.2]$$

Where : g = Gravitational acceleration (=9.81) [m/s^2]
h = Water level (with respect to the reference level) [m]
C = Chézy coefficient [$m^{½}/s$]
R = Hydraulic radius [m]
W_f = Flow width [m]
τ_{wi} = Wind shear stress [N/m^2]
ρw = Water density, normally 1000. [kg/m^3]

The first term describes local acceleration; the second term represents the convection acceleration; the third term stands for the water level gradient; the fourth term is for the bed friction, and the fifth term represents the wind friction.

The flow for the overland flow (in two dimensions) module is described by three equations: the continuity equation, the momentum equation for the x-direction and the momentum equation for the y-direction. The continuity equation is given as

$$\frac{\partial \zeta}{\partial t} + \frac{\partial (uh)}{\partial x} + \frac{\partial (vh)}{\partial y} = 0 \qquad [4.3]$$

Where: u = velocity in x-direction [m/s]
v = velocity in y-direction [m/s]
$V = (u^2+v^2)^{0.5}$; velocity
ζ = water level above plane of reference [m]
h = total water depth: ζ+d [m]
d = depth below plane of reference [m]

For the overland flow, two momentum equations are calculated, together with the continuity equation in 2D. The 2D equations in SOBEK do not incorporate the turbulent stress terms, accounting for the sub grid transfer of momentum between grid cells. The momentum equations in the two directions are:

$$\frac{\partial u}{\partial t} + u\frac{\partial u}{\partial x} + v\frac{\partial u}{\partial y} + g\frac{\partial \zeta}{\partial x} + \frac{gu|V|}{C^2 h} + au|u| = 0 \qquad [4.4]$$

$$\frac{\partial v}{\partial t} + u\frac{\partial v}{\partial x} + v\frac{\partial v}{\partial y} + g\frac{\partial \zeta}{\partial y} + \frac{gv|V|}{C^2 h} + av|v| = 0 \qquad [4.5]$$

Where: The terms are as define above.

The terms in the momentum equation represent the physical processes that govern the flow momentum. The local acceleration term describes the change in momentum due to the change in velocity over time, the convective acceleration term expresses the change in momentum due to the change in velocity along the channel, the fourth term represents the transport of momentum caused by a difference in pressure, and the fifth term which is the friction force term created by the shear stress along the bottom and sides of the channel is proportional to the friction slope. The local and convective acceleration terms represent the effect of inertial forces on the flow. The effect of wind becomes more important for large bodies of water and when the flood duration is large (in the order of days or weeks).

In SOBEK 1-and-2D, floodplain cell water depths are updated in response to flow from the channel, which depends only on the relative water surface elevations. (M.S. Horritt et al 2002) mentioned that in such an approach, only mass transfer between channel and floodplain is represented and it neglects effects such as channel-floodplain momentum transfer and the effects of advection and secondary circulation on mass transfer; however, it is the simplest approach to the coupling problem and should reproduce some of the behaviour of the 'real system'. The criteria for the connection between the 1D network and 2D grid cells is

$$\text{If } ((|X1 - X2| \le DX/2) and (|Y1 - Y2| \le DY/2)) \qquad [4.6]$$

Where: X1 = x map coordinate for 1D point
X2 = x map coordinate for 2D grid cell
Y1 = y map coordinate for 1D point
Y2 = y map coordinate for 2D grid cell
DX = width of grid cell in X direction
DY = width of grid cell in Y direction (DX and DY are equal)

Then the 1D point is assumed to lie completely within the 2D grid cell.

The connection between the 2D cells and the 1D network is in such a way that the centre of 1D node is internally moved to match with the centre of 2D grid cell, without changing the length of the connecting 1D branches. The 2D grid cell is counted as part of 1D node. The flow in 1D channel below the 2D grid level is treated as 1D flow, while the flow above the 2D grid level is treated as 2D flow with the area of 2D grid cell.

The interaction between the 1D and the 2D part takes place via mutual volumes and is described (Dhondia and stelling. www.sobek.nl) as follows:

$$\frac{dV_{i,j}(\zeta)}{dt} + \Delta y((uh)_{i,j} - (uh)_{i-1,j}) + \Delta x((vh)_{i,j} - (vh)_{i,j-1}) + \sum_{l=k_{i,j}^{1}}^{l=k_{i,j}^{L_{i,j}}} (Q_n)_l = 0 \qquad [4.7]$$

where: V = combined 1-and 2D volume;
u = velocity in x direction
v = velocity in y direction
h = total water height above 2D bottom;
ζ = water level above plane of reference (the same for 1D and 2D);
Δx = 2D grid cell size in x (or i) direction;
Δy = 2D grid cell size in y (or j) direction;
Q_n = discharge in the direction normal to the mass volume faces;
i,j,l,k,L = integer numbers for nodal point numbering (refer Figure 4-2).

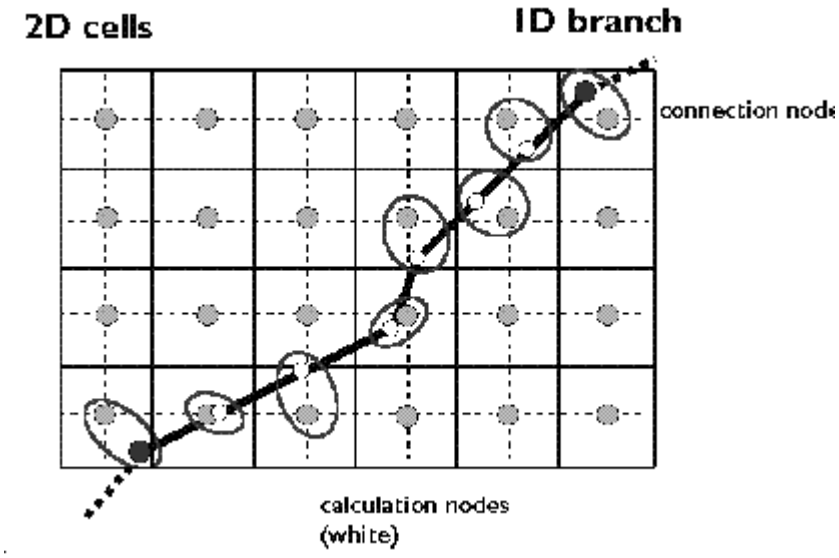

Figure 4-1: Connections between 1D and 2D layers (www.sobek.nl)

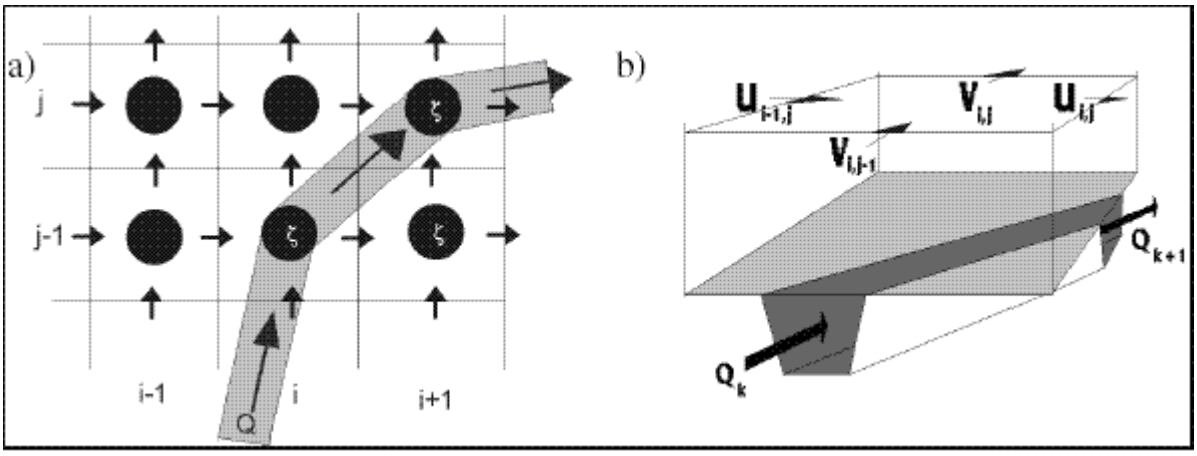

Figure 4-2: Schematization of the hydraulic model: a) combined 1-and 2D-staggered grid; b) combined finite mass volume for 1-and 2D computations. (www.sobek.nl)

The 1-and 2D coupled module of SOBEK is designed for conditions where channel width is narrower than the size of the grid cells. Use of wider channel than the grid cell results in more conveyance locally. Figure 4-3 illustrates the two conditions.

The overland flow module of SOBEK assumes flow to take place from a given grid cell only to one of its four neighbours. This is illustrated in Figure 4-4. In SOBEK, water depths are specified at the centre of each cell, and velocities are defined perpendicular to the edges of each cell. Thus, the spatial discretization makes use of a staggered grid structure.

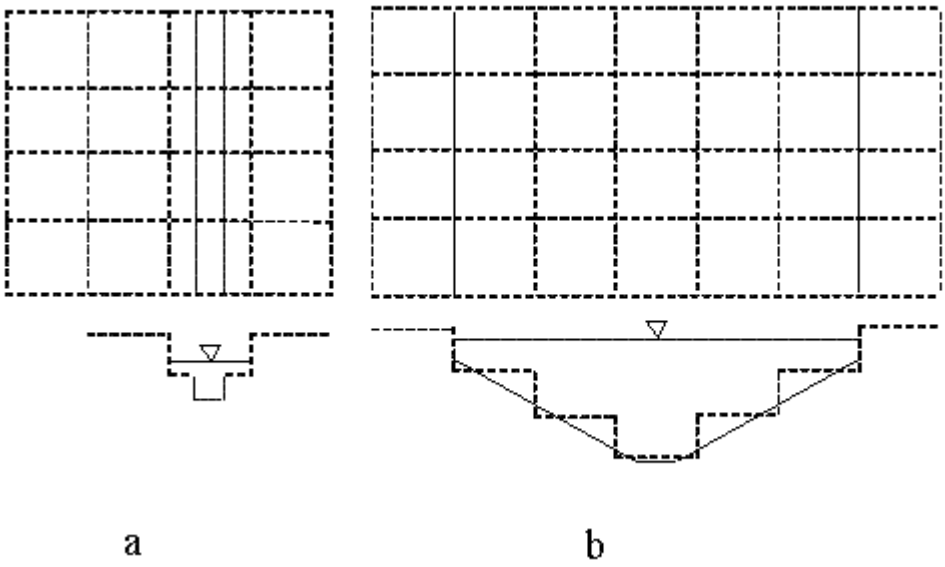

Figure 4-3: Illustration of cases when grid cell size is (a) larger than channel width, and (b) smaller than channel width. NB: broken lines refer to 2D grid elements and solid lines represent the channel.

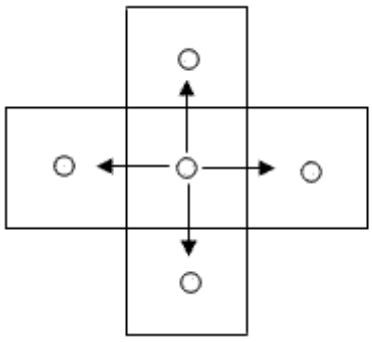

Figure 4-4: Possible flow directions from a grid cell to neighbouring cells in SOBEK.

4.2. Sobek calculation procedure

The calculation procedure for SOBEK 1- and 2D coupled model is explained in (Goorden 2004). For the overland flow, the velocity at future time is written in the form of equation (4.8) based on the momentum equation:

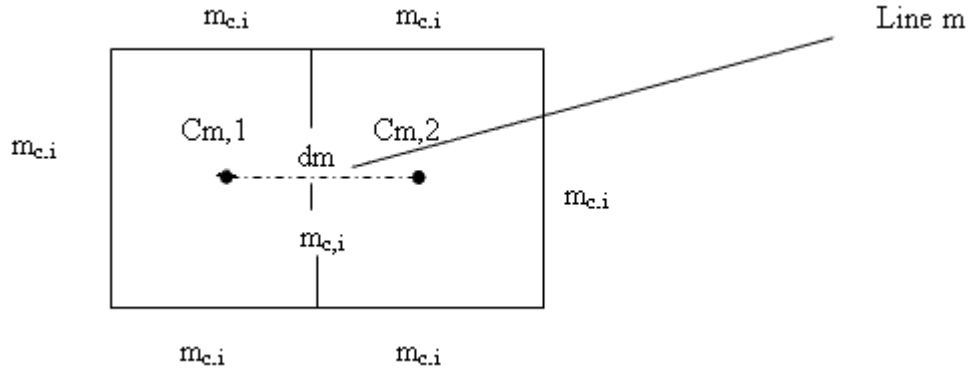

Figure 4-5: 2D grid cell overland flow model

$$u_m^{t+1} = u_m^t + \Delta t\left\{ g\frac{\theta(\zeta_{Cm,1}^{t+1} - \zeta_{Cm,2}^{t+1})}{dm} + g\frac{(1-\theta)(\zeta_{Cm,1}^{t} - \zeta_{Cm,2}^{t})}{dm} + Adv(u^t) + (1-\theta)\frac{g.u_m^t\left|u_m^t\right|}{C^2(\zeta_m^t - b_m)} + \theta\frac{g.u_m^{t+1}\left|u_m^t\right|}{C^2(\zeta_m^t - b_m)}\right\}$$

[4.8]

Where:

Adv = The discretisation of the advection which depends on a few neighbouring velocities

C = Chezy's coefficient

$m_{c,i}$ = Reference to the edges that form the boundary of the cell

ζ_m = Water surface level above some reference level at m

$\zeta_{cm,1}$ = Water surface level above some reference level at Cm,1

dm = Distance between the neighbouring cell centres

Cm,1 and Cm,2 = Centre of cells which are to the right and left from edge m

u_m = Velocity orthogonal to the edge

The direction Cm,1 to Cm,2 is taken positive: $u_m = \vec{u}.n_m$

b_m = Bottom level (above reference level) of line m

The norm of u_m is calculated by

$$\left|u_m\right| = \sqrt{u_m^2 + v_m^2} \qquad [4.9]$$

v_m = Velocity parallel to the edges $m_{c,i}$

The integration scheme in time is based on the θ method

The model uses a fractional time step method to solve the momentum balance. In the first fractional time step the advection is calculated and then the friction term and the pressure gradient of the momentum are calculated in the second fractional time step. Substituting the velocity from the first fractional time step in the discretized momentum balance results in equation (4.10).

$$u_m^{t+1} = u_m^t + \Delta t\{g\frac{\theta(\zeta_{Cm,1}^{t+1} - \zeta_{Cm,2}^{t+1})}{dm} + g\frac{(1-\theta)(\zeta_{Cm,1}^{t} - \zeta_{Cm,2}^{t})}{dm} + \frac{g.u_m^{t+1}\left|u_m^t\right|}{C^2(\zeta_m^t - b_m)}\} \qquad [4.10]$$

Where: u_m^t is calculated in advection

The velocity in the future time, which is expressed in equation 4.10 is rewritten in SOBEK with the coefficients r(u) and f(u):

$$u_m^{t+1} = r(u)_{(m)} + f(u)_{(m)} \cdot (\zeta_{(Cm,1)}^{t+1} - \zeta_{(Cm,2)}^{t+1}) \quad [4.11]$$

Where:

$$\mathrm{r(u)_{(m)}} = \left(\frac{1}{\Delta t} - \frac{g|u_m^t|}{(\zeta_m^t - b_m)C^2} \right)^{-1} \left(\frac{u_m^t}{\Delta t} + (1-\theta)\frac{g}{dm}(\zeta_{(Cm,1)}^t - \zeta_{(Cm,2)}^t) \right) \quad [4.12]$$

$$\mathrm{f(u)_{(m)}} = \left(\frac{1}{\Delta t} - \frac{g|u_m^t|}{(\zeta_m^t - b_m)C^2 \Delta t} \right)^{-1} \theta . \frac{g}{dm} \quad [4.13]$$

Where: $(\zeta_m^t - b_m)$ = water depth at line m is taken from the outflow cell

The velocity expressed in terms of the velocity coefficients f(u) and r(u) is substituted in the mass balance. SOBEK calculates the wetted cross-section in an explicit way. After substituting the terms for the velocity, the mass balance equation results in a linear equation for the water levels in each cell. This is rewritten in a matrix form:

$$\mathrm{A} \begin{pmatrix} \zeta_1^{t+1} \\ \zeta_2^{t+1} \\ \cdot \\ \cdot \\ \zeta_n^{t+1} \end{pmatrix} = \mathrm{b}$$

In SOBEK, the above linear system of equations is calculated by use of an iterative method, called the conjugate gradient.

4.3. HECRAS calculation procedure

In HECRAS, the total discharge is distributed to the channel and the floodplain according to their conveyance. Thus, the combined 1-dimensional equations for both the floodplain and the channel are written as:

$$\frac{\partial A}{\partial t} + \frac{\partial(\Phi Q)}{\partial x_c} + \frac{\partial[(1-\Phi)Q]}{\partial x_f} = 0 \quad [4.14]$$

$$\frac{\partial Q}{\partial t} + \frac{\partial(\Phi^2 Q^2 / A_c)}{\partial x_c} + \frac{\partial[(1-\Phi)^2 Q^2 / A_f]}{\partial x_f} + gA_c[\frac{\partial Z}{\partial x_c} + S_{fc}] + gA_f[\frac{\partial Z}{x_f} + S_{ff}] = 0 \quad [4.15]$$

The equations (4.14) and (4.15) can be rewritten in an implicit finite difference form by incorporating storage term (S) and average lateral inflow ($\overline{q_l}$) in equations (4.16) and (4.17)

$$\Delta Q + \frac{\Delta A_c}{\Delta t}\Delta x_c + \frac{\Delta A_f}{\Delta t}\Delta x_f + \frac{\Delta S}{\Delta t}\Delta x_f - \overline{q_l} = 0 \quad [4.16]$$

$$\frac{\Delta(Q_c \Delta x_c + Q_f \Delta x_f)}{\Delta t \Delta x_e} + \Delta(\beta V Q) + g\overline{A}\left(\frac{\Delta Z}{\Delta x_e} + \overline{S_f}\right) = 0 \qquad [4.17]$$

Where: V = Velocity (m^3/sec)

Δx_e= Equivalent flow path (used to replace the friction force term from the banks by using an equivalent force with a single friction slope for the entire cross section).

$$\Phi = \frac{K_c}{(K_c + K_f)} \qquad [4.18]$$

K_c = Channel conveyance

K_f = Floodplain conveyance

Equation (4.18) assumes the friction slope for both the channel and floodplain to be the same but in actual case the situation is different. Moreover, an equal channel and floodplain water level (Z) has been used in the momentum equation. This implies presence of a horizontal water surface for the channel and left and right floodplains.

HECRAS solves the flood routing problem by transforming first the finite difference form of the equation in to linear system of algebraic equations. For a single channel without a storage area, the coefficient matrix has a banded structure. However, sparse terms enter and leave at the boundary locations and at the storage areas. The coefficient matrix is stored using a skyline storage algorithm, and a modified Gauss elimination algorithm with seven pointers was developed. The pointers eliminate the meaningless operations on zero elements. The whole procedure is explained in HECRAS technical manual.

4.3.1. Mixed flow regime in HECRAS

HECRAS uses the specific force (SF) equation to determine which flow regime is controlling, as well as locating any hydraulic jumps.

$$SF = \frac{Q^2 \beta}{g A_m} + A_t \overline{y} \qquad [4.20]$$

Where: A_m = Flow area in which there is motion

A_t = Total flow area

For steady state mixed flow regime calculations, if the downstream boundary condition is supercritical, the program calculates a subcritical flow profile assuming a critical state at that location. If the specific force for the supercritical state of the user specified upstream boundary condition is greater than the specific force of the previously computed subcritical water surface at this location, the program starts calculating a supercritical flow profile at this section. If the condition is vice versa, the program begins calculating supercritical profile calculation downstream of the location where it defaulted to a critical depth in the previous run. When it reaches a cross section with a valid subcritical and supercritical answer, the one with a greater specific force is considered to be the correct solution. If the subcritical answer has a greater specific force, the program assumes that a hydraulic jump occurred between that section and a previous cross section. The program then goes to the next downstream location that has a critical depth answer and continuous the process.

Most 1D model approaches have an algorithm written for a subcritical flow state. When a mixed flow (subcritical, supercritical, hydraulic jump and drawdown) regime is encountered in unsteady flow, then the solution becomes complicated. The derivatives in the governing equations become very large and cause oscillations as the flow passes through critical state. These oscillations can grow large enough to cause the program unstable. The models use some kind of approximation when a supercritical flow is attained in the solution domain. For a supercritical flow, MIKE11 reduces the value of β to account for supercritical flow as per the Froude number of the flow. Thus, the model results will be less accurate with increasing Froude number. Limitations of this procedure are: the results for supercritical flow conditions overestimated water levels and delayed peaks (Kutija 1993; Kutija and Hewett 2002), and additional calculations must be performed in order to obtain the Froude number for every discretization point at every point at every time step as the reduction coefficient for the convective momentum term has to be calculated on the basis of the local Froude number (Kutija 2002).

In order to solve the stability problem in a mixed flow regime, HECRAS applies a reduction factor to the two inertia terms in the momentum equation as the Froude number goes towards 1.0. This procedure is proposed by Fread et al.(www.nws.noaa.gov). The modified momentum equation is

$$\sigma\left[\frac{\partial Q}{\partial t}+\frac{\partial\left(\frac{\beta Q^2}{A}\right)}{\partial x}\right]+gA\left(\frac{\partial h}{\partial x}+S_f+S_e\right)=0 \qquad [4.21]$$

Where: $\sigma = F_T - F_r^m$ $(F_r \le F_T;\ m \ge 1)$

$\sigma = 0$ $(F_r > F_T)$

σ = Local Partial inertia factor

F_T = Froude number threshold at which factor is set to zero. It ranges from 1.0 to 2.0.

F_r = Froude number.

m = an exponent which changes shape of the curve. This exponent can range between 1 and 128. Smaller values of m tend to stabilize the solution in some cases while larger values of m provide more accuracy.

4.4. Data requirements, processing and preparation

The data requirements for floodplain modelling can be categorized into: Data input for analysis, calibration and verification. The analysis part mainly requires geometric information (channel cross section area and floodplain DEM), bed friction coefficients, boundary and initial conditions. The calibration and verification stages require independent observed flow characteristics: inundation area, flow discharge, depth and velocity.

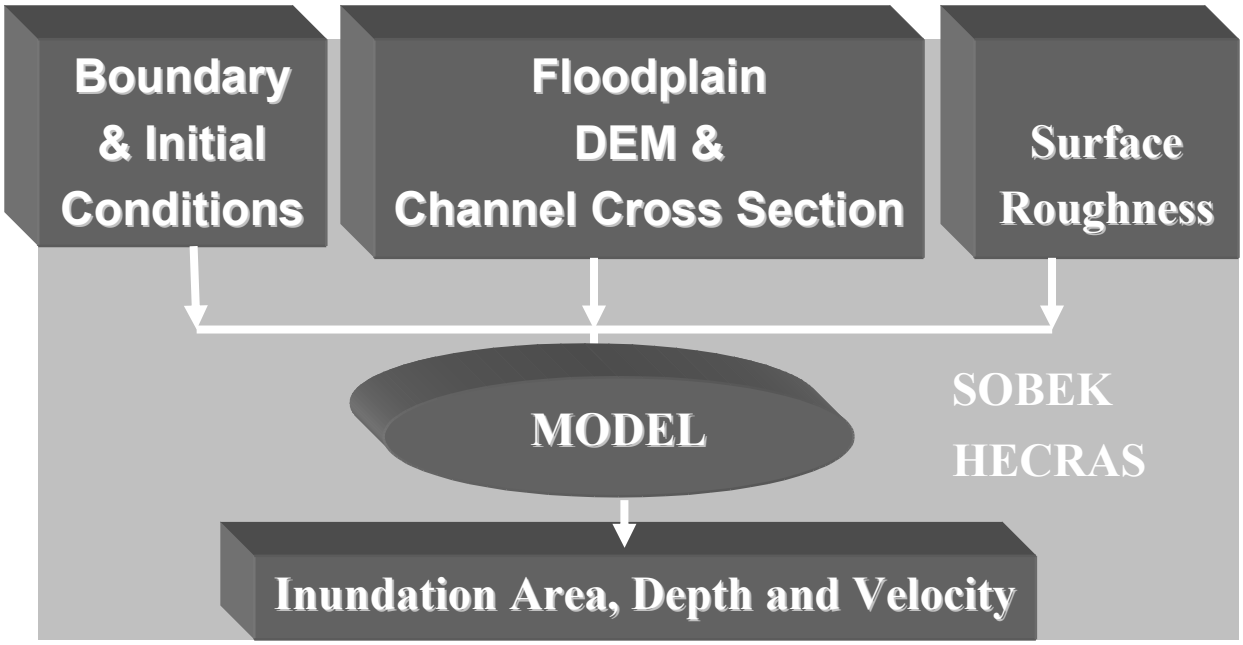

Figure 4-6: Floodplain modelling inputs and outputs

4.4.1. Geometric Information

Topographic information for fifteen municipalities of Honduras was gathered during February and March 2000 using an airborne Light detection and ranging (LIDAR) system to create a high resolution DEM of each site (USGS 2002). Statistical comparison of elevation differences between GPS ground surveys and the LIDAR airborne surveys gave a mean difference of -0.134 m and a standard deviation of 0.097m (USGS 2002).

The classical problem in LIDAR post processing is how to separate ground hits from surface object hits on vegetation or buildings. Laser pulses reflect on the ground as well as on buildings, trees, cars, and other objects. The LIDAR raw data is in the form of elevation values for mass points and need to be interpolated and resampled to grids to obtain elevation of grid elements. Bed elevations for the 1D model were taken from the LIDAR derived cross sections.

The methodology usually employed to detect the bare earth is based on a series of filters and mathematical operations on the data. The most essential of these are: 1) a majority filter that helps to screen out anomalous or spurious data; 2) a local filter that is effective at screening out tall and moderate sized buildings; 3) a median filter that is particularly effective at screening out short to medium height buildings; 4) a slope filter that is designed to eliminate topographic changes associated with objects such as buildings and trees protruding from the ground; 5) a variance filter that focuses on eliminating large clusters of buildings; and 6) an eucladean allocation operation that creates a surface from the areas identified as most likely to be associated with ground height (Huyck et al. 2002).

5	5	4	3	2
5	9	3	2	1
5	4	3	3	2
4	3	3	3	3
3	3	3	3	0

a

5	3	2	1	1
4	3	2	1	1
3	3	2	1	1
3	3	3	0	0
3	3	3	0	0

b

Figure 4-7: Results of the minimum filter: a) Data before filtering; b) Data after filtering (Huyck et al. 2002).

For extracting buildings, a rank (minimum) filter was used. Subtracting the filtered map from the original DEM resulted in candidate points for buildings' footprints. Figure 4-7 illustrates how the minimum filter works. A map of buildings for part of the city, which was edited latter by comparing it with the LIDAR DEM and the orthophoto of the area, was obtained after digitizing these candidate points. This task required some trial and error procedure and the final result was compared by overlaying it over an orthophoto of the study area. Finally, the elevation values under the buildings were estimated by interpolation. The bridges were also removed in a similar manner. The candidate buildings footprints and the extracted buildings for part of the study area are shown in Figure 4-8 and Figure 4-9

The LIDAR data acquisition was performed during low flow seasons when the rivers water depth can be assumed negligible compared to the water depth during high flows. Based on this assumption, cross sections at selected points in the channel network were extracted from the LIDAR DEM using HECGEORAS package, which is an ARCVIEW extension. As the software makes calculation based on the TIN structure of the DEM, its computational time depends on the Z-tolerance. Use of smaller Z-tolerance values; for example, less than one results in excessive computational time. Thus, a larger Z-tolerance was used and the cross sections were edited based on raster based cross sections as obtained using ERDAS.

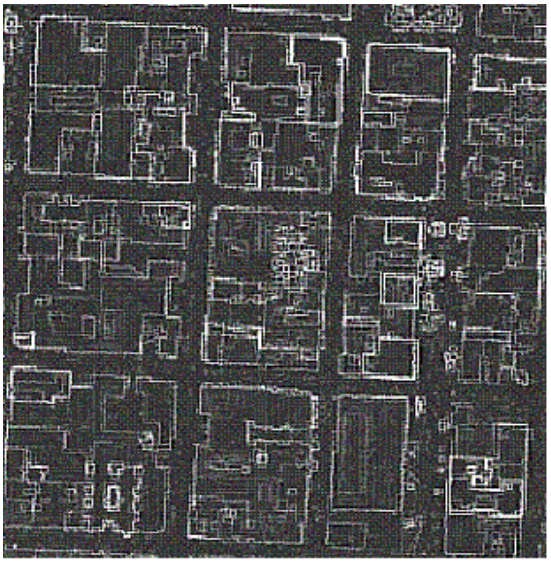

Figure 4-8: Candidate building footprints

Figure 4-9: Buildings extracted from the LIDAR DEM overlaid over an orthophoto of the city.

4.4.2. Comparison of DEM resampling methods

The benefit of comparing the DEM resampling methods is of two fold: to investigate which method is more appropriate and to verify whether there is a significant increase in accuracy with increasing resolution. Such a comparison is expected to give an answer only for the study area. The latter helps to answer, partly, the question: whether the use of a high resolution DEM is justifiable or not. In addition, it helps to investigate the loss of information in changing the original resolution.

The three resampling methods compared were nearest neighbour, bilinear and bicubic. In case of the first, for each output cell, the value of input cell closest to it is used as output value. Bilinear interpolation uses the values of four surrounding cells of the input map to calculate an interpolated value for each pixel in the output map. Bicubic interpolation uses the values of sixteen surrounding cells of the input map to calculate interpolated value for each cell in the output map. Figure 4-11 shows the positions of the input and output cells for the three methods. In ILWIS, in reference to Figure 4-11, the output map in case of bilinear resampling is calculated by making two interpolations in the y direction and then one interpolation in the x direction. For the bicubic resampling, there are first four interpolations in the y-direction and then one interpolation in the x-direction by fitting a third order polynomial through each set of four known points.

For comparison purpose, a subset of the study area was chosen in such a way that it incorporates buildings, streets, and channel and channel banks. In total, nine surfaces were created using three resampling methods (nearest neighbour, bilinear and bicubic) and varying grid cell sizes (4.5m, 7.5m, and 10m). To assess the success of each method, the error at an arbitrary selected point was considered to be the difference between the elevation value at 1.5m grid cell and the resampled value for that location. The minimum and maximum error values, mean error, standard deviation and the root mean square error (RMSE) were also calculated in Comparison of DEM resampling methods in page 41 and Table 5-1.

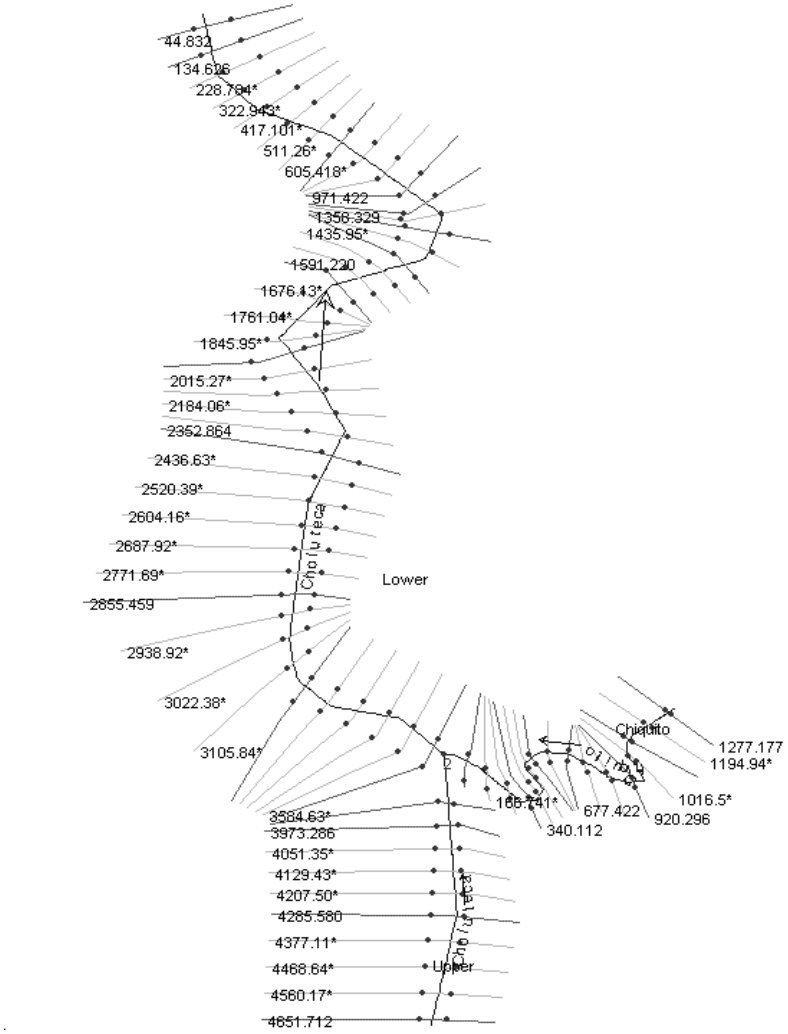

Figure 4-10: River cross-section cut lines as extracted from the LIDAR DEM.

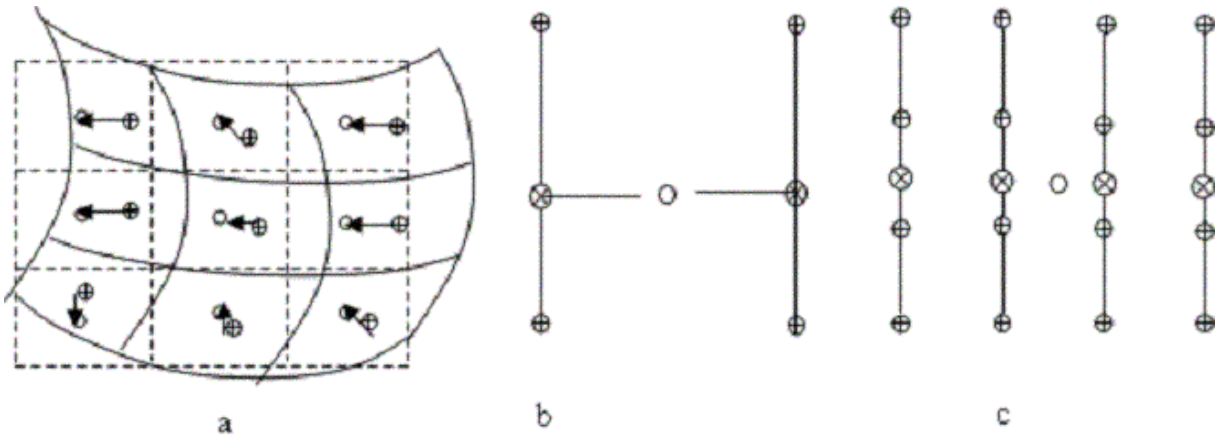

Figure 4-11: Position of input and output cells for a) Nearest neighbour, b) Bilinear, and c)Bicubic interpolation methods (is output pixel, is for input pixel, and is for interpolated value).

4.4.3. Bed friction coefficients

The bed friction is the friction between the flowing water and the channel bed exerting a force on the flowing water always in the direction opposite the water flow. Bed friction values depend on several factors including: surface roughness, presence of obstructions, channel alignment and irregularities,

etc. One of the methods to define these values in SOBEK is using the Manning's coefficient (n). Several reference books provide tabulated values for this coefficient and they can be referred to define the bed friction values for the study area based on floodplain and channel characteristics, which can be deduced from the aerial photographs, LIDAR data, buildings and road maps of the area. A GIS can be used to represent the spatial variation of these values and prepare input files for the modelling purpose. For the city of Tegucigalpa, the USGS estimated ranges of Manning's n values of 0.037 to 0.046 for the channels and 0.050 to 0.075 for the floodplain. Thus, values of 0.04 for the channel and 0.07 for the floodplain were used in this study. However, it has to be noted that model outputs could vary for different model structures but the same surface roughness values. In addition, buildings were represented in the model as solid objects, hollow objects or partially solid objects with large surface roughness values. For representation as partially solid objects, roughness values of 1 for buildings and 0.025 for areas without buildings were specified while for hollow object representation buildings were assumed to have the same surface roughness values as other features in the floodplain. The possible representations of buildings for flood modelling and the associated possible flow vectors are illustrated in Figure 4-12.

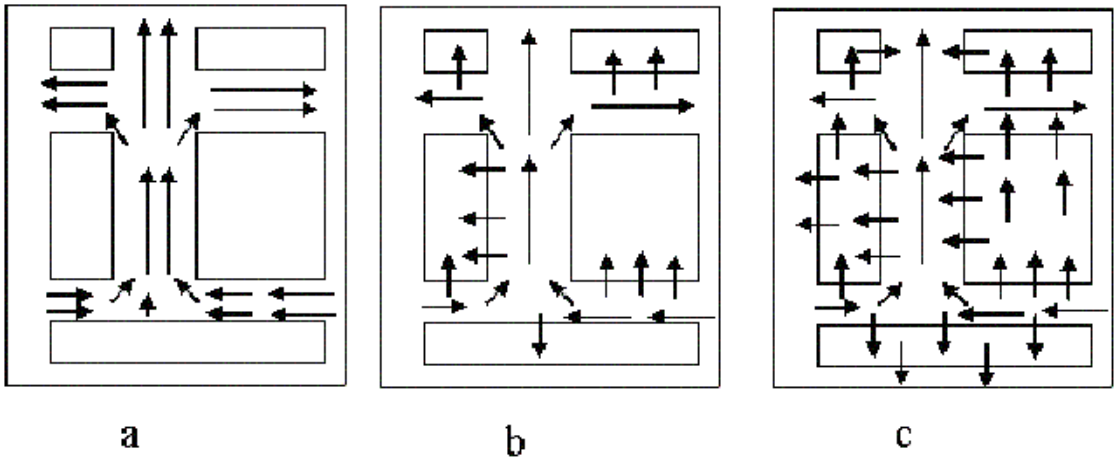

Figure 4-12: Flow vector when buildings are represented as a) solid objects, b) partially solid objects, and c) hollow objects

The sensitivity of the model (HECRAS) to bed friction has been presented in section 5.3. This was performed by specifying the possible parameter ranges, and randomly generating about thirty five couple of surface roughness values with in the specified range for both the floodplain and the channel. Thus a total of thirty five model runs were made for both the 50-year and 100-year return period floods.

4.4.4. Boundary conditions

Boundary conditions are used to define, in the model, the influence of external environment on the study area. For flood models these are commonly specified at the upstream and the downstream locations of the reach of interest. Lateral inflow (or out flow) data also constitutes a boundary condition. Mathematically, three types of boundary conditions can be identified: Dirichlet condition (specified head boundary), Neumann condition (specified flow boundary), and Cauchy condition (head-dependent flow boundary).

The available boundary conditions in SOBEK include water level, water depth, flow, and discharge-head relation. Here, a head-dependent (Cauchy) flow downstream boundary condition was specified. This condition is also called mixed boundary condition, as it relates boundary heads to boundary flows. It is dependent on the difference between a specified head, supplied by the user, on one side of the boundary and the model calculated head at the other side. The upstream boundary conditions were provided as flow hydrographs.

The effects of using different downstream boundary conditions and their extent of influence were investigated using the 1D hydrodynamic model HECRAS. This was performed only for the part of the river network which is downstream of the two streams junction. Different boundary conditions: normal depth, constant water levels and artificially steeper channel at the downstream end were specified and the extent of their effect to the upstream portion of the reach was investigated. For this purpose, an inflow of 12 hours, with a peak of 900 m^3/sec with a triangular distribution, was used. A steady state simulation was also performed using different downstream boundary conditions for upstream flows of 50, 200, 700, 800, and 900m^3/sec. The result is discussed in section 5.2. In this study, for the analysis part, a discharge hydrograph for the upstream of the channel and a hydraulic free fall for the downstream stretch of the river were adopted.

The USGS (USGS 2002) performed a flood frequency analysis for 34 stations in Honduras following the guidelines established by the U.S. Water Resources council. The stations Peak flows for exceedance probabilities of 0.5, 0.1, 0.04, 0.02, and 0.01 were estimated. A log-pearson type III distribution was fitted to the data for each station. This distribution uses a three parameter fit (mean, standard deviation and skew). The average of the station skews calculated for each set of station data with more than 20 years of record defined a generalized skew coefficient for Honduras (average = 0.166; standard error = 0.523). For the ungauged locations, a regression analysis was performed to obtain a relationship between the 50-year flood discharge and basin characteristics. In the area of Tegucigalpa municipality, there are two downstream gauging stations on the Rio Choluteca river at Tegucigalpa. Their weighted discharges, when adjusted by the drainage areas ratios, averaged about the study area's 50-year flood discharge by regression (USGS 2002). The 50-year flood discharges were estimated using the following regression equation:

$$Q_{50} = 0.0788(A)^{0.56664}(p)^{0.7693}$$

Where: Q_{50} = the 50-year flood discharge, in cubic meters per second (m^3/sec)
A = catchment area, in Km^2
P = mean annual precipitation over the basin, in mm

The 100 year floods are transferred to the study area from the downstream station based on drainage area ratio. For investigating the effect of DEM resolution, triangular hydrographs with 12 hours duration and peaks of 100-years return period were used at the upstream boundary conditions. However the 50- and 100-year flood characteristics such as flood depth, velocity and inundation area were simulated based on 24 hour hydrograph duration.

5. Results and discussion

5.1. Comparison of DEM resampling methods

The intention of DEM production processes is to produce DEM data sets that are accurate representations of slope as well as elevation of the 'real world' topography as much as possible. While resampling the high resolution DEM to a lower one, the size of the grid cells are different and there is no one to one relationship between values of the input and output elements. This means usually two or more input values are used to estimate the output value for each element. For this reason, resampling methods are used to decide on the new value of each cell. The commonly used methods are nearest neighbour, bilinear and bicubic resamplig methods. In the case of nearest neighbour method, as illustrated in Figure 5-1, there is a possibility of occurrence of more than one point at an equal distance to the output grid cell. In such a case the value assigned to the new cell depends on how the code is written. The bilinear method makes the DEM smoother than the nearest neighbour as it averages neighbouring values together. Bicubic method results in both sharpening and smoothing of the input map. The results of the comparison using these methods are presented in Table 5-1

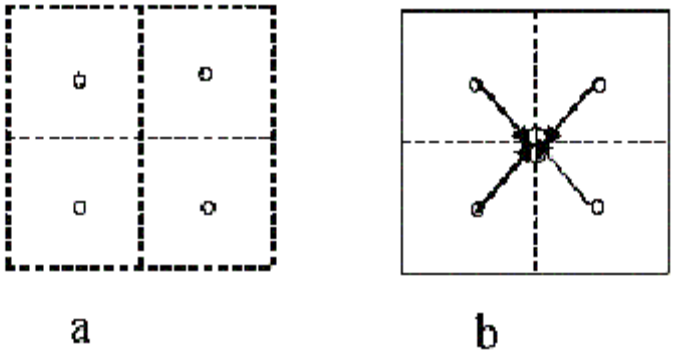

Figure 5-1: Occurrence of more than a single input cell at equal distance to the output cell for nearest neighbour resampling method: a) input grid b) output grid

For the low resolution DEM's (7.5m and 10m), Table 5-1 revealed remarkable differences between the resampling methods in terms of the magnitude of errors they introduced. For the 4.5 m grid cell size, all the methods resulted in nearly the same amount of error. The bicubic method exposed the fact that as the grid cell size increases the error increases. However, the other two methods resulted in the smallest error for the largest; i.e. 10 m grid cell. The bilinear method resulted in lower errors than the bicubic in two of the three cases. The same result was also obtained by Smith (Smith 2003). In all the methods, a significant amount of error was observed indicating the considerable loss of information in transferring high resolution DEM to a lower one. The largest error was introduced by the bicubic method.

Table 5-1: Results from the comparison of resampling method

Method	Grid cell size	Minimum error (m)	Maximum error (m)	Standard deviation (m)	RMSE (m)	Mean (m)
Nearest Neighbour	4.5	-3.01	24.31	3.1073	3.1385	0.561
	7.5	-16.75	22.97	3.5648	3.5448	0.131
	10	-13.58	13.57	2.8237	2.8119	-0.182
Bilinear	4.5	-3.01	24.31	3.1073	3.1385	0.561
	7.5	-14.07	22.16	3.2748	3.2571	0.137
	10	-12.47	13.22	2.7279	2.7144	-0.140
Bicubic	4.5	-3.01	24.31	3.1117	3.1384	0.536
	7.5	-15.42	23.59	3.4593	3.4429	0.192
	10	-29.96	13.19	14.3273	4.3239	-0.452

In addition to the magnitude, the spatial distribution of the error is also important from flood simulation point of view. A larger error is expected near river banks and edges of buildings. Figure 5-2 shows the spatial distribution of error for the bilinear resampling method using 7.5m grid cell. The figure clearly shows the error is larger at the edge of buildings and smaller for the channel. For a flood inundation mapping, error in slope as a result of the resampling procedure might also be important. This is addressed in section 5.6.

Figure 5-2: Spatial distribution of the error in elevation using a bilinear resampling.

5.2. Sensitivity to downstream boundary condition

A common practice for minimizing the effect of inappropriate downstream boundary conditions is to locate it far away from the area of interest. The sensitivity to downstream boundary conditions was investigated using the 1D model approach as use of the 2D model approach required a larger

computational time. Figure 5-3 shows the maximum water surface profiles for different types of downstream boundary conditions. The downstream boundary condition produced a significant effect on the maximum water surface profile only near the downstream end of the channel. Use of different cross section spacing (2m and 20m) resulted in different water surface profiles for the same type of boundary conditions (constant water levels at 904m and 904.5m, and artificially steeper channel). This could be because of a steeper profile near critical depth, which requires closer cross section spacing for a more accurate capture of the profile. Specifying a normal depth at a distance of 1500m downstream of the selected downstream boundary location resulted in a slightly different maximum water surface profile. For this purpose, there was no cross sectional data at far away from the selected site and thus the attributes of the last sub reach had to be extrapolated. The effect of using different boundary conditions disappeared at a distance of about one kilometre. Thus, it produced almost no effect on the area of interest for the study, which is at a distance of about 2 km upstream of the downstream boundary. One of the assumptions in using the governing flow an equations is the stream lines are parallel. However, specifying a supercritical flow depth resulted in curvature of the stream lines but it didn't propagate far upstream. The effect of downstream boundary condition also depends on the surface roughness values adopted for the channel and floodplain.

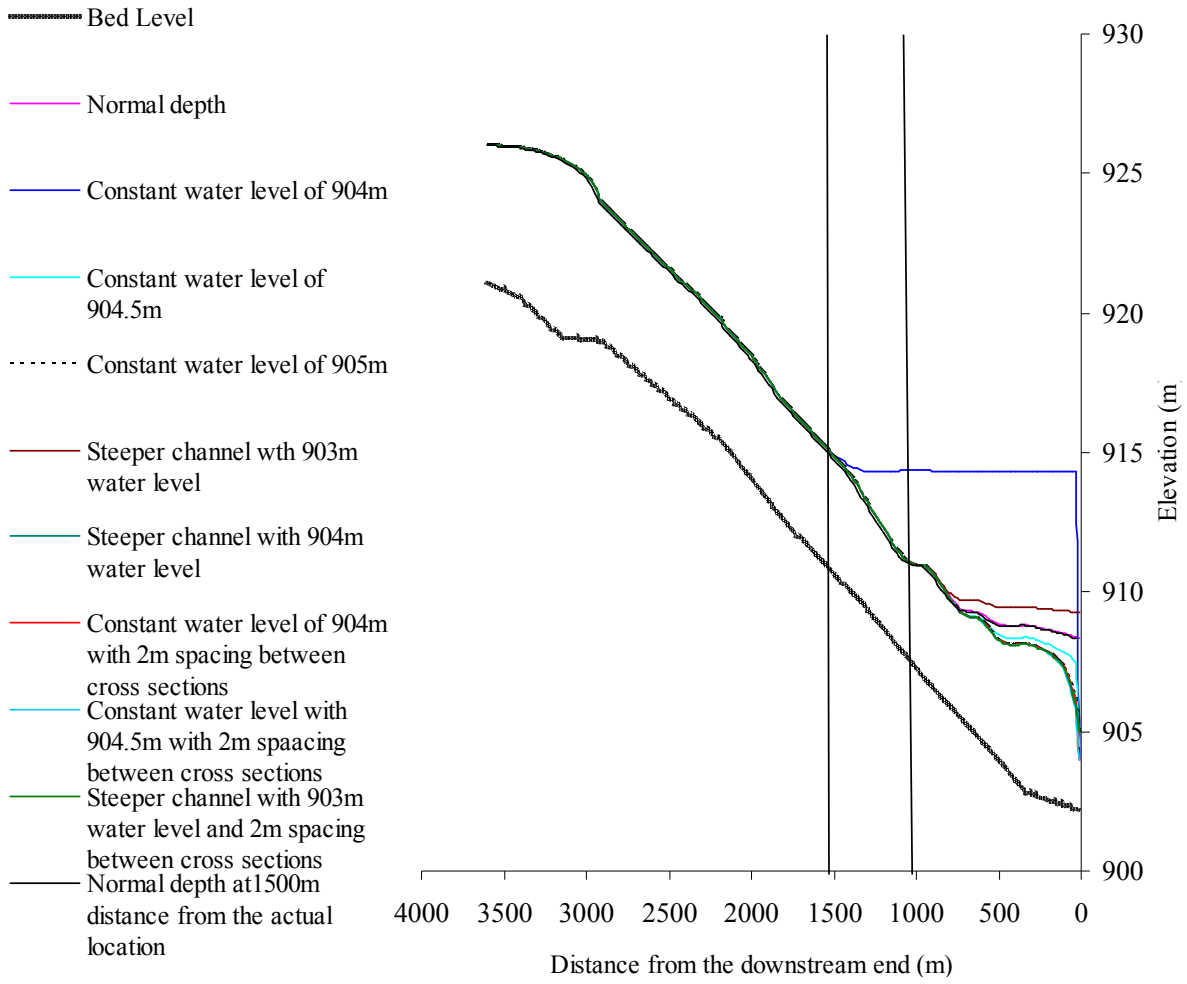

Figure 5-3: Maximum water surface profiles for different types of downstream boundary conditions using unsteady flow simulation.

As illustrated in Figure 5-4, specifying a normal depth resulted in a singular relationship between stage and discharge at that location and the loop effect was observed when the boundary condition was extended 1500 m downstream from the actual site.

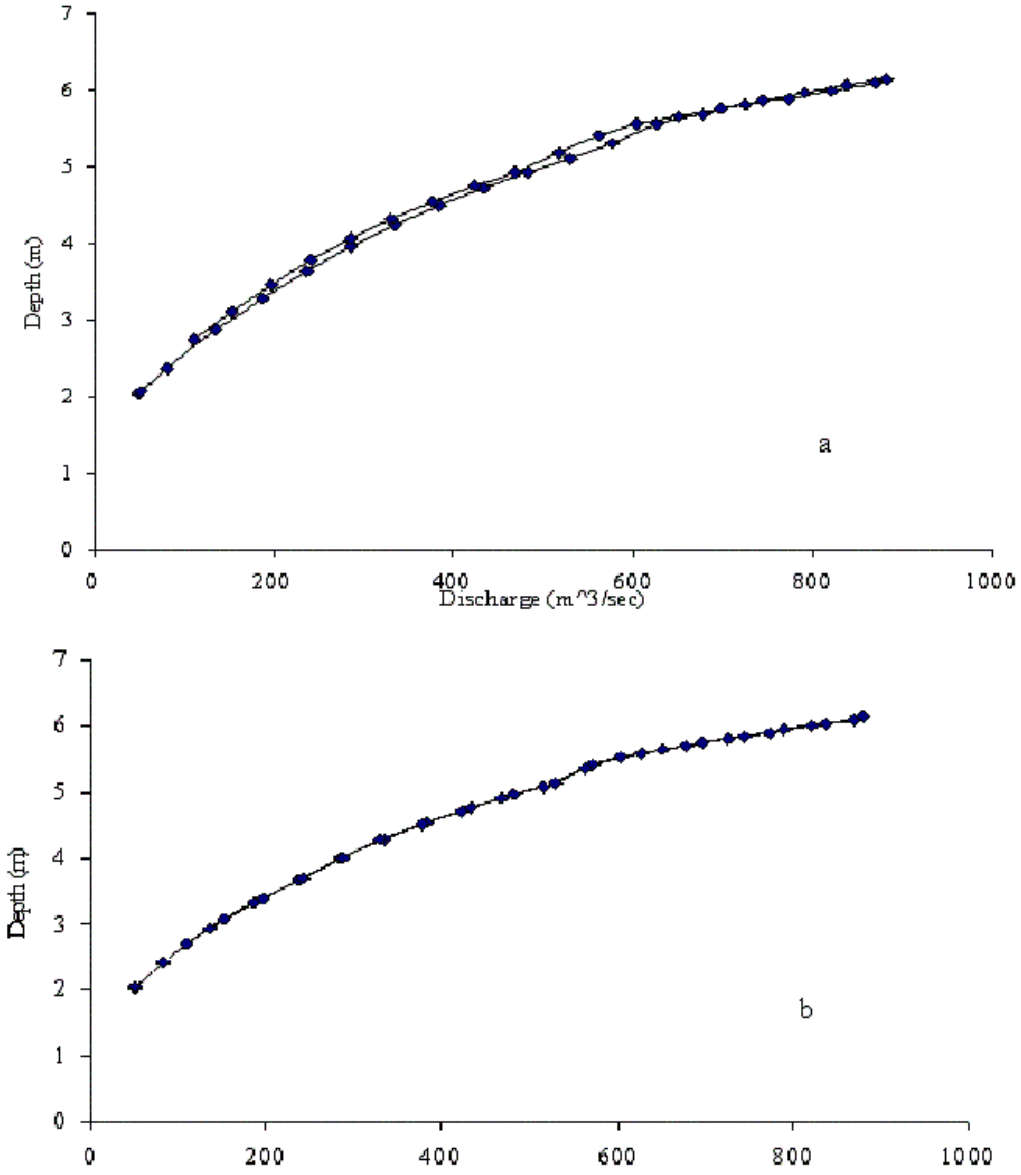

Figure 5-4: Rating curves at the selected downstream boundary condition location when downstream boundary condition is set a) at a distance of 1500m downstream of the selected location, and b) at the selected location as a normal depth.

The effect of downstream boundary condition was also investigated using a steady state simulation. The maximum water surface profiles for normal depth downstream boundary condition became the same as that for the other boundary condition types at an upstream distance. The locations of the same water level were occurred at distances of 600, 750, 850, 850, and 910m from the downstream end for discharges of 50, 200, 700, 800 and 900 m^3/sec respectively. This indicates that at lower discharges the specified upstream discharge controls most parts of the reach and the downstream boundary effect will have a larger extent as the flow increases.

5.3. Effects of hydrograph shape

The 'actual shape' of a discharge hydrograph for a certain catchment could be reproduced by the use of rainfall-runoff model approaches. However, since there was no sufficient data on hydrometric, climatic, and cacthment characteristics for the study area and also in consideration to the time constraint, the flood simulation is based on only peak flows as obtained from regional flood frequency analysis. Therefore, it was found necessary to see the effects of the shape of hydrographs on the flood characteristics. Three conditions were considered: normal distribution (bell shape), triangular distribution, and lognormal (skewed) distribution. For a given hydrograph duration, the main effect of different hydrograph shapes was obtained to be due to differences in volume of water, and distributions of discharge magnitudes over time. The maximum inundation area for the three cases is shown in Figure 5-5. Table 5-2 shows the flow characteristics for the three hydrograph shapes. It shows that there is no significant change in the bulk flow characteristics in response to the use of different hydrograph shapes. This should also be checked for conditions with equal volume of water but different hydrograph shapes.

Table 5-2: Flow characteristics for different types of hydrograph shape

Hydrograph shape	Inundated no. of cells	Inundation area (m^2)	Maximum depth (m)		Maximum velocity (m/s)		Normalized inundated area (%)
			Max	Mean	Max	Mean	
Triangular	27724	693100	9.583	3.99	17.772	2.12	99.22
Bell Shape	27943	698575	9.649	4.03	13.092	2.06	100.00
Skewed	27804	695100	9.615	4.03	12.957	2.08	99.50

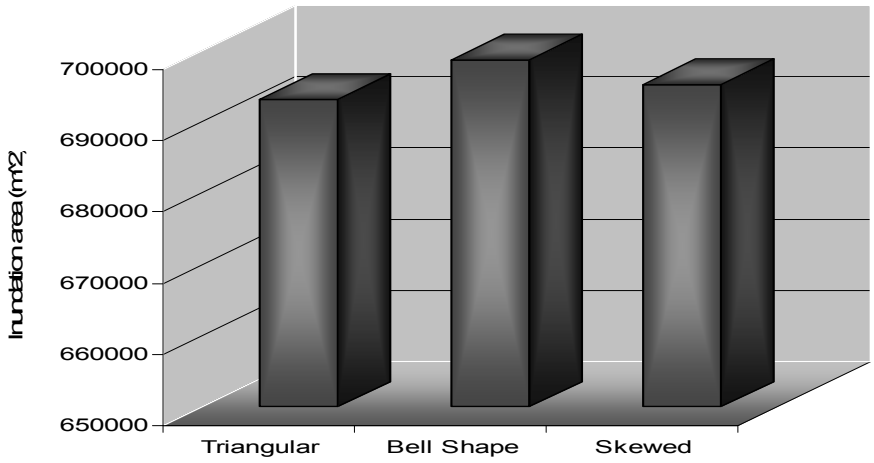

Figure 5-5: The maximum inundation area for the triangular, skewed and bell shaped hydrographs.

5.4. Sensitivity to surface roughness coefficient

Surface roughness values are usually used in a hydrodynamic modelling as calibrating parameters. However, any data on previous flood characteristics for this study area was not available. Therefore, it was found necessary to investigate the model's sensitivity to this parameter. Figure 5-6 shows the surface roughness response surface of the model approach for 50-year and 100-year floods. This was

performed using the 1D hydrodynamic model approach HECRAS. The inundation area was normalized to the maximum simulated inundation area. The figure clearly indicates that the inundation area is sensitive to the channel roughness values in both cases. The same extension of inundation area for different combination of roughness values could also be obtained as it can be seen on the response surfaces. This is an evidence for the problem associated to calibrating hydrodynamic and hydrologic models. It is challenging to obtain an 'optimum' parameter sets (the problem of non-uniqueness in hydrology). This fact for hydrodynamic models is also discussed by (Bates et al. 1996) and they indicated that the traditional single-parameter perturbation approach to sensitivity analysis may not fully capture all aspects of model behaviour. There are inflections for smaller values of the channel roughness which are observed on Figure 5-6. This is mainly associated to the weakness of the solver used in HECRAS. The numerical algorithm is written for subcritical flow, and supercritical flow is simulated by minimizing or completely eliminating the acceleration terms. This fact was observed while making simulations when the model became unstable for very small channel roughness values for which the flow regime became supercritical and mixed.

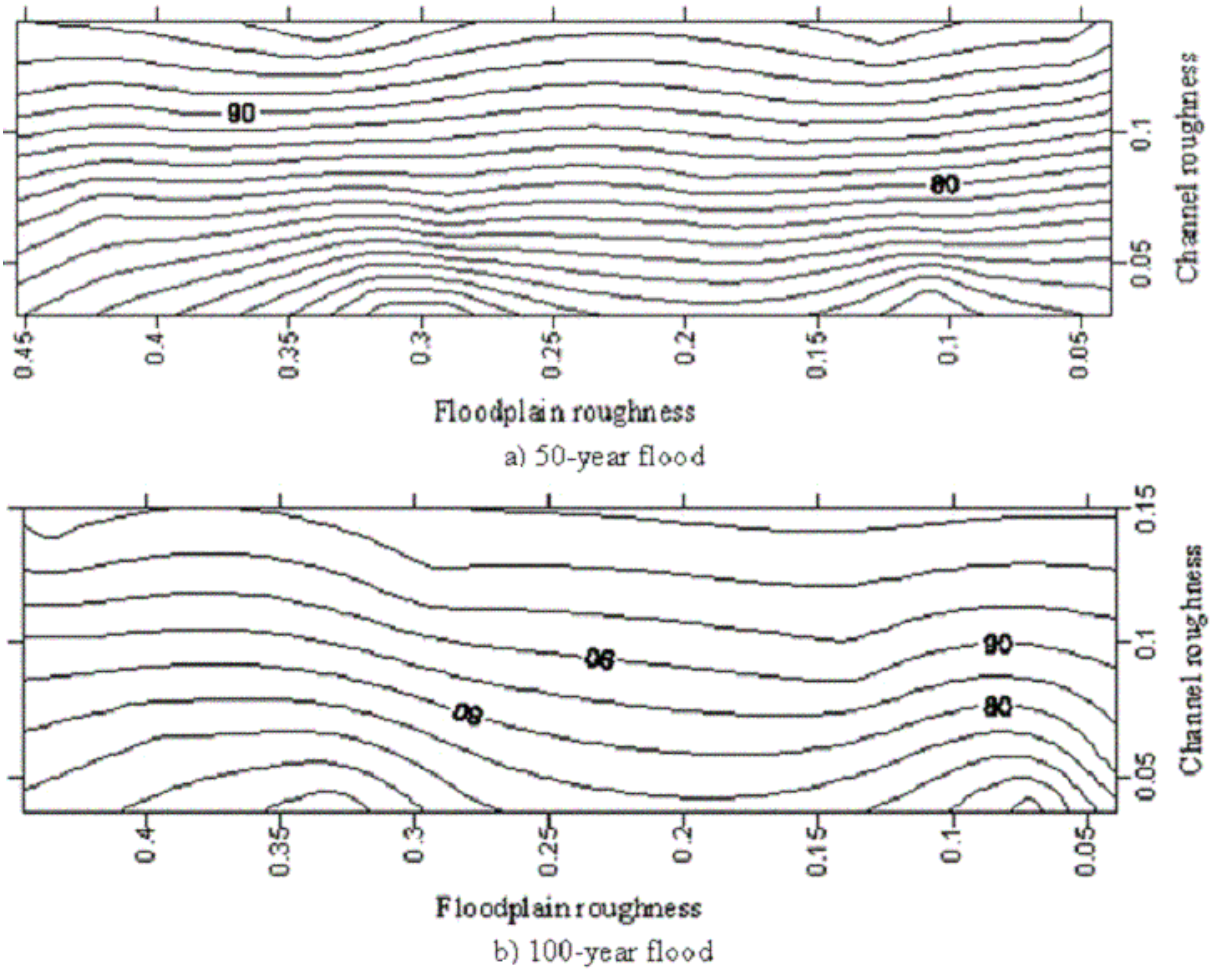

Figure 5-6: Contour map of the maximum inundation area(%) (normalized to the maximum) for different sets of channel and floodplain roughness values

5.5. Representation of buildings for flood modelling

One of the challenges in floodplain modelling is how to represent buildings. They can be represented as solid objects, partially solid objects, or hollow objects depending on how the surface roughness values are specified. When they are assumed to act like solid objects, no water is allowed to flow into

them and the roads together with other features serve as the only conveying and storage devices for the flood water. In the case of the second representation, buildings act as storage devices by storing the flood water during the flood event and releasing it afterwards with a larger delay. This is made by associating larger roughness values to building locations. When a single surface roughness value, which is relatively small, is provided for the whole floodplain; i.e. buildings represented as hollow objects, they serve both as conveying and storage devices simultaneously. This presupposes that they have an equivalent flow resistant effect as the other features in the floodplain. For the solid representation, the DEM should include the height of buildings. Another issue is how to account for differences in types of building as the roughness of individual buildings is different. This requires a sound judgment on the relative roughness of the buildings based on several data on these objects. However, it is not addressed in this study.

Table 5-3: Flow characteristics for the three possible types of building representations

Building representation	Inundated no. of cells	Inundation area (m^2)	Maximum depth (m)		Maximum Velocity (m/sec)		Normalized Inundation area (%)
			Max	Mean	Max	Mean	
Hollow	27724	693100	9.583	3.99	17.772	2.12	97.42
Solid	27220	680500	9.658	4.29	14.49	2.41	95.65
Partially solid	28459	711475	9.626	4	15.653	2.03	100.00

The results of the simulations for the three conditions are given in Table 5-3 and Figure 5-7. For the case of buildings as solid objects, a building was considered inundated when it was surrounded by water. The mean maximum depth and maximum velocity were the largest for buildings as solid objects. This may be since water can't enter the buildings, then it resulted in increase of the water depth, increasing speed. However, it is difficult to give the exact reason for this as the hydrodynamics of urban areas is very complex and only the bulk flow characteristics are considered here. The largest number of cells is inundated when buildings serve both as conveying objects (partially solid objects). The normalized inundation area is 100%, 97.42%, and 95.65% for buildings as partially solid, hollow, and solid objects.

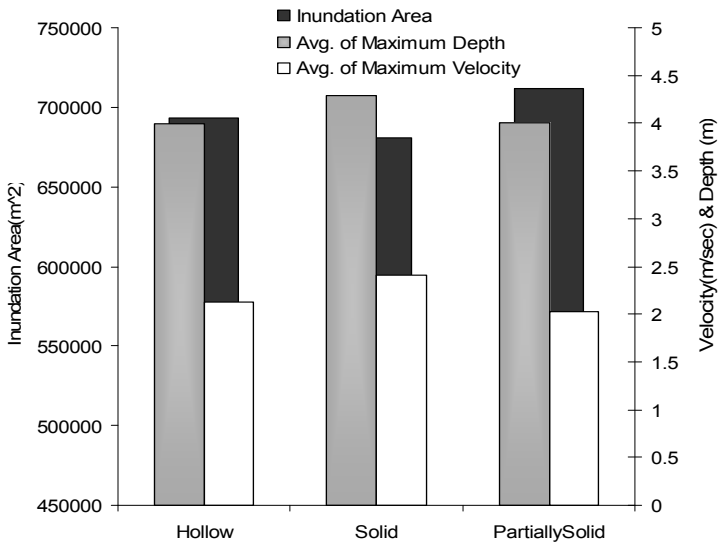

Figure 5-7: Bulk flow characteristics for different types of building representation.

Figure 5-8 and Figure 5-9 illustrates the inundation extent for the three conditions. The thick line is for the case of buildings as partially solid objects. The figures clearly illustrate that, the flood extent did not change significantly in whatever way buildings were represented. However, there is small difference at the upstream of the tributary from the east.

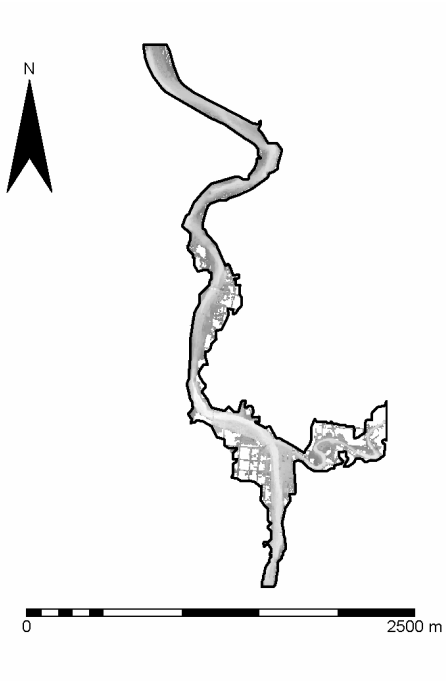

Figure 5-8: Inundation extent for buildings represented as solid objects.

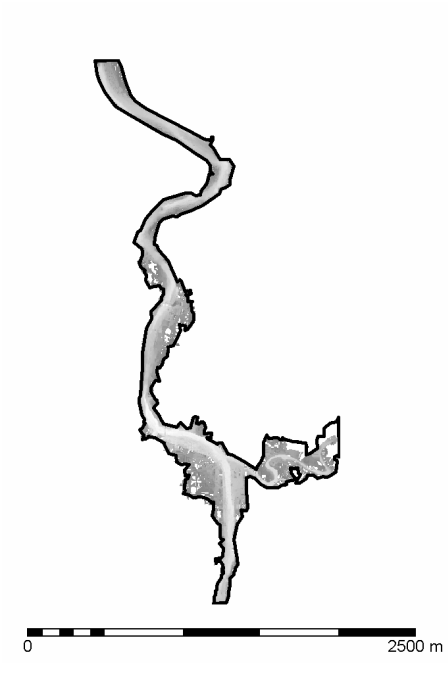

Figure 5-9: Inundation extent for buildings represented as hollow objects.

Streets often serve as the main water conveying elements in cities. This fact can be clearly observed from Figure 5-10 where the maximum inundation depth map is superimposed over an orthophoto of the city. The buildings were not inundated in this case as they were assumed to be solid objects and not participate in both conveying as well as storing water.

Figure 5-10: Propagation of flood over streets for buildings as solid objects (Black colour is for water)

5.6. The effects of DEM resolution on hydrodynamic flood modelling

Topography is one of the critical factors affecting the propagation of a flood wave in a channel and its floodplain. The outputs from a hydrodynamic modelling such as flow depth, velocity and flood extent

are interrelated and merely depend on the values of the inputs from the DEM: elevation values, slope and available flow area. For a complex topography, the relationship between flow depth, velocity and inundation area for hydrodynamic modelling of great interest but are difficult to be defined. For example, the model inputs from a DEM differ in magnitude with DEM resolution and this could result in different outputs (flow characteristics) from hydrodynamic modelling. By using a rectangular grid DEM structure, the elevation of the area under each grid cell becomes lumped property and is replaced by a single value. This procedure results in averaging or generalization of some features, such as dykes, other flow obstacles and local storage areas, which have sizes smaller than the selected grid cell size. Such averaging could result in poor flow dynamic representations in particular when low resolutions are adopted. In hydrodynamic flood modelling, it is of great interest to know to what extent the use of low resolution DEM and its associated generalization of important features affects the model outputs. There is often a need to select the appropriate resolution: a low resolution DEM could result in a larger loss of information (averaging) and a high resolution DEM could result in excessive computational time. Thus, the DEM resolution needs to be selected in such a way that there will be lesser computational time while reducing the effect of the averaging which could yield unacceptable model outputs. SOBEK stores the maximum flow depths and velocities occurring within each grid cell of the problem domain during the calculation period. These values have been averaged over space using GIS operations and are reported in Table 5-4 and Figure 5-11 and Figure 5-12 for different DEM resolutions.

Table 5-4: Maximum velocity and depth for different DEM resolutions

DEM resolution (m)	Maximum depth (m)			Maximum velocity (m/sec)		
	Max	Mean	Std. Dev	Max	Mean	Std. Dev
2.5	10.518	4.25	2.56	14.873	2.21	2.05
5	10.125	4.201	2.5	19.621	2.17	1.93
7.5	10.022	4.19	2.49	11.482	2.13	1.76
10	10.103	4.28	2.53	9.083	2.07	1.66
12.5	10.112	4.34	2.56	8.712	2.02	1.61
15	35.812	16.68	8.71	8.312	0.2	0.34

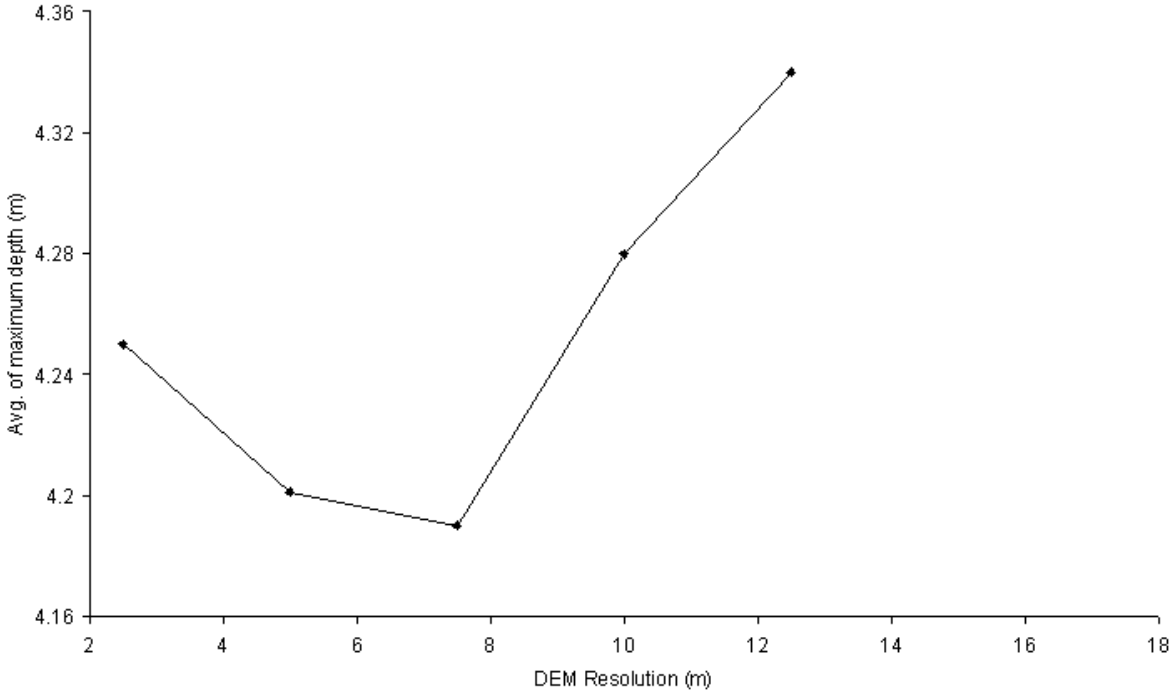

Figure 5-11: Variation of the average of the maximum depth with DEM resolutions.

Figure 5-13 shows the variation in maximum inundation area with DEM resolution. The maximum inundation areas when normalized to the maximum inundation area are 100%, 98.96%, 97.92%, 98.21%, and 98.94% for 12.5 m, 10 m, 7.5 m, 5 m, and 2.5 m grid cell sizes respectively.

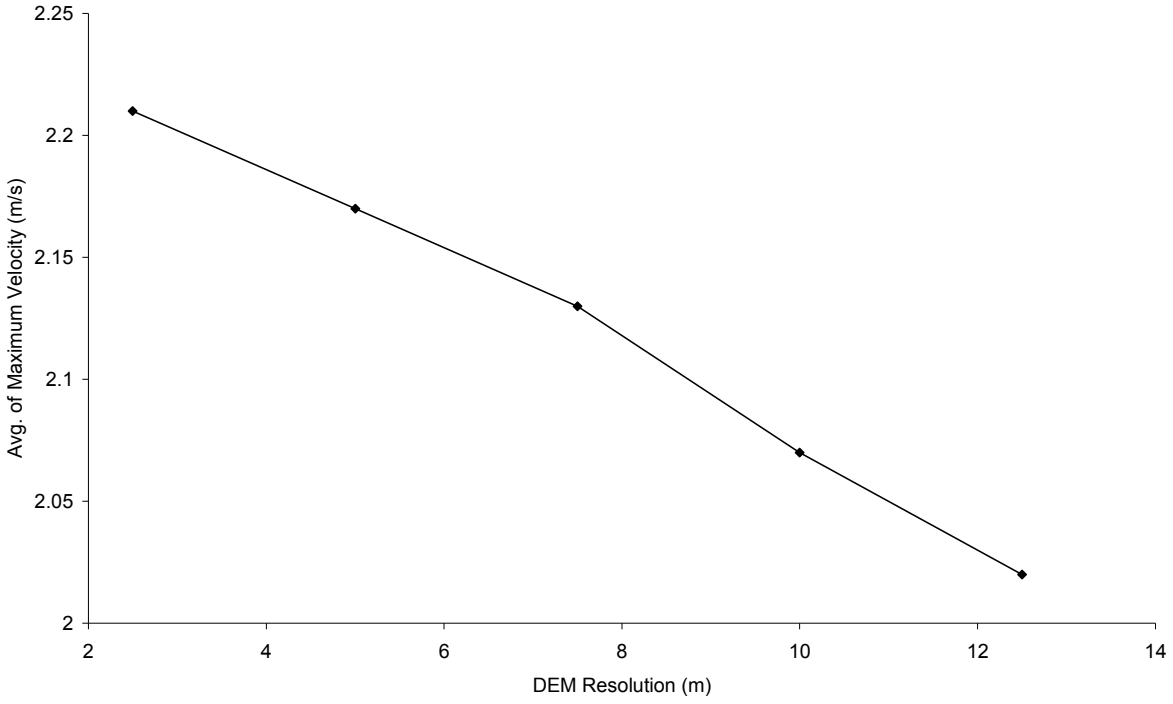

Figure 5-12: Variation of the average of the maximum velocity with DEM resolution

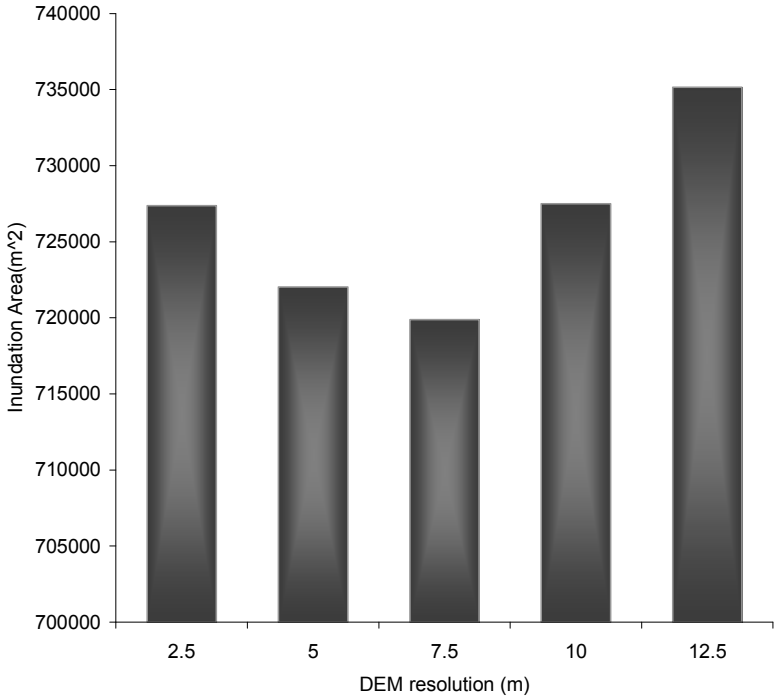

Figure 5-13: Maximum inundation area variation with DEM resolutions.

Figure 5-14 and Figure 5-15 illustrate the maximum inundation depth and extent maps for the 5 and 15m DEM resolutions. The results of other resolutions are presented in Appendix I. If the same discharge hydrograph is introduced for the upstream boundary condition, equal volume of water is expected to be stored in the model domain provided the same downstream boundary condition is introduced. This is to satisfy the law of mass conservation: for a certain time period, the inflow minus the outflow must be equal to the change in storage. Thus, a larger flood extent is usually expected to be associated to a smaller flood depth. Following this reasoning, it is surprising that this is not observed in Figure 5-14 and Figure 5-15 and the simulation results show inconsistencies. For the 15m resolution, the increase in inundation extent, and depth were found to be extremely large.

Three reasons were anticipated for the increase of flood depth and inundation area simultaneously and for the excess flood extent for the 15m resolution:

- The selected downstream boundary condition limits discharge outflow
- By the averaging procedure of the low resolution DEM much small scale topographic data is lost that affects flood routing process, and
- In SOBEK water is allowed to flow from a single cell to only one of its four neighbouring cells

The three possible reasons are compared below.

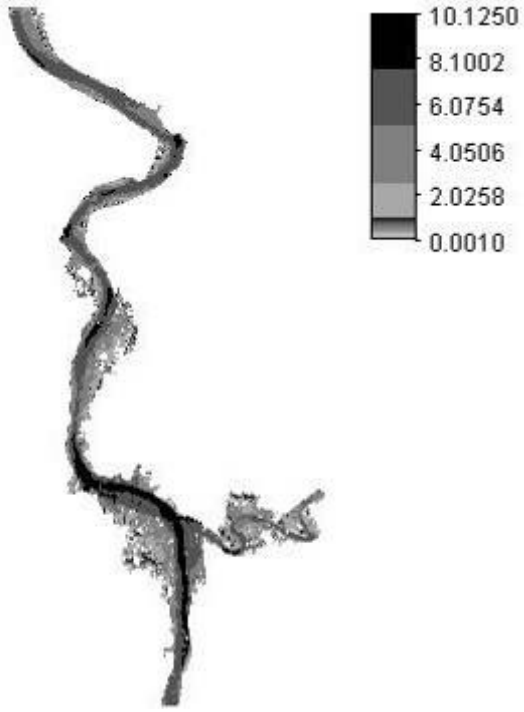

Figure 5-14: Maximum depth maps for 5 m DEM resolution

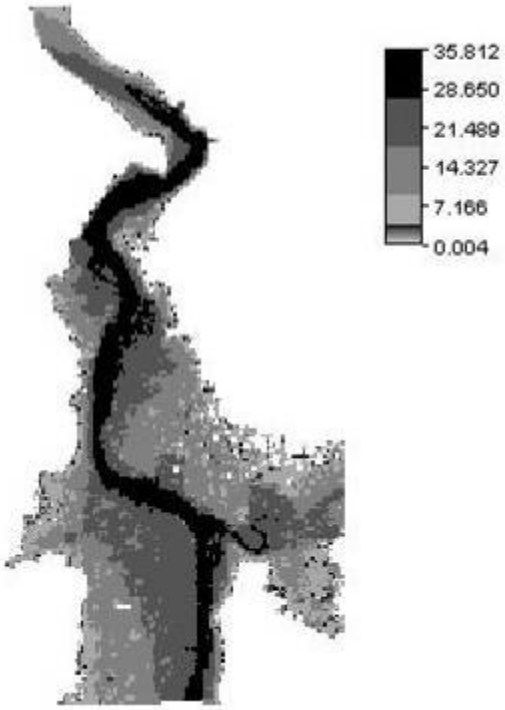

Figure 5-15: Maximum depth maps for 15 m DEM resolution

The first anticipated reason is the effect of downstream boundary condition. In this study, a hydraulic free flow condition was introduced at the downstream end by specifying a lowered constant water level. In this case, the computation for the last element will be based on the computed water level on one side and the specified water level on the other side of the boundary and has an advantage when there is no backwater effect at the specified downstream boundary location. For such type of boundary condition, the water curvature is expected not to propagate to a larger extent in the model domain. However, when specifying constant water level, the use of different DEM resolutions might result in different hydraulic gradients at the downstream boundary location as illustrated in Figure 5-16. Here, the elevations of two cells were taken for the 5- and 15 m DEM resolutions at the downstream end (the outlet) to illustrate the situation.

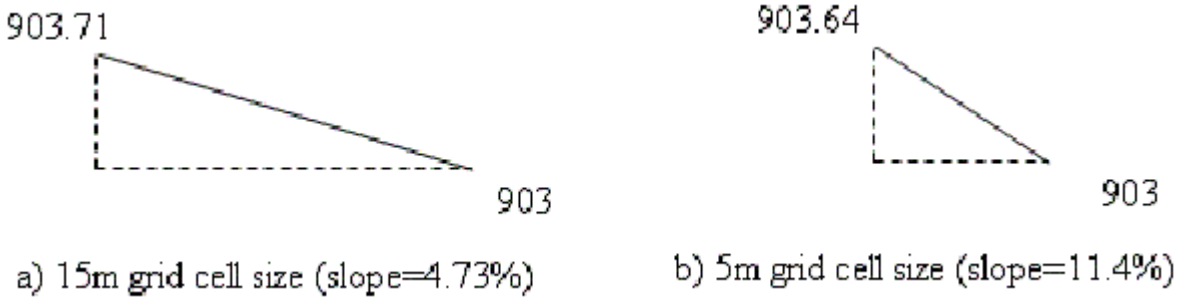

Figure 5-16: Hydraulic steepness at the downstream boundary

In order to test the effect of the downstream boundary condition, additional simulation was performed for the 15m DEM resolution making the channel at the downstream end steeper which is equivalent to the gradient of the 5m grid cells. Analysing the results proved that the inundation area and depth did not change significantly. Moreover, the simulation video showed that water propagated further into

the floodplain even before the flood wave introduced at the upstream boundary had reached at the downstream end. Thus, the downstream boundary condition had no significant effect on the increase of the flooded area and the increase of flood depth simultaneously as they are observed for the low resolution DEM.

The second reason anticipated was the averaging effect of the low resolution DEM. To study this effect, two cross sections and one profile for part of the channel were extracted from the 2.5, 5 and 15 m resolution DEM's as shown in Figure 5-17, Figure 5-18 Figure 5-22. Cross sectional plots which cover both the channel and left and right bank floodplains at selected locations are also given in Figures 5-19 to 5-21. As shown in Figure 5-22, the 15m DEM resulted in a channel bed with larger elevation values than the other resolutions at the upstream part of the selected profile. This is also supported by Figure 5-35 to 5-38. These figures show that there are larger elevation differences between the channel and floodplain parts for the 5m DEM than for the 15m DEM. In such a case, the computation could result in a relatively large amount of discharge entering the floodplain when low resolution DEM is used since such a resolution averages out some of the obstacles to flow at the channel-floodplain interaction. Moreover, there could also be an increase of water depth in the floodplain as well as in the channel since steepness, which significantly affects the flow velocity, is also a notion of grid cell size and water is expected to flow slowly in the floodplain than the channel due to several obstacles. This fact can further be supported by Figure 5-12 where the velocity has been shown to decrease with a decrease in DEM resolution. The cross sectional plots also show that the 15m resolution results in an increased channel width than the others and averages out the important features, which affect the flow dynamics, near channel and floodplain interaction. Figure 5-23 to 5-34 show the DEM for part of the model domain using different visualization techniques. They clearly illustrate how details are dropped out and the simplified model domain deviates by far from the 'real problem domain' when using low resolution DEM. Some of the major dropped out features are shown in Figure 5-23 with the three circles. In addition, the channel capacity is underestimated for the 15m DEM as shown in these figures. Use of the three types of visualizations illustrates how different types of model domains for the same study area are obtained by using different resolutions. As such it should be expected that such different model domains result in different model output. In general, by using low resolution DEM, all the inputs to a model such as elevation values, slope, channel dimensions and overland flow area, as obtained from the DEM will be affected. This will result in model outputs which could differ significantly as the DEM resolution is changed. One thing which was not done in this study and which could limit the amount of features mainly flow obstacles averaged is to perform a GIS continuity analysis on the DEM and obtain these features. The resampling procedure should then be done in such a way that it respects these features by manually or automatically editing the resulting low resolution DEM.

The third possible reason for the simultaneous excess flood depth and extent using the low resolution DEM is in SOBEK water is allowed to flow from a certain finite difference element to only one of its four neighbouring cells. This introduces a difficulty to depict the flow path with a reasonable accuracy as the cell size increases. This fact is illustrated in Figure 5-39 where a water particle is shown to follow several flow directions and zigzag paths when using the high resolution DEM. These heterogeneities and small scale process become significant when higher resolutions are used. However, the heterogeneities are lumped by the use of the low resolution DEM. Considering only the shaded grid elements in Figure 5-39, there are discharge outflows in the north-east and east

boundaries of these groups of cells for the 5m DEM but there is an outflow only in the east direction for the 15m DEM. This implies by using the 15m DEM the cell to the east of this element receives more discharge than it actually receives while the cell to the north of this element receives smaller discharge. Figure 5-39 is computed for a condition where there is a possibility for a grid cell to discharge to eight of its neighbours. Thus, the problem propagates in SOBEK where the discharge is only to the four neighbours of a cell. This problem gets more complicated for a complex topography such as urban areas and it is difficult to address all the factors affecting the flow dynamics for such an area.

Generally, even though the hydraulic gradient at the downstream boundary could have an impact on the computed flood characteristics, it is not the significant reason for the observed excess water in this problem domain for low resolutions. It is instead more related to the combination of the other two reasons explained above: the averaging effect of the low resolution topographic definition and the definition of flow direction for rectangular grid DEM structure and in particular for SOBEK. This indicates that accurately depicting the flow direction and also other flow characteristics is significantly affected by to what detail the topography is represented and what type of spatial discretization (though this requires further investigation) we are adopting in our model approach.

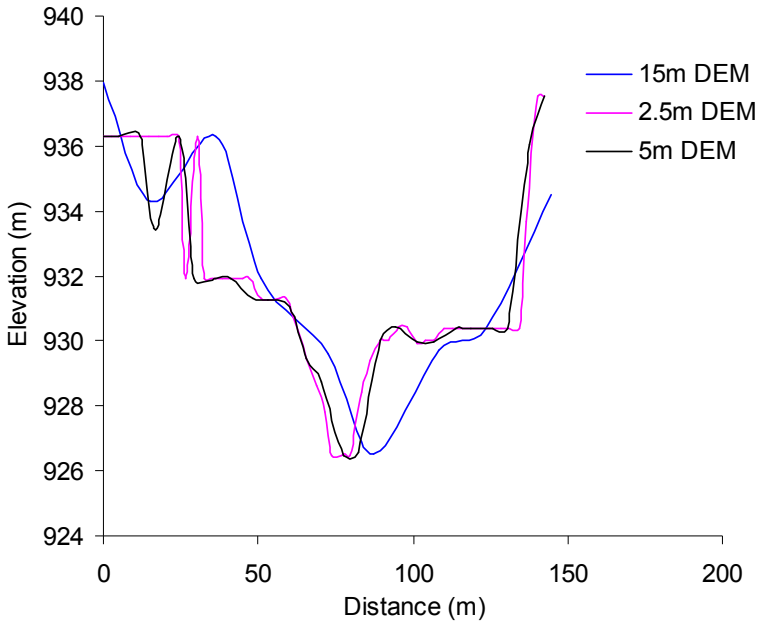

Figure 5-17: Channel cross sections on the tributary river

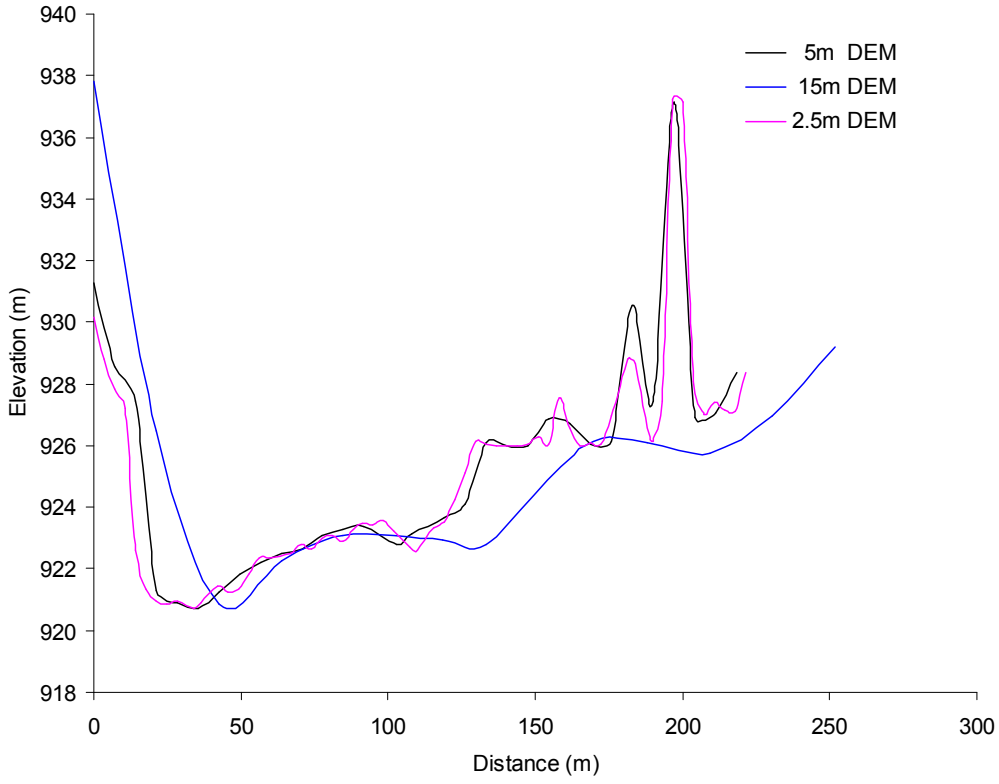

Figure 5-18: Channel cross sections below the junction of the river with its tributary

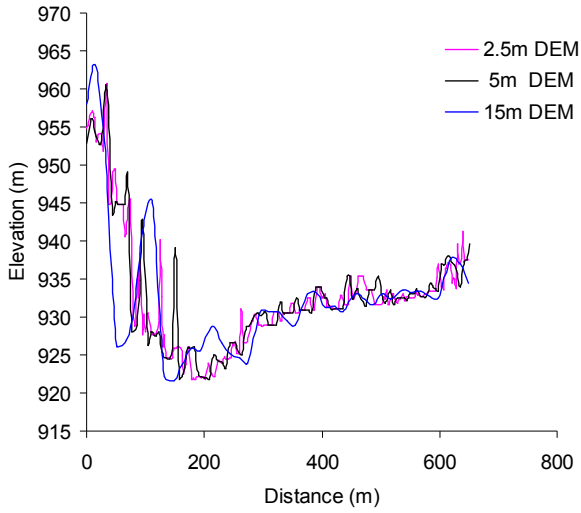

Figure 5-19: Cross sectional plot for both the channel.

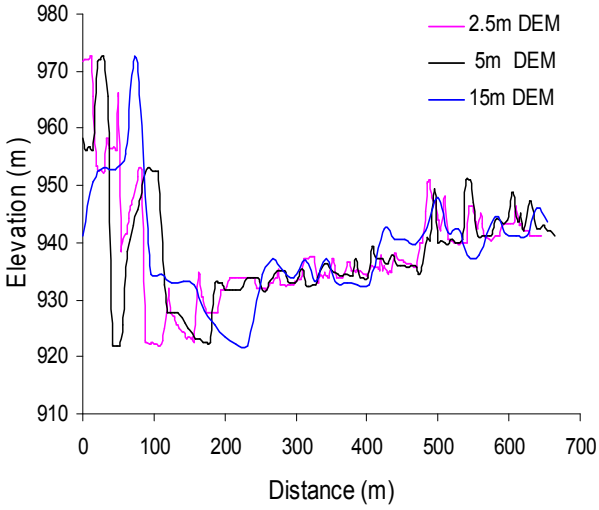

Figure 5-20:Cross sectional plot for both the right bank floodplain

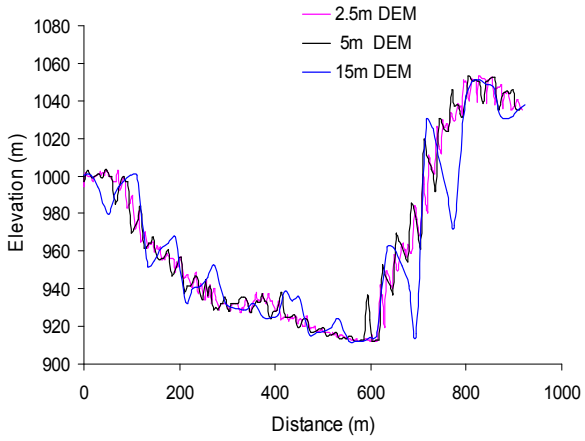

Figure 5-21: Cross sectional plot for both the left bank floodplains

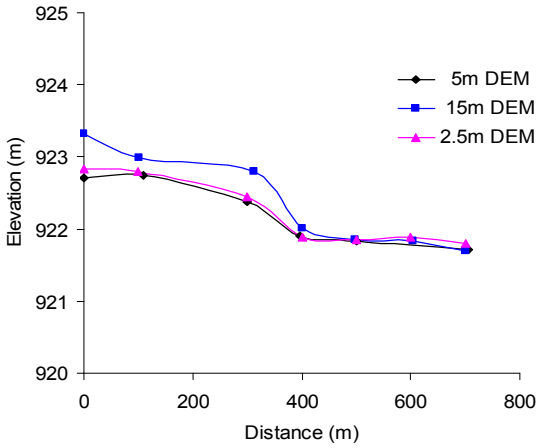

Figure 5-22: Channel profile at selected location

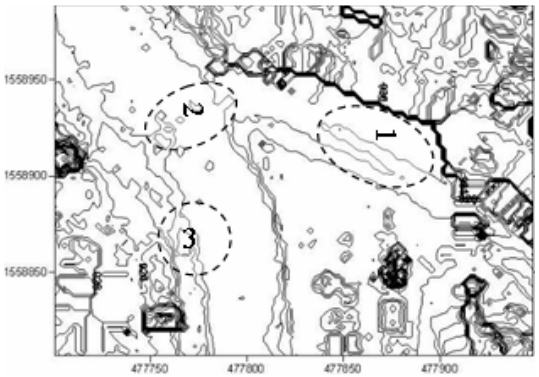

Figure 5-23: Elevation contour map for 2.5 m DEM

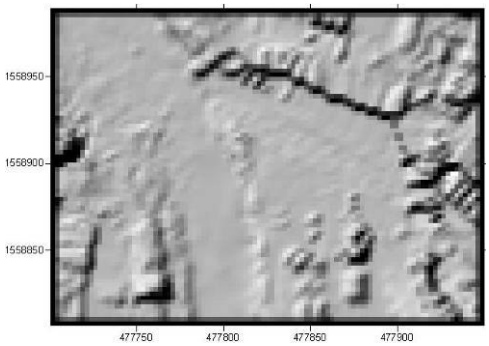

Figure 5-24: Shaded relief map for 2.5 m DEM

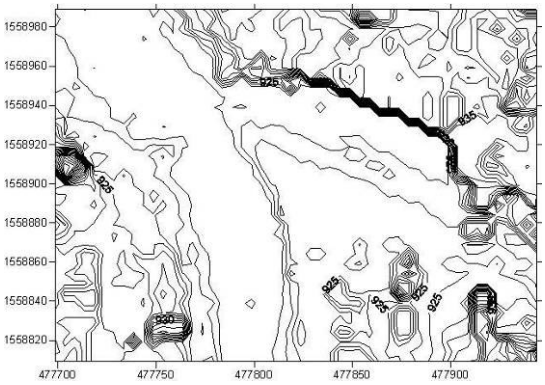

Figure 5-25: Elevation contour map for 5 m DEM

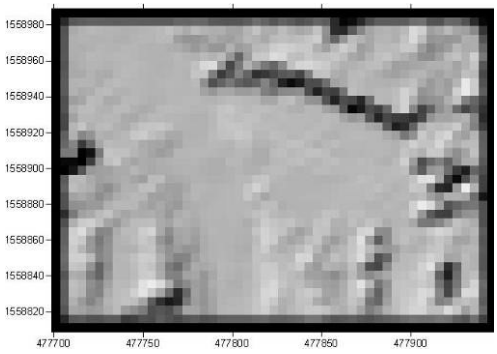

Figure 5-26: Shaded relief map for5 m DEM

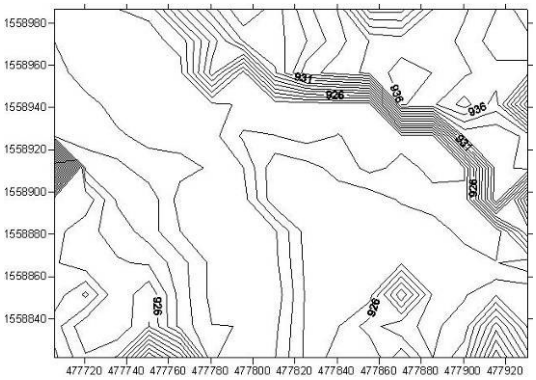

Figure 5-27: Elevation contour map for 15 m DEM

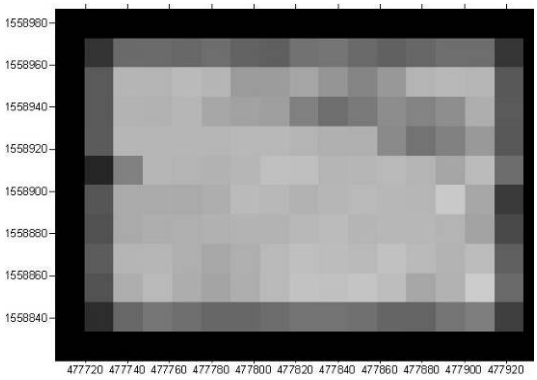

Figure 5-28: Shaded relief map for 15 m DEM

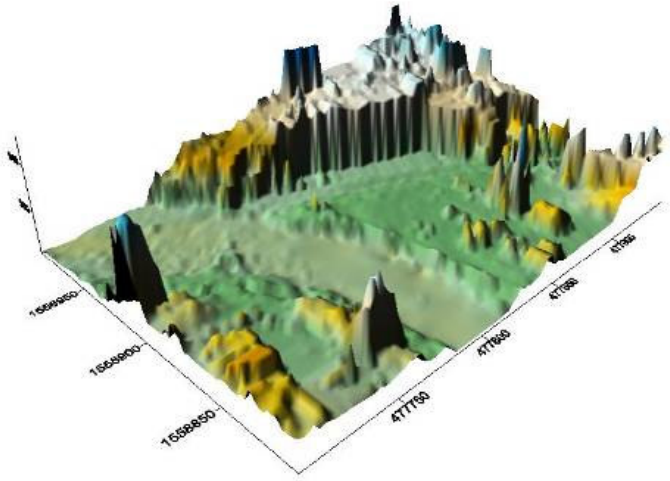

Figure 5-29: Surface plot 2. 5m DEM

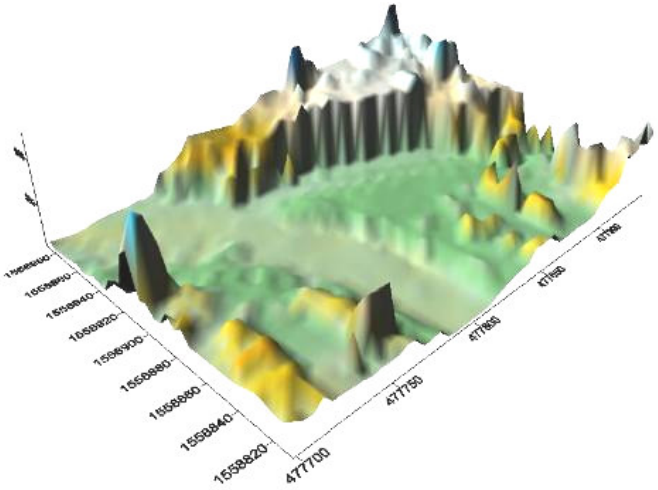

Figure 5-30: Surface plot 5 m DEM

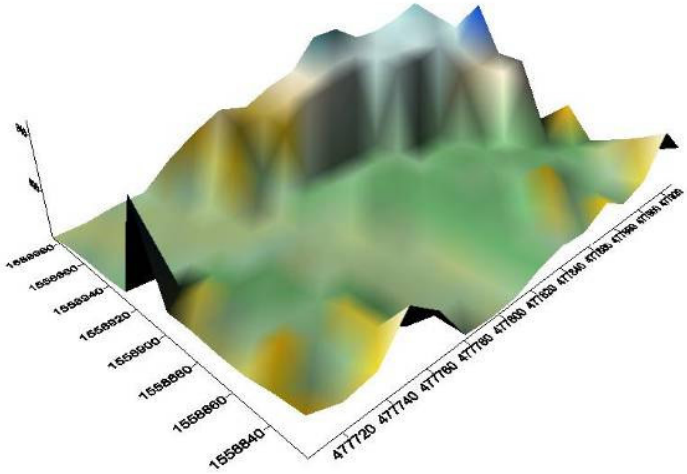

Figure 5-31: Surface plot 10 m DEM

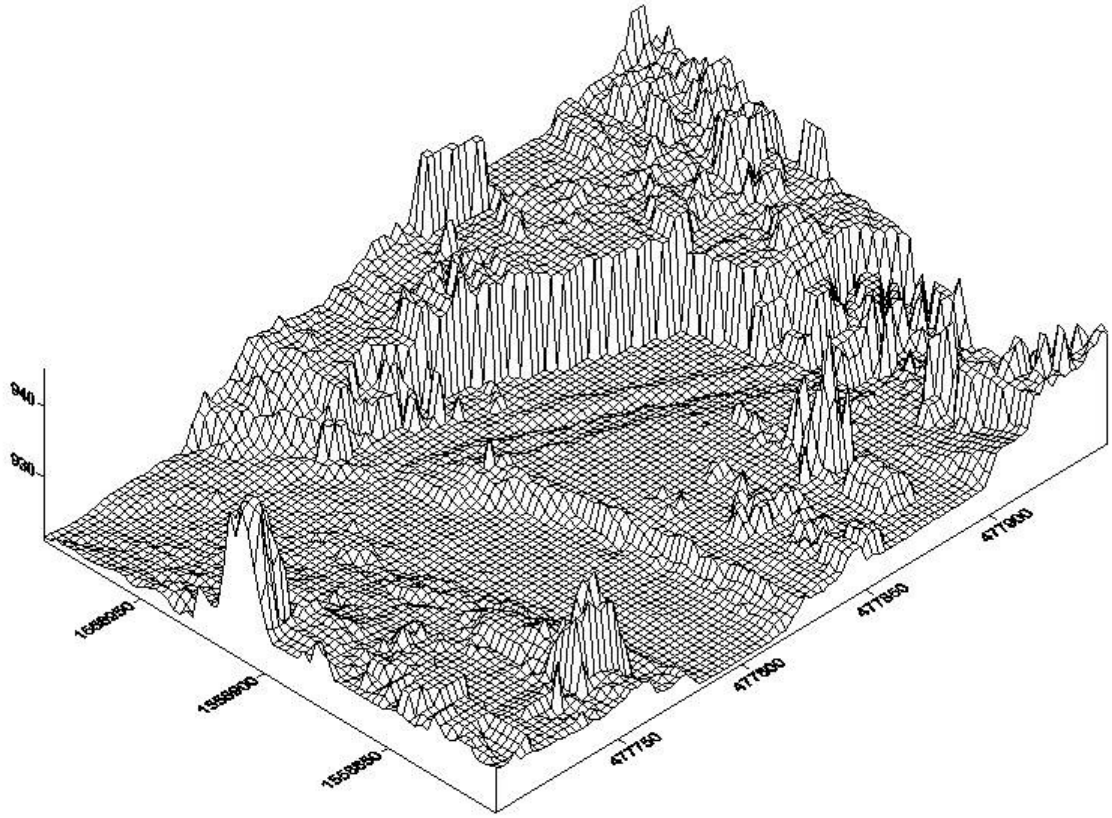

Figure 5-32: Wiremesh map for 2.5 m DEM

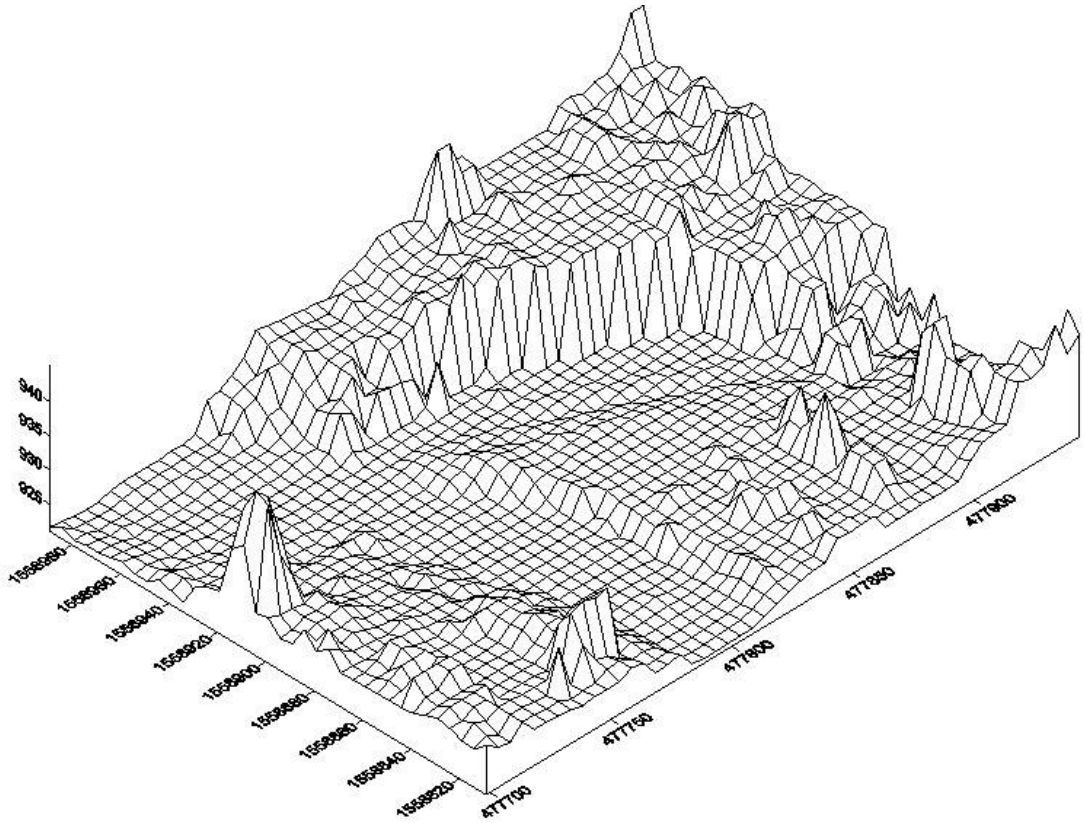

Figure 5-33: Wiremesh map for 5 m DEM

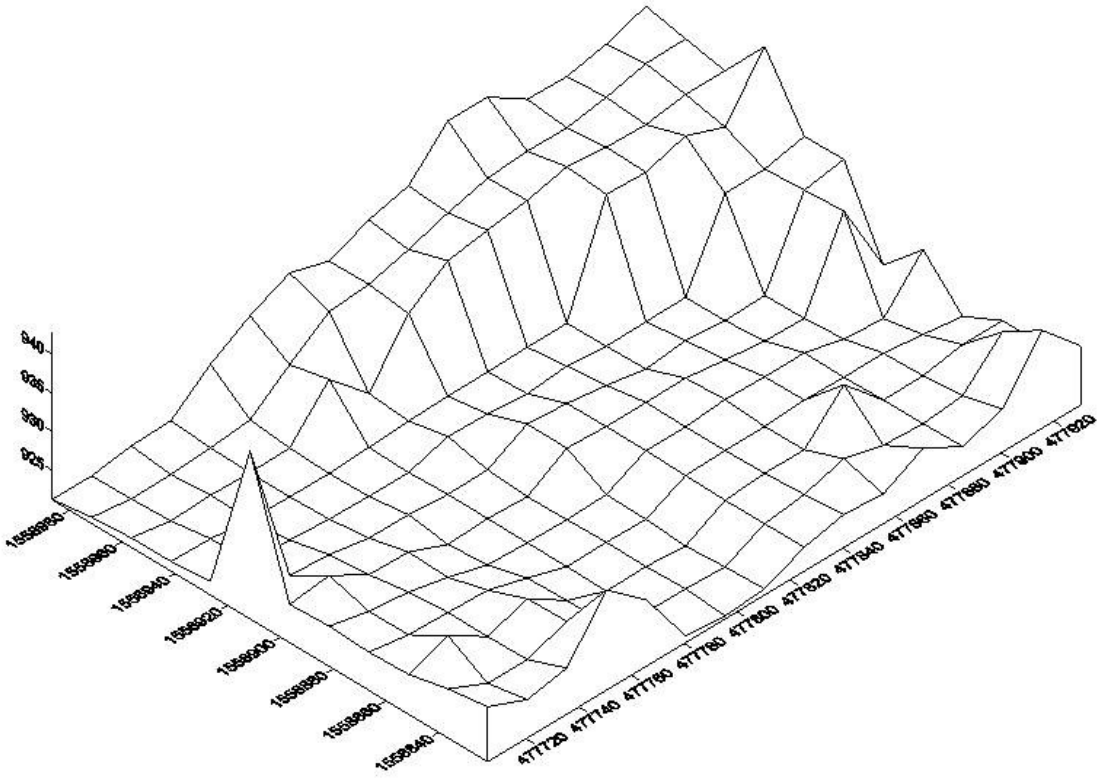

Figure 5-34: Wiremesh for 15m DEM

Comparison of the computational time indicated that it increases adversely for small grid cell sizes. Reducing the grid cell size by half was observed to increase the simulation time by a factor of about 12.58. This is illustrated in Figure 5-40.The simulation was performed using a 1.8 Ghz Pentium IV PC. For the same PC, the simulation for 2.5m DEM size was interrupted after 13days simulation due to annual network maintenance. For this reason, the simulation with the 2.5m DEM was performed using another computer inconsideration to the time limit for this thesis to be completed and as such its computational time is not included in Figure 5-40.

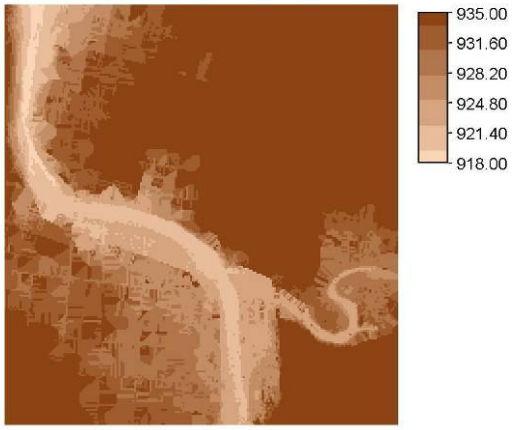

Figure 5-35: DEM map for5 m resolution

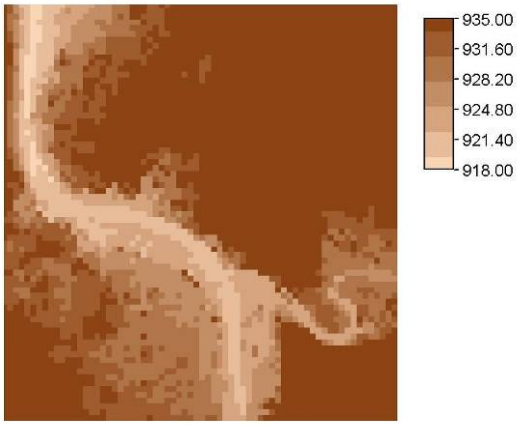

Figure 5-36: DEM map for 15 m resolution

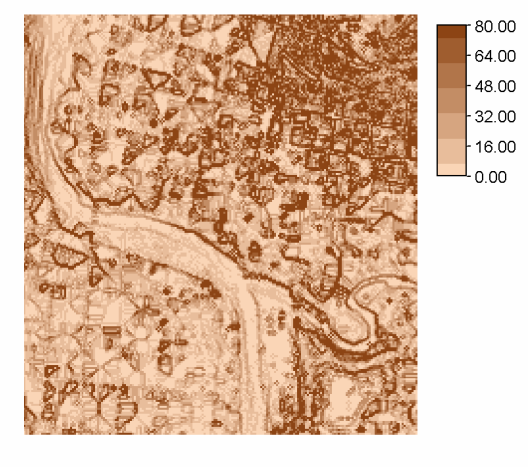

Figure 5-37: Slope map for 5 m DEM resolution

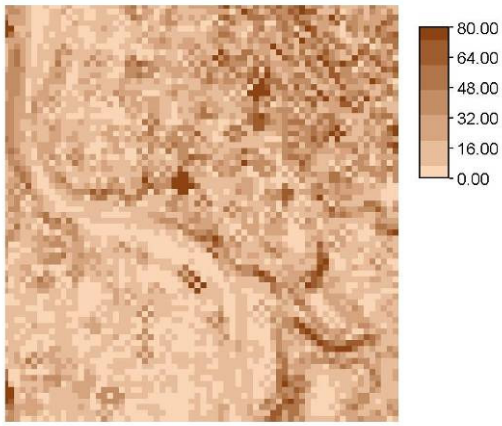

Figure 5-38: Slope map for 15 m DEM resolution

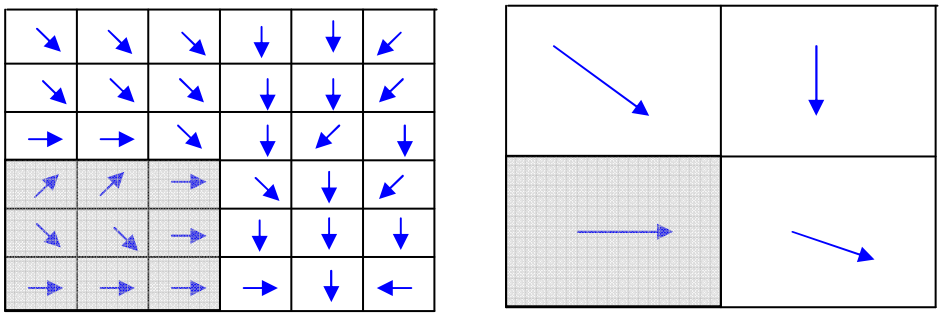

Figure 5-39: The effect of DEM resolution on flow direction for a finite difference discretization. Left 5 m and right 15 m resolution

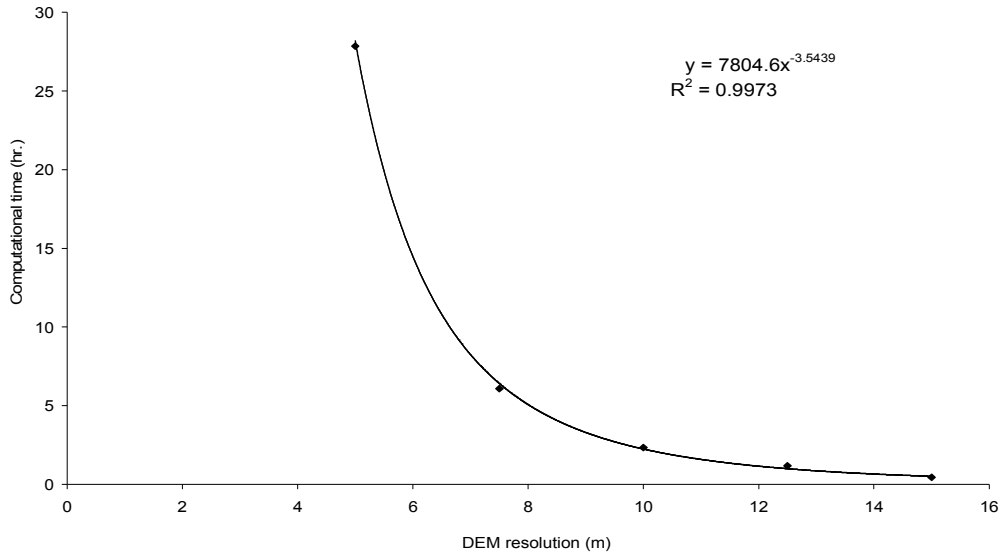

Figure 5-40: Change of computational time with DEM resolution

5.7. Simulation results for the 100 and 50 year return period floods

It is a common practice to use the flood inundation area, depth, velocity and duration maps to study a floodplain's vulnerability and risk to floods. These information as obtained from the hydrodynamic modelling of the study are for the 50-and 100-year return period floods are shown on Figure 5-43 to 5-46. The simulations were performed using a 5m DEM resolution and 24 hour hydrograph duration.

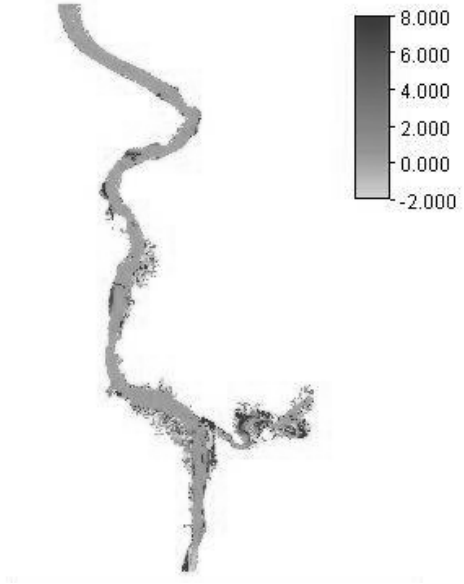

Figure 5-41: the difference between the times of occurrence of the maximum depth and velocity (hrs.) for 50-year return periods floods

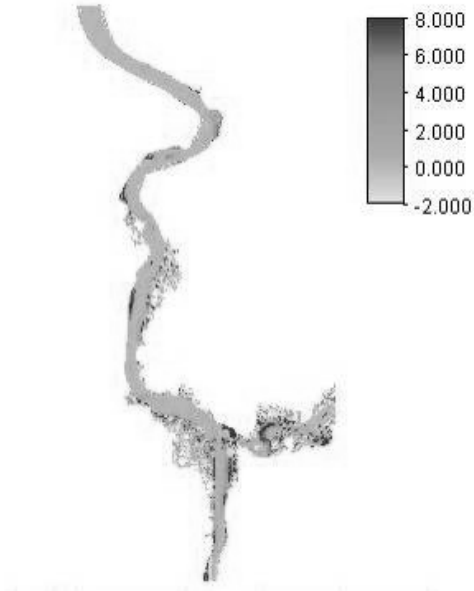

Figure 5-42: the difference between the times of occurrence of the maximum depth and velocity (hrs.) for 100-year return periods floods

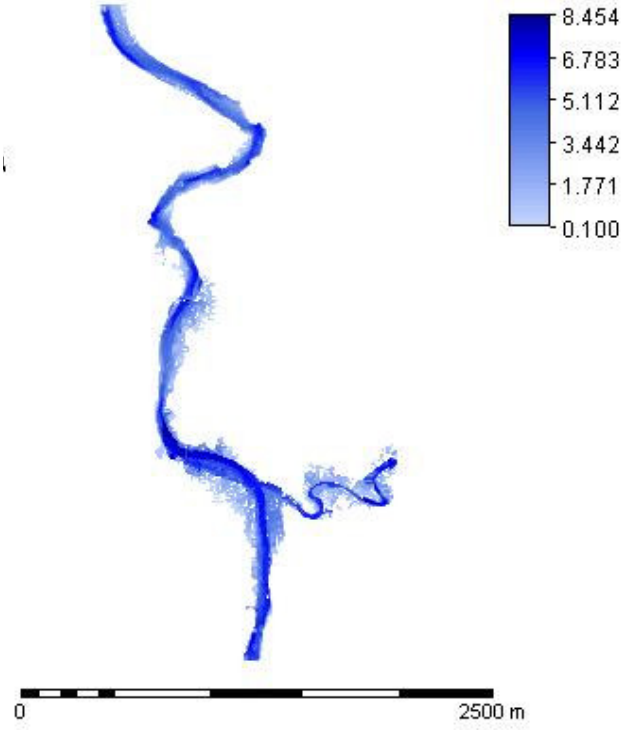

Figure 5-43: Maximum depth (m) for 50-year return periods floods

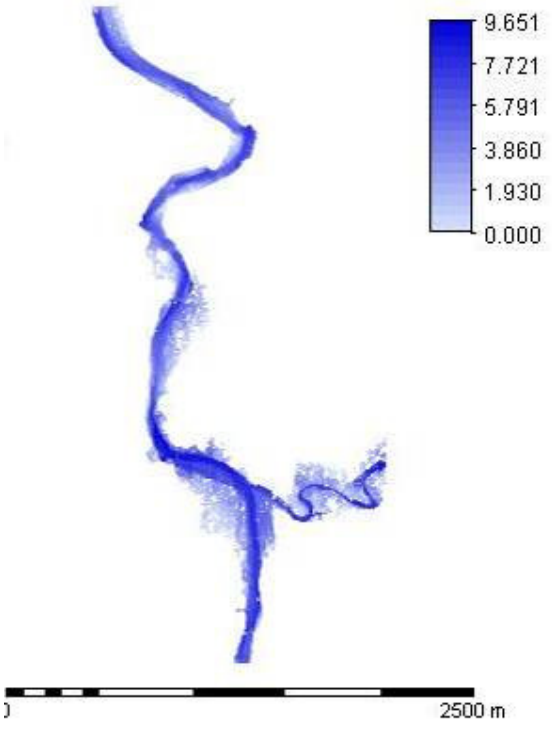

Figure 5-44: Maximum depth (m) for 100-year return periods floods

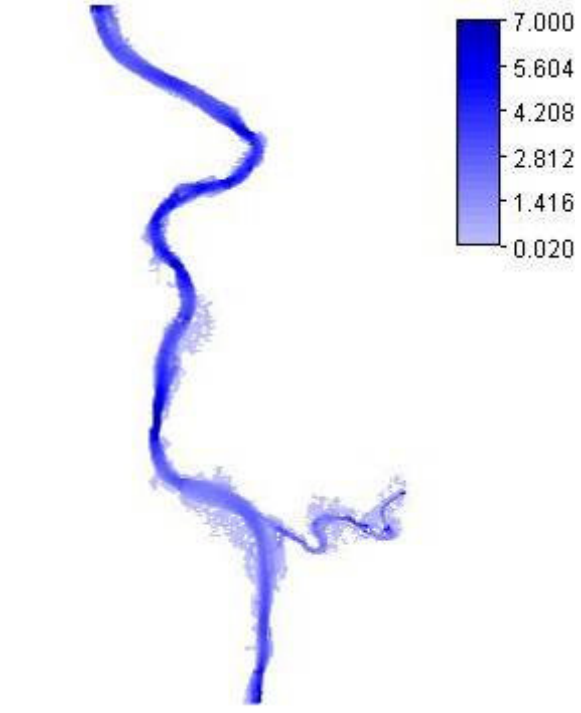

Figure 5-45: Maximum velocity (m/s) for 50- year return periods floods

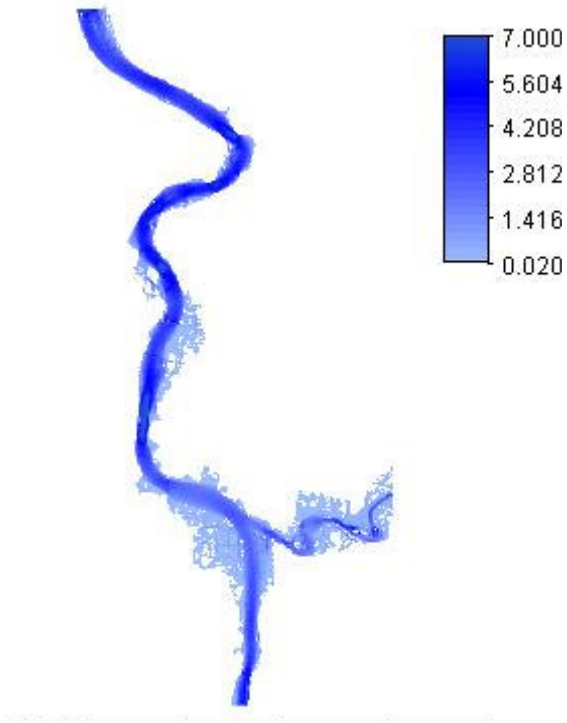

Figure 5-46: Maximum velocity (m/s) for 100-year return periods floods

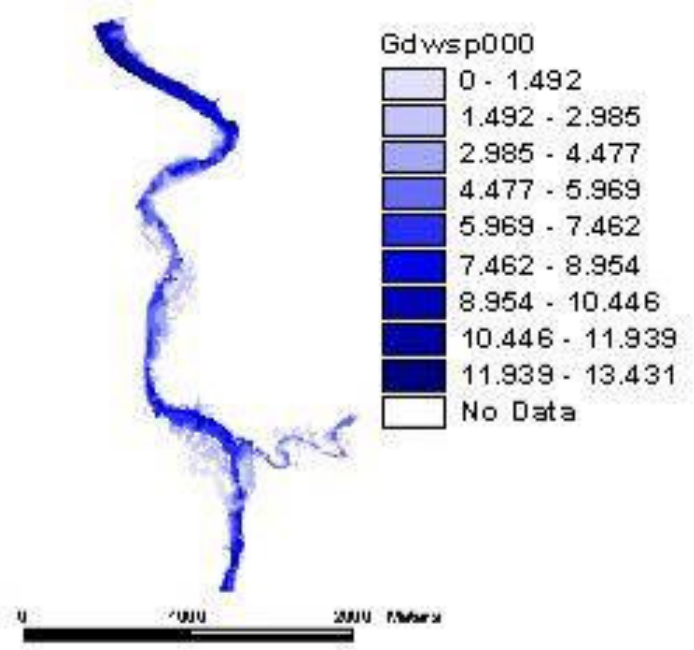

Figure 5-47: Maximum inundation depth for 100-year return period flood as obtained from the 1D model

The 100-year return period inundation extent was also produced using the one dimensional HECRAS flood model. It resulted in an inundation of 27,377 DEM grid cells when projected on 5m grid cell size as opposed to the 28,529 inundated cells using the two dimensional hydrodynamic model SOBEK. The difference might be due to differences in model structure; difficulties in defining the problem domain, mainly the channel cross section and alignment, in the 1D model; and interpolation of the maximum inundation depth map from the 1D model. Moreover, the absence of calibration data also affects the comparison. The maximum inundation depth map using the 1D model is given in Figure 5-47.

6. Conclusion and recommendations

Society's need to get reliable information on flood characteristics is increasing as the occurrence of these devastating events is becoming a common experience in almost every parts of the world. In the past, several types of flood models have been developed to satisfy this need. The structure of these models has been mainly dictated by advances in computational facilities. However, the reliability of their results is merely dependent on the availability of inputs to parameterize them. Availability of high resolution DEM in response to advances in airborne topographic data acquisition is expected to play a vital role in this regard.

This thesis was based mainly on the available LIDAR data set for the city of Tegucigalpa, Honduras. As the main limitation of these type of DEM's is their failure to give information beneath structures such as bridges, this kind of study must be supported by a field visit. This has been the main limitation of the thesis. Moreover, defining the channel alignment and cross sections must be supplemented by the conventional surveying techniques. Despite these limitations, the available data has been shown to be sufficient to answer the main research questions.

The model's reliability and sensitivity for changes in different inputs was investigated. Sensitivity analysis of the 1D model approach, HECRAS, for different downstream boundary conditions: normal depth, constant water levels, artificially steeper channel, and hydraulic free flow, was performed. The effect did not propagate to the area of interest for this study. However, such a conclusion needs to be made cautiously as the response depends also on other factors such as the surface roughness values used for the simulation. Surface roughness sensitivity of the 1D model approach also revealed the weakness of the model to solve supercritical flows and the possibility of occurrence of more than one parameter set with the same model output. It was very difficult to define the channel alignment and cross sections as inputs to the 1D model. This even became very complex for the meandering part of the channel. Defining the channel and floodplain areas separately was also a difficult task since there is no clear boundary between the two. Therefore obtaining a reliable simulation results from a one dimensional model, while a 2D model is less sensitive to this provided a finer grid cell size is adopted, is a function of how accurately the model domain, that is the channel alignment and cross sections, is represented and indirectly more on the modeller's experience.

The other challenges in flood modelling are how to represent buildings, and how to define the system boundary conditions. Buildings were represented as solid, partially solid and hollow objects. However, the bulk flow characteristics were not significantly changed for these different types of representation. For the upstream boundary condition, the peak flood was obtained from national flood frequency analysis. 'Accurately' depicting the shape of the hydrograph for the upstream boundary conditions requires performing hydrological modelling for the hill slope of the catchment. This needs to be performed in future studies. For the downstream end, a free hydraulic fall was assumed.

The terms used here for the 50-and 100-year floods are simple indications of the magnitude of the peak floods. Nevertheless, these values should not be taken as strictly accurate values since they were based on regional flood frequency analysis for ungauged catchments which could give crude results. Moreover, in this study an extrapolation of the 100-year flood from neighbouring stations was performed to obtain its values for the upstream boundary condition. It is believed that there are several sources of errors in statistical hydrology and it needs careful treatment. However, the study gives a good indication of the magnitude of flood events and their characteristics in the study area and the implications of high resolution DEM for flood modelling.

The resolution of the DEM source, in this case the LIDAR DEM, and the resolution required for hydrodynamic flood modelling are often quite different. Therefore, the DEM resolution must be suited to the models need by using appropriate resampling methods. This study showed that there would be larger loss of information in transferring the DEM resolution to the resolution required by the model. The change in model's output for different resolutions was also tested. In general, the average of maximum velocity decreased with a decrease in DEM resolution while the average of maximum depth and the maximum inundation extents did not show a straight line relation with the DEM resolution. Moreover, the excessive increase in inundation extent for the 15m DEM is an evidence for the fact that there is a limit to the maximum grid cell size to be used for flood simulation. Three possible reasons were proposed and compared to determine the most important factor resulting in different flow characteristics with different DEM resolutions: the change in gradient at the downstream boundary with changes in DEM resolution, the filtering effects of low resolution DEM's, and the way the flow direction is depicted by the model approach, i.e. the spatial discretisation. It has been illustrated that the combination of the latter two reasons could be the main reasons for the larger variation in flow characteristics for different grid cell sizes mainly for the 15m DEM. The computational time also increased with an increase in DEM resolution. This became expensive for smaller grid cell sizes making use of the high resolution LIDAR DEM, without any transformation to other grid cell sizes and in the consequence without any loss of information, difficult. This problem could be improved in the future with the larger availability of high speed computational facilities. The need to reduce the excessive computational time required by distributed models is due to three reasons as stated by (Ivanova et al. 2004) (1) make feasible distributed model calibrations, (2) perform ensemble averaging of the model results to incorporate uncertainties in model forcing and parameterizations, (3) conduct real-time operational forecasting with distributed hydrologic (in this case hydrodynamic) models.

This study integrated State of Art techniques in data processing and Earth observation and hydrodynamic flood models to study flood hazard in Tegucigalpa, Honduras. Integrating Earth observation systems, GIS, and complex flood models which display impressive three dimensional outputs undeniably will have the potential to increase our capability to predict and manage flood events. However, the study showed that there are a lot of uncertainties related to the current hydrodynamic models. This must be investigated and well understood before using the models for flood simulation. It is also recommendable if the available models incorporate methods of quantifying the associated uncertainty.

Appendix

I. Discharge hydrographs used for DEM resolution comparison and simulating the 50-and 100-year flood maps

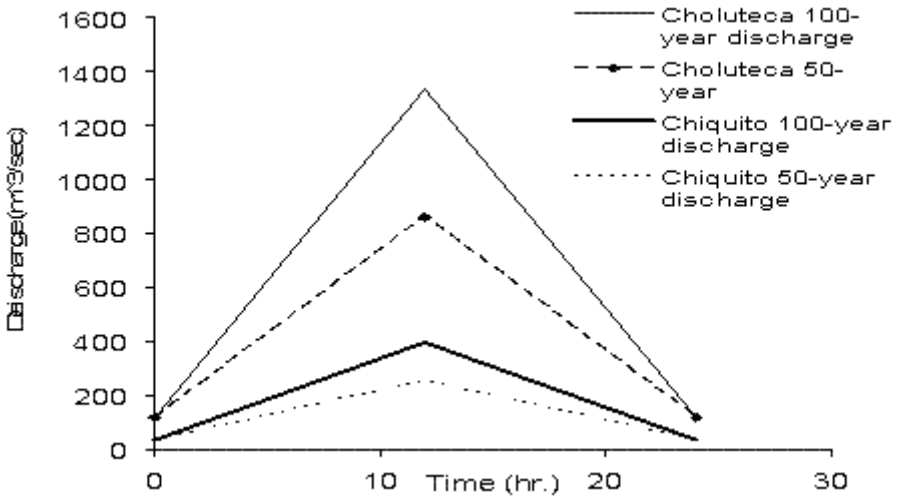

II. Different possible shapes of discharge hydrographs

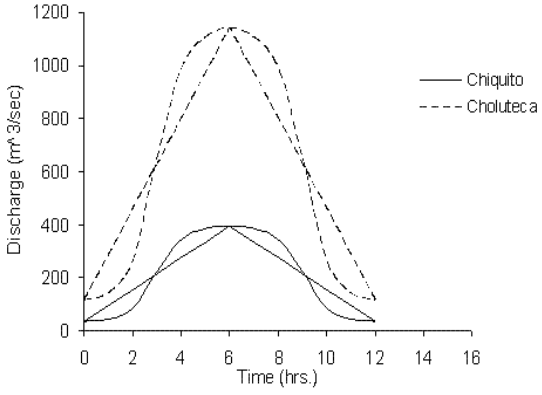

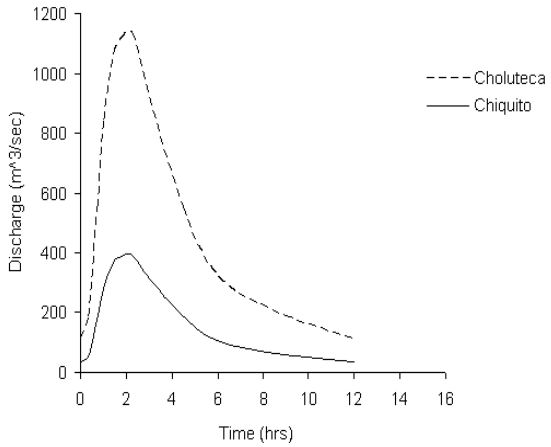

III. Flood Maps for different DEM resolutions

a) 2.5 m DEM

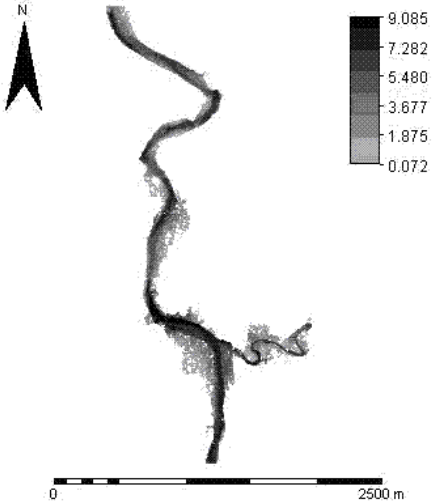

b) 5 m DEM

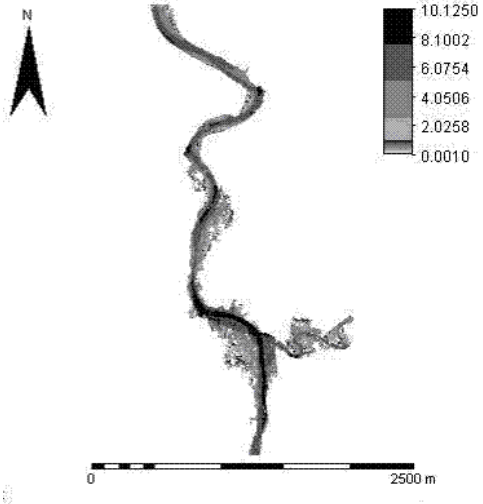

c) 7.5 m DEM

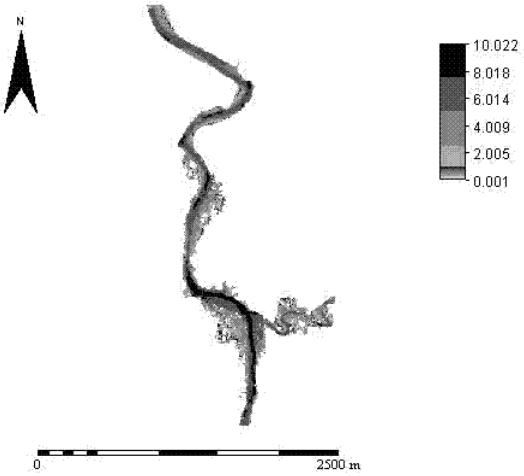

d) 10 m DEM

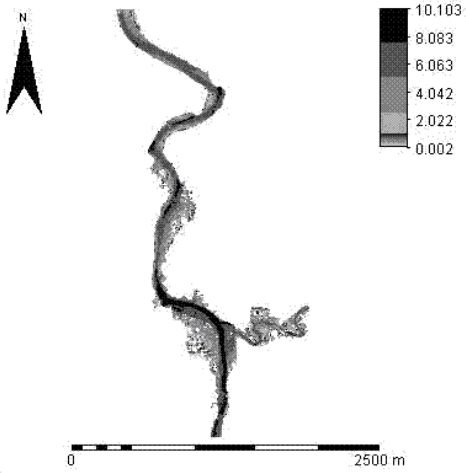

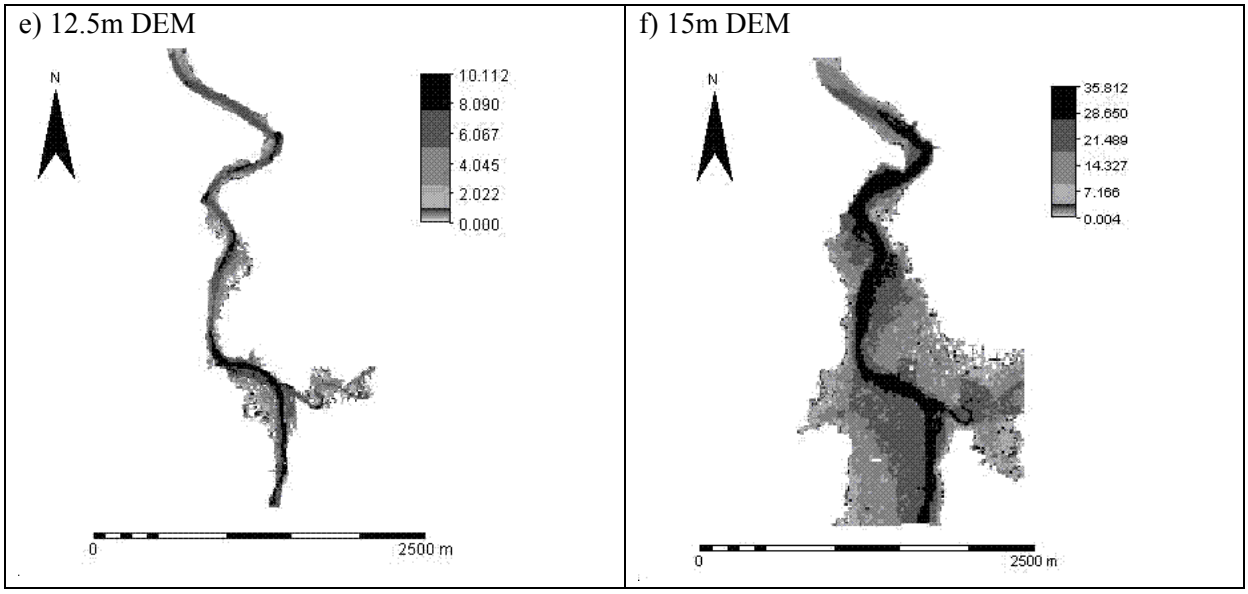

IV. Flood maps for the 50- and 100-year return periods

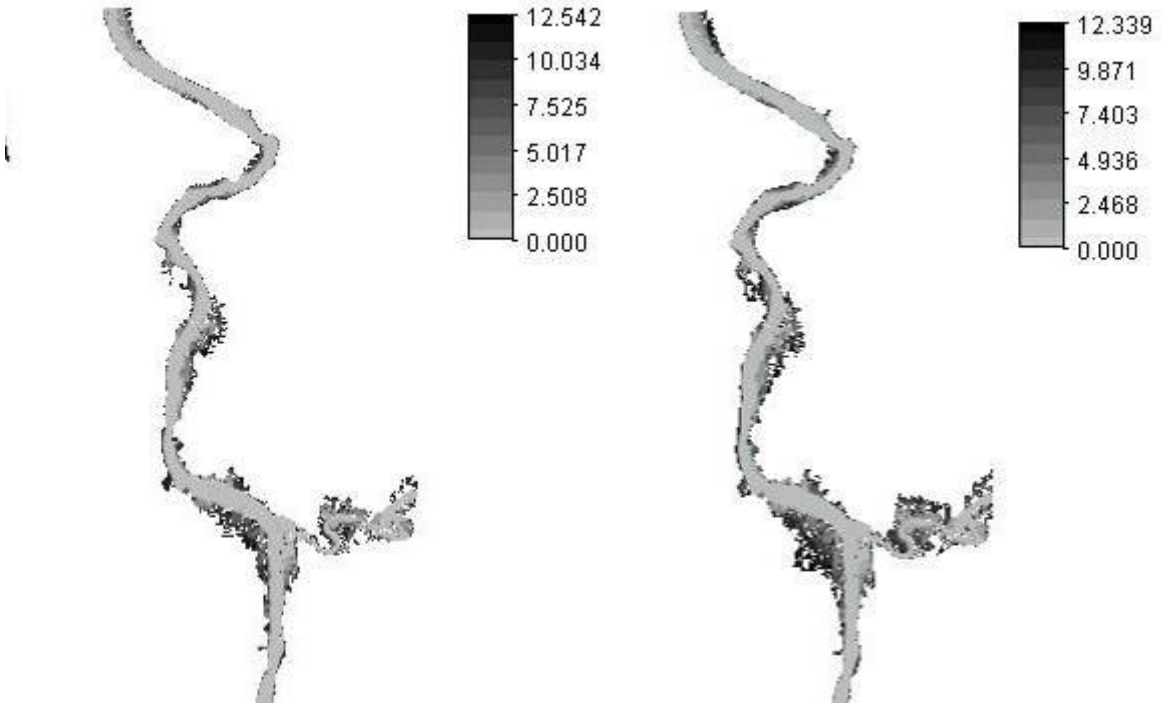

a) 50-year flood b) 100-year flood

i. ***Time to wet map for 50-year and 100-year return periods floods***

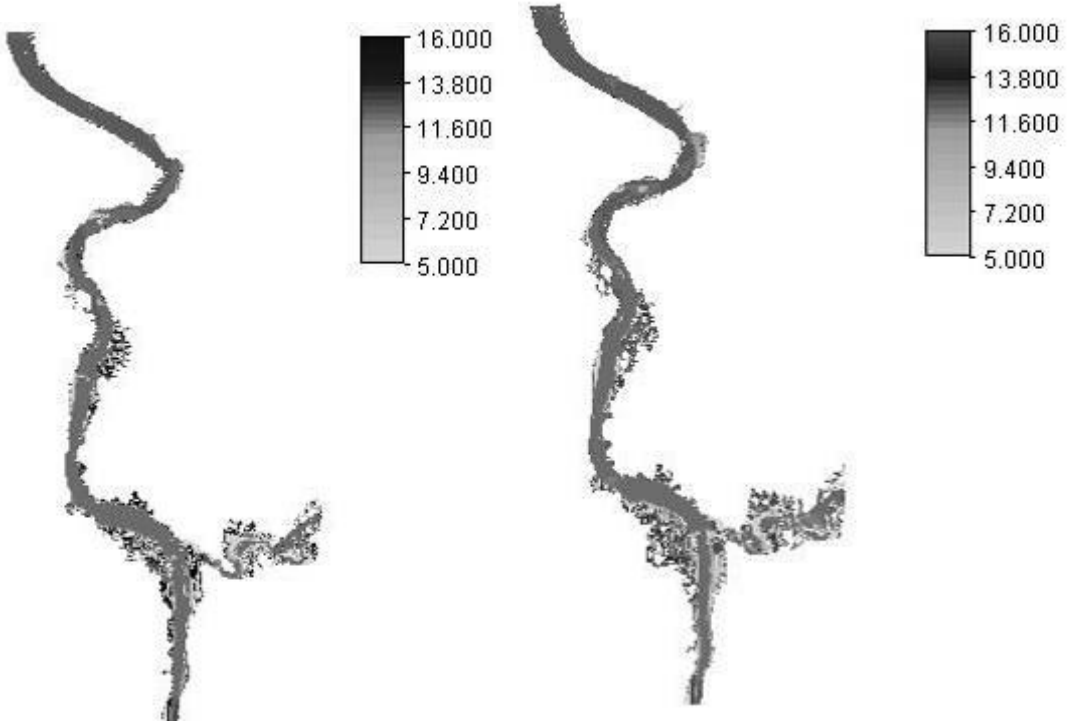

a) 50-year flood b) 100-year flood

ii. Time to maximum velocity (hrs.) for 50-year and 100-year return periods floods

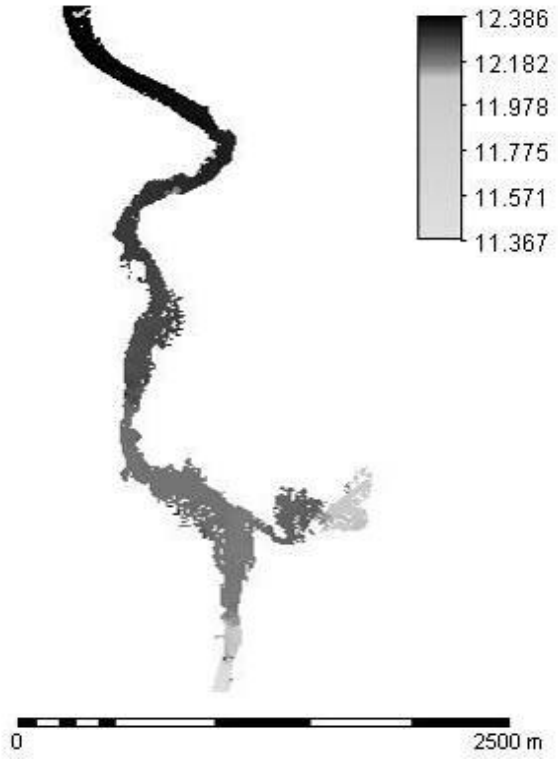

a) 50-year flood

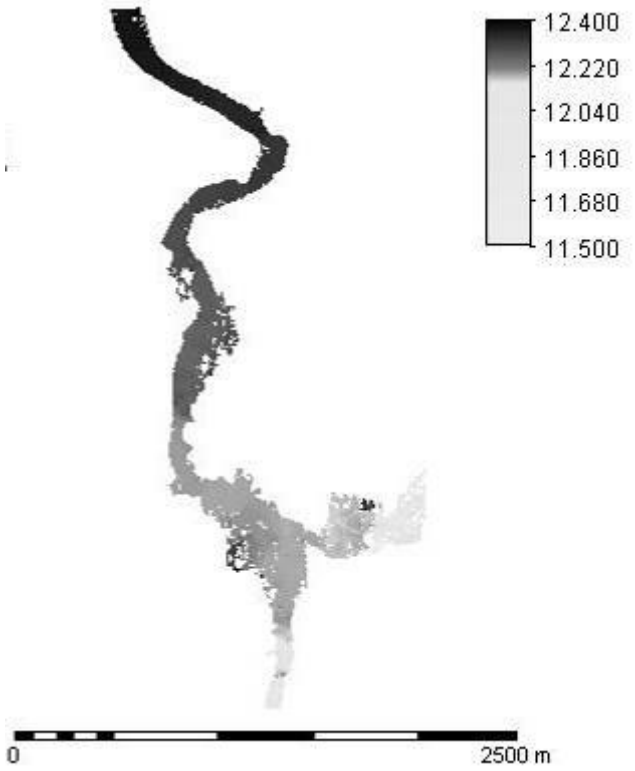

b) 100-year flood

References

Anderson M.G., P.D. Bates, and Walling D.E., (1996). The general context of floodplain process research. Floodplain processes. M. G. Anderson, D. E. Walling and P. D. Bates, Editor. Chichester, John Wiley & Sons Ltd.

Band L.E., and Moore I.D. (1995). Scale: Landscape attributes and geographical information systems. Scale issues in hydrological modelling. J.D. Kalma, and M. Sivapalan, Editor. Chichester, England, John Willey & Sons.

Beven K.J., and A.Binley (1992). "The future of distributed models: model calibration and uncertainty prediction." Hydrological Proccesses **6**: 279-298.

C. K.Huyck, R.T.Eguchi, and B. Houshmand (2002). Bare-Earth Algorithms for Use with SAR and Lidar Digital Elevation Models, Multidisciplinary Center for EarthQuake Engineering Research, University Buffalo, State University of New York.

Chow, V. T. (1956). Hydrologic studies of floods in the United States. International Assoc. Sci. Hydrl. Publ.**:** 134-170.

Chow, V. T. (1964). Handbook of Applied Hydrology, MacGraw-Hill Inc.

D.L. Fread, and J.M.Lewis "selection of Δx and Δt computational steps for four-point Implicit Nonlinear Dynamic Routing Model." *URL:* www.nws.noaa.gov/oh/hrl/rvrmech/papers.htm

D.L. Fread, M.J., Janice M. Lewis. An LPI Numerical Implicit Solution for Unsteady Mixed-flow Simulation. URL: www.nws.noaa.gov/oh/hr/rvrmech/papers.htm

E.C. Penning Rowsell, a. S. M. T. Risks and Resources: Defining and managing floodplain. Floodplain processes. M. G. Anderson, D. E. Walling and P. D. Bates, Editor. Chichester, England, John Wiley & Sons Ltd.

FEMA Flood Hazard Mapping. **2004**.

G. Aronica, B.Hankin, & K. Beven (1998). "Uncertainty and equifinality in calibrating distributed roughness coefficients in a flood propagating model with limited data." Advances in water resources **22**(4): 349-365.

Goorden, N. (2004). Overland-channel flow modelling with Flowsim. Department of fluid mechanics. Delft, Delft university.

J.F. Dhondia, and G.S. Stelling, Application of One Dimensional-Two Dimensional Inetegrated Hydraulic Model for Flood Simulation and Damage Assessment. URL: www.sobek.nl. Access date: July 22/2004.

Kate Marks, P.Bates (2000). "Integration of high-resolution topographic data with floodplain flow models." Hydrological Proccesses **14**: 2109-2122.

Keith Smith, and Roy Ward (1998). Floods physical processes and human impacts. Chichester, England, John Wiley & Sons.

Kutija, V. (1993). "On the numerical modelling of supercritical flow." Journal of Hydraulic research **31**(6): 841-848.

M.S. Horritt, and P.D.Bates (2002). "Evaluation of 1D and 2D numerical models for predicting river flood inundation." Journal Of Hydrology **268**: 87-99.

Maidment, D. R., Ed. (1993). HandBook of hydrology, McGraw-Hill,Inc.

P Ph Jansen, L.v.Bendegom, J van den Berg, M de Vries, and A Zanen, ed. (1979). Principles Of River Engineering. London, Pitman Publishing Limited.

P.D. Bates, M.G. Anderson, d.A. Price, R. J. Hardy and C.N. Smith (1996). Analysis and development of Hydraulic models for floodplain flows. Floodplain processes. M. G. Anderson, D. E. Walling and P. D. Bates, Editor. Chichester, England, John Wiley & Sons Ltd.

Rientjes, T. H. M. (2004). Inverse modelling of the rainfall-runoff relation: a multi objective model calibration approach. Delft, Delft university.

Smith, S. L. H., D.A, and Longley, P.A (2003). The Effect of Changing Grid Size in the Creation of Laser Scanner Digital Surface Models. **2004**. URL: www.geocomputation.org. Access Date: Oct. 12/2004.

Tennakoon, K. B. M. (2004). Parameterisation of hydrodynamic models and Flood Hazard Models for Naga city, Philippines. Enschede, ITC.

USGS (2002). Flood-Hazard Mapping in Honduras in Response to Hurricane Mitch. M. C. Mastin. Tacoma, Washington.

Uwe Arnold, B.Datta, and Peter Haenscheid. (1989). Intelligent Geographic Information System (IGIS) and surface water modelling. New directions for surface water modelling, IAHS Publ. no. 181.

V. Y. Ivanov, E.R.Vivoni, Rafael L. Bras, D. Entekhabi (2004). "Preserving high-resolution surface and rainfall data in operational scale basin hydrology: a fully distributed physically-based approach." Journal of hydrology **298**: 80-111.

Kutija, V., and C.J. Hewett (2002). "Modelling of supercritical flow conditions revisited; NewsC scheme." Journal of Hydraulic research **40**(2).

Ward, R. (1978). Floods A Geographic Perspective, MacMillan Press Ltd.

Werner, M., (2004). Spatial flood extent modelling A performance based comparison. Delft Universty: Delft.

Yevjevich, V. (1994). Floods and society. Coping with floods. G. Rossi, N. Harmancioglu and V. Yevjevich, Editor. Dordrecht, The Netherlands, Kluwer Academic Publisher.